MICROCOPY RESOLUTION TEST CHART

NATIONAL BUREAU OF STANDARDS 1963-A

REPORT NO. CG-D-09-80

LEVEL

(12)

LORAN-BASED BUOY POSITION
AUDITING SYSTEMS--ANALYTICAL EVALUATION

AD A088266

U.S. DEPARTMENT OF TRANSPORTATION
RESEARCH AND SPECIAL PROGRAMS ADMINISTRATION
Transportation Systems Center
Cambridge MA 02142

FEBRUARY 1980

DTIC
ELECTE
AUG 2 7 1980

C

FINAL REPORT

Prepared for

U.S. DEPARTMENT OF TRANSPORTATION
UNITED STATES COAST GUARD
Office of Research and Development
Washington DC 20593

80 8 25 142

18 (10) Jr. ... A./Wolfson, Peter D./Engels
/Martin C./Poppe, Jr, James M./Holtz
Leon M./DePalma

Technical Report Documentation Page

1. Report No.	2. Government Accession No.	3. Recipient's Catalog No.
CG-D-09-80	AD-A088266	(11) Feb 10 /

4. Title and Subtitle	5. Report Date
(1) LORAN-BASED BUOY POSITION AUDITING SYSTEMS—ANALYTICAL EVALUATION	February 1980
	6. Performing Organization Code

7. Author's J.A. Wolfson,* P. Engels,* M.C. Poppe, Jr.,** J.M. Holtz ** L.M. DePalma ***	8. Performing Organization Report No.
	(14) DOT-TSC-USCG-80-2

9. Performing Organization Name and Address	10. Work Unit No. (TRAIS)
*U.S. Department of Transportation Research and Special Programs Administration Transportation Systems Center Cambridge MA 02142 (13) 256 /	CG019/R0004
	11. Contract or Grant No.
	13. Type of Report and Period Covered

12. Sponsoring Agency Name and Address	
U.S. Department of Transportation United States Coast Guard Office of Research and Development Washington DC 20593	(9) Final Report, Feb. — Dec. 1979
	14. Sponsoring Agency Code

16. Abstract

An analytic evaluation and comparison of the following candidate Buoy Position Auditing System (BPAS) configurations is presented in this report: transmission of digital Time Difference (TD) data from a Loran-C receiver on the buoy, retransmission of Loran-C pulses from the buoy, and combination of helicopter Loran-C data and helicopter-to-buoy microwave ranging data in a variable geometry solution. The candidate BPAS configurations utilize Loran-C in the differential mode. A model is developed to characterize differential Loran-C errors, accounting for the expected effect of the land/sea water conductivity interface. The error model is utilized alone, or with a microwave ranging system error model, to estimate buoy position-fix accuracy afforded by each BPAS configuration. Accuracy estimates and data on cost, complexity, and technical risk are employed to recommend a BPAS configuration for testing. It is concluded that Loran-C pulse retransmission is not a viable BPAS configuration. The variable geometry BPAS configuration is highly accurate, due to calibration of Loran-C errors by processing of redundant data, but is not presently cost-effective. The digital TD transmission BPAS configuration is recommended for testing, due to its simplicity and low cost. An experiment is outlined whereby the accuracy of the TD transmission configuration can be assessed to determine its utility in the U.S. Coast Guard buoy audit mission.

17. Key Words	18. Distribution Statement
Buoy Position Finding Aids to Navigation Differential Loran-C Loran-C Pulse Retransmission	DOCUMENT IS AVAILABLE TO THE PUBLIC THROUGH THE NATIONAL TECHNICAL INFORMATION SERVICE, SPRINGFIELD, VIRGINIA 22161

19. Security Classif. (of this report)	20. Security Classif. (of this page)	21. No. of Pages	22. Price
Unclassified	Unclassified	258	

Form DOT F 1700.7 (8-72)   Reproduction of completed page authorized

407083 sll

PREFACE

The purpose of this Transportation Systems Center (TSC) report is to:

1. provide an evaluation and comparison of methods for auditing the positions of U.S. Coast Guard buoys (aids to navigation) using retransmission of radio location signals,

2. recommend a buoy position audit system (BPAS) configuration,

3. provide a test method to determine the operational acceptability of the technique.

The project was sponsored by Captain Donald A. Feldman of the United States Coast Guard (G-DST-1). Peter D. Engels and Joseph A. Wolfson of the Transportation Systems Center were responsible for the preparation of the report as well as overseeing and contributing to all subject areas. The error analyses were performed by Leon M. DePalma and James M. Foltz of The Analytical Sciences Corporation (TASC) in Reading, Massachusetts. The BPAS system hardware configurations, availability, operations and associated costs studies were performed by Martin C. Poppe, Jr. of Cambridge Engineering in Cambridge, Vermont. These three gentlemen also contributed to all phases of this report.

The authors would also like to acknowledge Kathleen Kvicala whose typing skills were critical to the timely completion of this report. Acknowledgement is also due to William Nucefora for a splendid job of editing and compilation.

iii

METRIC CONVERSION FACTORS

Approximate Conversions to Metric Measures

Symbol	When You Know	Multiply by	To Find	Symbol
	LENGTH			
	inches	*2.5	centimeters	cm
	feet	30	centimeters	cm
	yards	0.9	meters	m
	miles	1.6	kilometers	km
	AREA			
	square inches	6.5	square centimeters	cm²
	square feet	0.09	square meters	m²
	square yards	0.8	square meters	m²
	square miles	2.6	square kilometers	km²
	acres	0.4	hectares	ha
	MASS (weight)			
	ounces	28	grams	g
	pounds	0.45	kilograms	kg
	short tons (2000 lb)	0.9	tonnes	t
	VOLUME			
	teaspoons	5	milliliters	ml
	tablespoons	15	milliliters	ml
	fluid ounces	30	milliliters	ml
	cups	0.24	liters	l
	pints	0.47	liters	l
	quarts	0.95	liters	l
	gallons	3.8	liters	l
	cubic feet	0.03	cubic meters	m³
	cubic yards	0.76	cubic meters	m³
	TEMPERATURE (exact)			
	Fahrenheit temperature	5/9 (after subtracting 32)	Celsius temperature	°C

Approximate Conversions from Metric Measures

Symbol	When You Know	Multiply by	To Find	Symbol
	LENGTH			
mm	millimeters	0.04	inches	in
cm	centimeters	0.4	inches	in
m	meters	3.3	feet	ft
m	meters	1.1	yards	yd
km	kilometers	0.6	miles	mi
	AREA			
	square centimeters	0.16	square inches	
	square meters	1.2	square yards	
	square kilometers	0.4	square miles	
	hectares (10,000 m²)	2.5	acres	
	MASS (weight)			
	grams	0.035	ounces	
	kilograms	2.2	pounds	
	tonnes (1000 kg)	1.1	short tons	
	VOLUME			
	milliliters	0.03	fluid ounces	
	liters	2.1	pints	
	liters	1.06	quarts	
	liters	0.26	gallons	
	cubic meters	36	cubic feet	
	cubic meters	1.3	cubic yards	
	TEMPERATURE (exact)			
	Celsius temperature	9/5 (then add 32)	Fahrenheit temperature	

TABLE OF CONTENTS

TABLE OF CONTENTS (continued)

TABLE OF CONTENTS (continued)

LIST OF ILLUSTRATIONS

LIST OF ILLUSTRATIONS (Continued)

ix

LIST OF TABLES

LIST OF TABLES (Continued)

1. INTRODUCTION AND SUMMARY

1.1 BACKGROUND AND OBJECTIVES

The U.S. Coast Guard (USCG) maintains a network of moored buoys (aids to navigation) to control maritime traffic in the shipping channels of rivers, harbors and harbor entrances. These buoys can be moved off station or destroyed as a result of severe storms, ice flow or collision with vessels. Since an off-station buoy is presently identified by periodic inspections with a buoy tender or by an "aid discrepancy report" from a mariner, a significant time delay may occur before a warning is issued and the buoy is returned to its correct location. An effective Buoy Position Auditing System (BPAS) will both reduce this delay and enable the Coast Guard to maintain the navigational capability provided by the buoy network, thus minimizing the likelihood of property damage and shipping delays which can result from displaced buoys.

In October 1977, the USCG Research and Development Center published Report No. CG-D-61-77, "A Study of Aerial Semi-Precise Survey Systems for Position Auditing of Coast Guard Aids to Navigation". This report specified the following requirements for a buoy position auditing system:

1.   Economical operation
2.   Buoy position error less than ± 30 meters
3.   Response time of a few hours and completion within 48 hours
4.   Minimal development time and modest equipment and manpower procurement requirements.

This report also concluded that no system is presently available which can meet all these requirements.

The Naval Research Laboratory (NRL) also studied the problem and arrived at a slightly different set of requirements:

1. Buoy position accuracy of 15 meters
2. Auditing up to four times a day.

NRL also concluded that no current system exists which can meet these requirements but recommended that retransmission of a radiolocation signal from the buoy compared to a reference station signal might form the basis for such a system.

This report evaluates three system concepts for determining the position of buoys using retransmission of radio location signals. The retransmitted signals from the buoys will be received and processed at either a mobile platform such as a helicopter or a shore station. The buoy signals will be compared against similar signals from fixed reference locations to provide a more accurate differential mode of operation. It is intended that the buoy monitoring operation will be accomplished in conjunction with other routine USCG operations and that the buoy audit will not increase workload or change routine operational procedures on the part of USCG personnel.

The three candidate electronic Buoy Position Auditing Systems (BPAS) selected for evaluation are:

1. Transmission of digital Time Difference (TD) data from a Loran-C receiver on the buoy. Each buoy is equipped with a Loran-C receiver which detects the signal and provides a time difference readout. The buoys are interrogated in sequence from a helicopter or shore-based control station. Each interrogation results in a return link using a continuous wave carrier which is modulated with the time differences as low bit-rate digital data.

2. Retransmission of Loran-C pulses from the buoy to a remote Loran-C processor in response to a command from the central station (fixed or mobile). Here, the retransmission is the received Loran-C pulse itself (after suitable filtering and amplification) modulated on a suitable carrier.

3. A combination of helicopter position data (from a Loran-C receiver and an altimeter) and helicopter-to-buoy range data (from a precision ranging system), in a variable geometry solution. Monitoring of buoy

1-2

position relative to a moving platform can be accomplished by two-way ranging. The platform emits a ranging signal which is transponded back by the buoy. As the platform moves, the changing geometry relative to the buoy will generate multiple lines of position, enabling buoy location by triangulation. Alternatively the ranging measurements could be made from a network of shore stations.

The configurations are referred to as "TD Transmission", "Pulse Retransmission", and "Variable Geometry", respectively, in this report.

All three candidate configurations employ differential Loran-C, which exhibits cost, accuracy and/or operational advantages over other methods of locating and tracking buoys (Appendix E contains a list of other methods). Implementation of a Buoy Position Auditing System based on differential Loran-C could lead to coordination of the buoy audit mission with harbor and harbor entrance navigation, for which differential Loran-C is also under consideration by the USCG.

The major objectives of this study are to:

o   Identify viable Loran-C system configurations meeting the requirements of a buoy-based system

o   Construct a tradeoff between cost/complexity and performance for the selected configurations

o   Define the associated base station equipment required to receive and process signals received from the buoys

o   Construct a typical operating scenario for each system to determine audit rates and buoy power requirements

o   Define a candidate system for experimental verification of the selected approach

o   Perform error analyses of the candidate BPAS configurations to estimate system accuracy and identify critical hardware parameters and operational restrictions

1-3

o   Employ the error analysis results, together with data on cost, complexity, and technical risk, to recommend a BPAS configuration for testing

o   Outline an experiment to verify the recommended configuration.

1.2 SYSTEM CONSTRAINTS

The USCG has imposed certain cost, equipment, and operational constraints on the Buoy Position Auditing System. The constraints are intended to serve as guidelines for comparison of the candidate configurations. The constraints fall into three categories, depending on whether they pertain to the buoys, shore station, or helicopter.

The following constraints pertain to the buoys and are relevant to all three candidate BPAS configurations:

o   Buoys to be audited: 1,000 to 4,000 lighted buoys

o   Time of audit: daylight

o   Power source: 12 volt, 1,000-6,000 amp-hr battery presently on buoy

o   Maximum battery drain: 1 amp-hr/day or 365 amp-hr/year

o   Maximum buoy equipment cost: $1,000

o   Space for buoy equipment: spare battery compartment (or mounted to exterior).

The $1,000 constraint on buoy equipment cost is a very important factor influencing the recommendations made herein. Due to the expense involved in servicing the electronic systems located on the buoys, a requirement for positioning system service at intervals other than normal battery changing/charging intervals is not permitted. In the future, buoy batteries may be

charged by solar cells thereby permitting a greater battery drain during a buoy audit than is presently feasible. Further, systems requiring sophisticated adjustments are also undesirable, as these would increase the level of training required for buoy tender personnel.

The following constraints pertain to the shore station used in the TD Transmission and Pulse Retransmission configurations:

o   Shore station-to-buoy communications link: line-of-sight

o   Antenna for communications link: mounted on existing tower

o   Maximum frequency of audits: daily

o   Equipment cost: $20,000 to $50,000 per control station.

Since communications from the shore station to the buoy must be line-of-sight from an antenna mounted on an existing tower, some buoys (particularly, ocean buoys) may have to be audited from a helicopter. Both a shore station and a helicopter may be needed to audit the buoys in each harbor, in the TD Transmission and Pulse Retransmission BPAS configurations.

The following constraints are applicable to the helicopter involved in all three configurations:

o   Typical altitude: 300 m (1,000 ft)

o   Maximum velocity: 150-220 km/hr (80-120 kt), depending on helicopter model

o   Maximum round-trip flight time: 3 hrs

o   Weather conditions at time of audit: good visibility

o   Helicopter-to-buoy communications link: line-of-sight

o   Effect of audit on flight pattern: desirable to have no effect, since helicopter will not be dedicated to buoy audit mission

o   Crew requirements: minimal tasks, no additional manpower

o   Audit completion time: 12 hrs from helicopter takeoff to data-processing completion

o   Antennas: permanently mounted

o   Size and weight of other equipment: portable, capable of being hand-carried by one person

o   Maximum helicopter equipment cost: $50,000

o   Maximum frequency of audits: weekly.

The helicopter is not dedicated to the buoy audit mission, details of the flight pattern cannot be chosen to optimize BPAS performance. However, the USCG permits specification of the general features of the flight pattern to assure line-of-sight transmission to each buoy (for all configurations) and favorable buoy/helicopter geometry (for the Variable Geometry configuration).

The position-fix accuracy required of a BPAS is not readily definable. Accuracy requirements depend on the buoy type; e.g., major obstruction buoys must be audited more precisely than ocean buoys. Furthermore, accuracy requirements cannot be defined meaningfully without first specifying the procedure, whereby position-fix data from a buoy audit is used to decide whether or not buoys are "on station" (Section 4.4). The USCG has not placed an accuracy constraint on BPAS at the present time. The Coast Guard's intentions are to evaluate the error analysis presented in this study, compare the analysis with experimental results and then determine the utility of the BPAS concept in USCG operations. Although a specific accuracy constraint has not been imposed, the Buoy Position Auditing System must be a "precision" system capable of better than 30 m rms position error for critical buoys. This conservative assumption is based

on accuracy guidelines for aerial "semi-precise" imaging systems, which are considered for the buoy position auditing problem in Ref. 8. The selected hardware should have a negligible effect on the potential accuracy of Loran-C. Further, the use of differential Loran-C (i.e. the measurement of Loran-C signals at a fixed location to calibrate the Loran-C signals received in the area of operation) is considered fundamental to meeting the stated less than 30 meter accuracy requirement. As part of establishing a buoy audit system, it is necessary to obtain authorization from the Federal Communication Commission (FCC) to use the necessary communication channels. Systems which permit the use of existing communication channels and further, which transmit data in a format permitted by the presently allocated use of those channels, are desirable. With the present crowded conditions in all frequency bands, the request for a wideband (e.g. 1MHz) communication channel would most likely be granted only in L-band or higher frequency ranges.

1.3 SYSTEM DESCRIPTIONS

The TD Transmission, Pulse Retransmission, and Variable Geometry BPAS configurations are described generically in this section. The candidate BPAS configurations all employ differential Loran-C operated in the hyperbolic mode. As in the case of conventional (non-differential) Loran-C, a position fix is computed as the intersection of two hyperbolas, each associated with a time difference measured at the Loran-C user location. However, the user TDs are first corrected based on the TDs measured at a pattern monitor (a Loran-C receiver which is established at a known location and operated continuously during the buoy audit). If the pattern monitor is located near the Loran-C user, differential Loran-C can significantly reduce the effect of temporal TD variations and thereby exhibit much smaller position-fix errors than conventional Loran-C. The differential Loran-C algorithm for the TD Transmission BPAS configuration is detailed in Appendix A (Section A.4.1). It is assumed that buoy TDs are recorded by personnel on the buoy tender when the BPAS equipment is first installed (time t_o). (The TDs are recorded with the buoy directly above the desired buoy anchor position.) Pattern monitor TDs are likewise assumed to be measured at time t_o, and are subtracted from the buoy TDs to form differential TDs. New differential TDs are computed based on buoy and pattern monitor TDs measured during the buoy audit. The change in differential TDs between time t_o and the audit time is used to estimate the new buoy position relative to the desired anchor position.

Figure 1.3-1 is an overview of a Loran-C based, buoy audit system. A buoy equipped with a Loran-C signal processor and a command/control receiver is maintained in a standby condition until an AUDIT command is received from a base station. Following the receipt of an AUDIT command, the buoy electronics are activated, causing Loran-C and buoy identification data to be transmitted back to the base. At the base, the data are further processed and recorded, and finally used to determine buoy position. Four data acquisition techniques are indicated in Figure 1.3-1. The first three provide for the reception of buoy data by either a helicopter, shore, or ship based data processing system. Although not envisioned as an auditing platform, the placement of a base station on a buoy tender permits the location of buoys which have drifted from their mooring point and further, permits the establishment of the correct buoy position at the time of deployment. The fourth acquisition technique provides for relaying an unprocessed buoy telemetry signal through a helicopter, back to the shore-based station. This technique the helicopter to increase the radio range or virtual line of site range from the shore-based processor to the buoy under audit.

Two Loran-C retransmission systems were considered in the study. The first, a time-difference (TD) transmission, employs a selectively addressable Loran-C receiver and digital data transmitter. The second uses a selectively addressable Loran-C (analog) signal pulse retransmitter on the buoy.

1.3.1 Time Difference Transmission

A diagram showing the TD Transmission BPAS is shown in Figure 1.3-2. Loran-C signals are received and processed by an automatic Loran-C receiver. The output of this receiver provides Loran-C time difference and signal quality information. These data are merged with buoy identification data and transmitted back to the base station on a narrow band, VHF telemetry link. At the base station, the data are received by a compatible VHF telemetry receiver and data demodulator. The demodulator data output is formatted and recorded. The recorded data is directed to a data position processor/center where a determination of buoy location is made using the time difference data from the buoy and differential correction data received from various pattern monitor receivers.

LORAN-C
SIGNALS

LORAN-C + ID

HELICOPTER
'BASE'
PROCESSOR

HELICOPTER TELEMETRY
RELAY

DIRECT TELEMETRY TO SHORE
AND/OR
TO BUOY TENDER

BUOY

SHORE
BASE
PROCESSOR
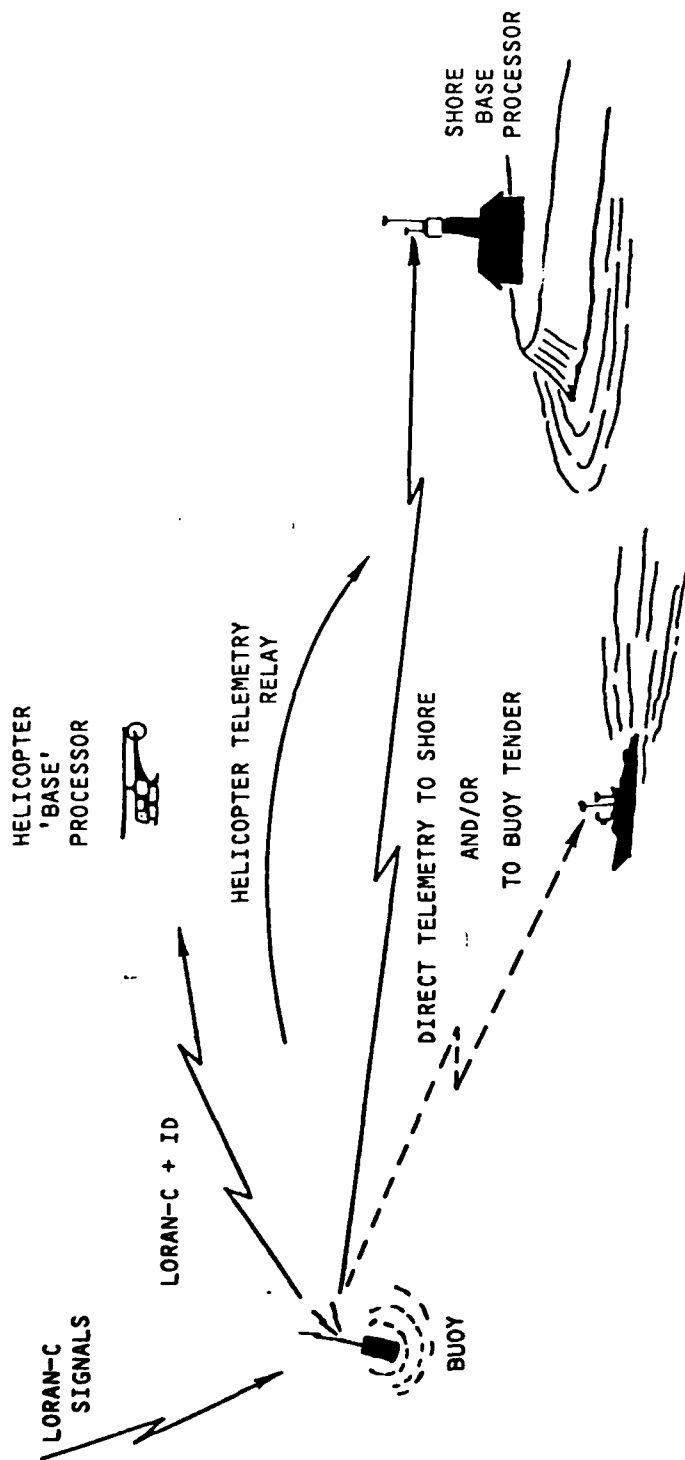
Figure 1.3-1   A Loran-C Based Buoy Audit System, System Configuration
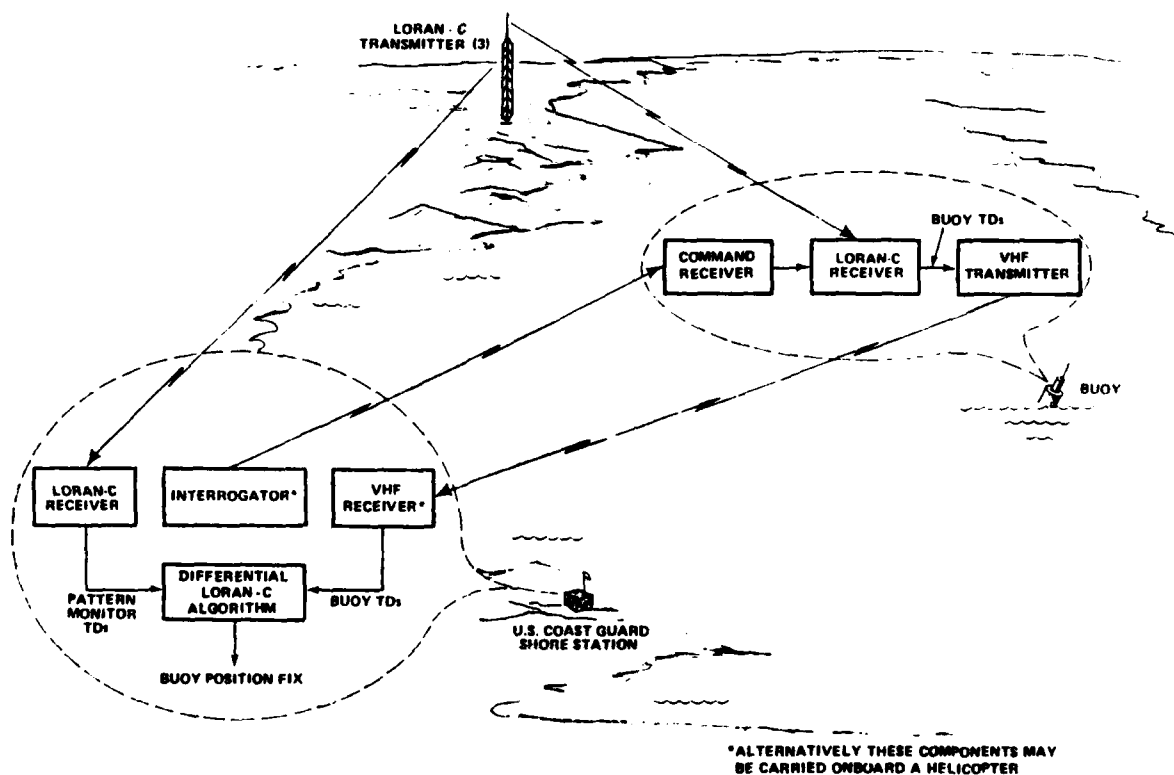
Figure 1.3-2 TD Transmission BPAS Configuration

1.3.2 Pulse Retransmission

The Pulse Retransmission BPAS configuration (Figure 1-3.3) differs from the TD Transmission configuration in that a Loran-C pulse retransmitter, instead of a Loran-C receiver, is installed on each buoy. The Loran-C signals are received at the buoy, and are processed by an analog pulse processor. The output of this processor is an analog signal which is a transformation of the original pulse. The processed pulse, pulse processing parameters necessary to complete the processing of the pulse, and identification data are transmitted back to the base station on a wideband telemetry link. At the base station, the processing of the Loran-C pulses is completed to obtain Loran-C time differences. This is accomplished using a special purpose Loran-C processor. As shown, the base station processor makes use of local Loran-C signals. Primary use of these signals is to aid in the processing of the retransmitted signals by providing timing and preliminary pulse information. The digital output from the special purpose Loran-C processor is recorded and directed to a data position processor/center where buoy position is determined using differential techniques. The primary reason for considering the pulse retransmission technique is the potential for cost reduction in the buoy electronics. Essentially, the electronics on the buoy may be thought of as the 'front end' of a Loran-C receiver, where the special purpose base station Loran-C procesor performs the remaining functions required to process the Loran-C signal to time difference data. By moving this electronics processing to the base station, the Loran-C processing in the buoy is simplified, resulting in a potential cost saving.

1.3.3 Variable Geometry

In the Variable Geometry BPAS configuration (Figure 1.3-4), the buoy audit is conducted from a helicopter which carries a Loran-C receiver, a precision ranging system, and an altimeter. The ranging system is used to determine the ranges from the helicopter to the buoys, where each buoy is equipped with a transponder. Simultaneous Loran-C TDs, range data, and altitude data are stored on magnetic tape and delivered to a USCG shore station for processing. The helicopter Loran-C TDs are combined with pattern monitor TDs in a differential Loran-C algorithm to compute helicopter position fixes. Buoy position fixes are then estimated from helicopter position-fixes, range data, and altitude data in a least-squares algorithm. The Loran-C and ranging equipment required for the Variable Geometry

LORAN - C
TRANSMITTER (3)

COMMAND
RECEIVER

LORAN - C
PULSE
RETRANSMITTER

BUOY

LORAN-C
RECEIVER

INTERROGATOR*

PULSE
DEMODULATOR*

SPECIALIZED
LORAN - C
RECEIVER*

DIFFERENTIAL
LORAN - C
ALGORITHM

PATTERN
MONITOR
TDs

BUOY TDs

U.S. COAST GUARD
SHORE STATION

BUOY POSITION FIX

*ALTERNATIVELY THESE COMPONENTS MAY
BE CARRIED ONBOARD A HELICOPTER
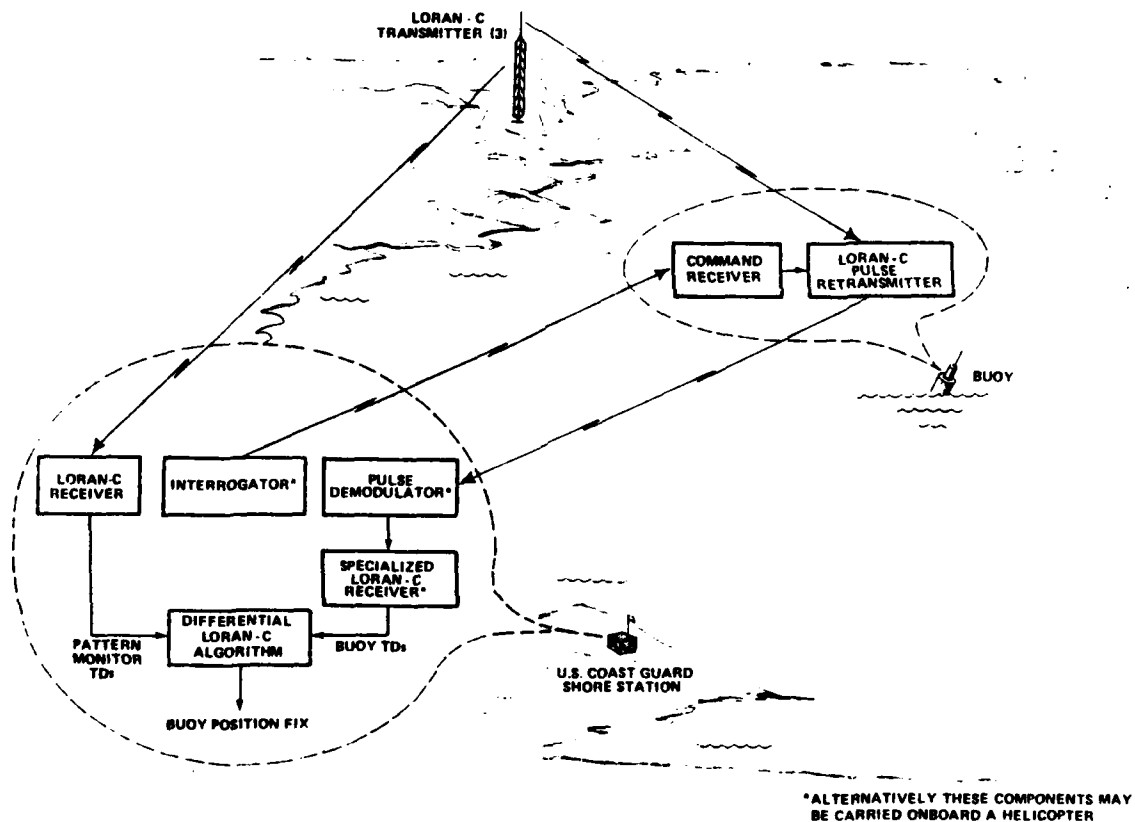
Figure 1.3-3   Pulse Retransmission BPAS Configuration
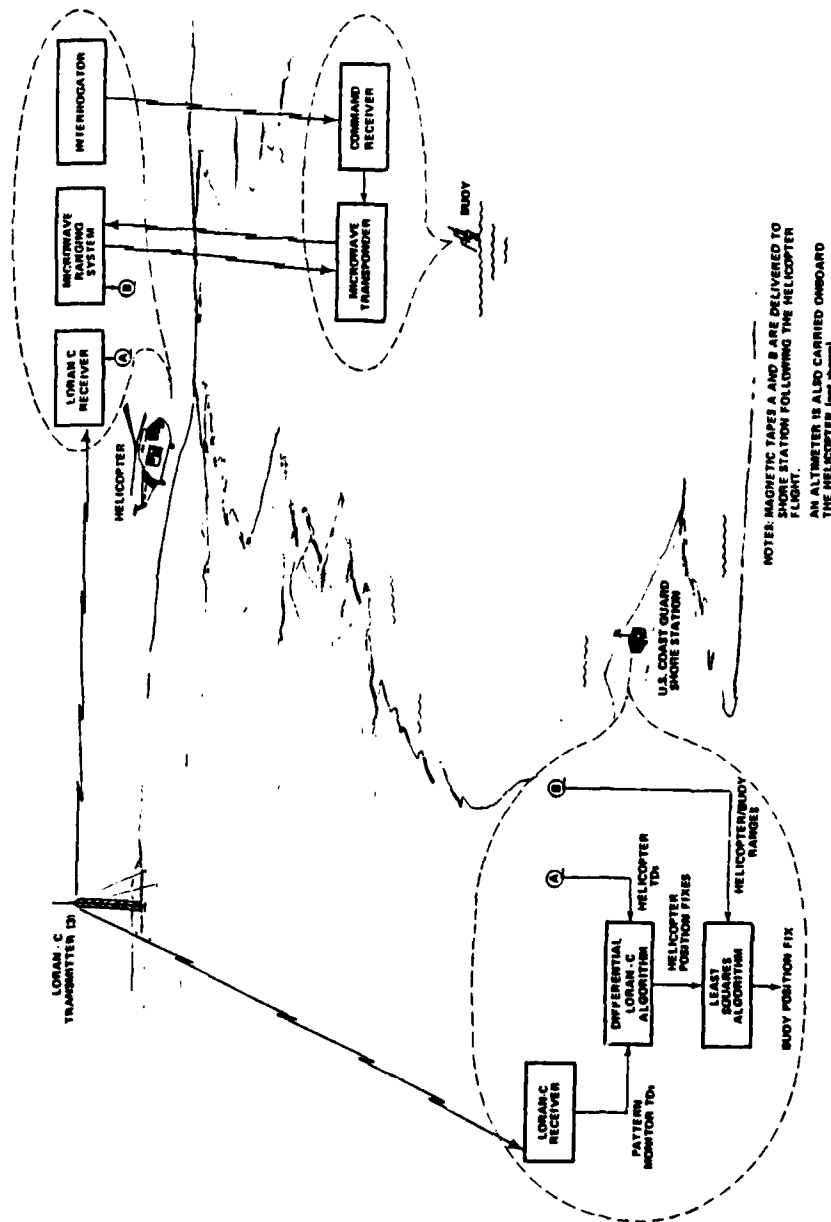
Figure 1.3-4 Variable Geometry BPAS Configuration

configuration is not presently available. However, according to manufacurers of similar equipment, its development should not impose substantial technical risk.

The following precision ranging system concepts are being considered for possible application to the BPAS problem:

o   Pulse ranging system operating in C-band or X-band (4-12.5 GHz)

o   CW systems using coded phase modulation operating in UHF band
    (300 - 3,000 MHz).

The design and operational characteristics of conventional pulse ranging position location systems are summarized in Refs. 20 and 30. In general, the available ranging systems are more sophisticated than required for the BPAS application. The manufacturers of the Trisponder (Del Norte Technology, Inc.) and Mini-Ranger (Motorola) systems were contracted to determine the feasibility of designing a simplified ranging system for application to the Variable Geometry BPAS configuration (see correspondence in Appendix D). Del Norte Technology has not expressed an interest in such an endeavor. Motorola has indicated that a system could be designed which uses a modified version of the Mini-Ranger equipment (Appendix D).

CW ranging systems usually employ a continuous carrier which is phase or frequency modulated by a deterministic wave form. Range measurements is accomplished by measurement of the phase shift between the transmitted and received wave forms. These systems are generally more efficient than pulse techniques; in addition since the average power and peak power requirements are identical, the required power profile is more compatible with the low power available from buoys.

1.4 SUMMARY OF KEY RESULTS

Error analyses have been conducted to estimate worst case BPAS accuracy and to identify critical hardware design parameters and operational restrictions for each configuration. The error analyses are based on a worst case differential

Loran-C error model (with GDOP = 1) which accounts for the expected effect of the land/sea water conductivity interface. This error model is used alone, or in combination with ranging system and altimeter error models (for the Variable Geometry configuration) to estimate buoy position-fix accuracy. A summary comparison of the three candidate BPAS configurations is contained in Table 1.4-1. The accuracy estimates presented in Table 1.4-1 are based on a selected subset of buoys in Boston Harbor, a differential Loran-C pattern monitor at Boston Light (a fixed aid), and certain assumptions regarding helicopter flight pattern and fix-taking strategy (Chapter 3).

Accuracy of the TD Transmission configuration is highly sensitive to buoy-to-pattern monitor separation. Estimated buoy position-fix errors are 10 to 30 m rms for a buoy-to-pattern monitor separation less than 11 km (the Loran-C error model results predict a maximum position error increase of 2.6 m per km of separation).* An improvement in TD Transmission accuracy can be achieved by deploying multiple pattern monitors so as to reduce the maximum buoy-to-monitor separation. However, a buoy-to-monitor separation less than 3 km is required to reduce the position error to less than 10 m rms. An alternative approach to reduce TD Transmission buoy position errors is to use data from multiple pattern monitors in a scheme to calibrate the Loran-C errors at the time of each audit. This scheme would permit accuracy improvement with a reasonable number of pattern monitors. Although detailed analyses of the calibration approach were beyond the scope of the present study, it is expected that significant improvement could be achieved with as few as three pattern monitors.

The TD Transmission BPAS configuration is very sensitive to Loran-C geometry. Buoy position fix errors are scaled by the Geometric Dilution of Precision (GDOP)—e.g., the position errors for San Francisco Harbor are approximately 4 times the position errors for Boston Harbor. However, in those locations where GDOP is poor the addition of more pattern monitors can reduce the buoy position errors to within acceptable limits. The Variable Geometry

---

*The reader is cautioned that this is a theoretical result based on "worst case" assumptions and should be interpreted accordingly.

Table 1.4-1

Comparison of BPAS Configurations

Consideration	TD Transmission	Pulse Retransmission	Variable Geometry
Accuracy (1σ)(worst case) based on assumptions enumerated in Section 3.2	10 to 30 meters (dependent on buoy pattern monitor locations) (with GDOP = 1)	10 to 30 meters (assumes same measurement capability as TDT)	<10 meters (dependent on helicopter dynamics compensation during data gathering and non-straight line flight path)
Cost/Buoy	$1,060 to $1,360	$1,540 to $1,750	$2,500 to $3,500
Cost/Base Station	$7,000	$63,000	$19,000 to $24,000
Audit Capability	10 buoys per 8 min. 20 sec. (60 buoys per 10 min.)	1 buoy per 6-10 min. (6-10 per hour)	7 buoys per 15 min.
Buoy power requirements (A-H = Ampere-Hours) based on 1 audit per week	0.23 A-H/day average	0.27 A-H/day average	0.21 to 0.73 A-H/day average
Max. per day of audit	0.33 A-H/day	0.60 A-H/day	0.26 to 3.36 A-H/day
Frequency Allocation	Standard VHF Communication Channel	Standard VHF Communication Channel and wide band L-band	Wide band L-band or X-band
Ability to work with helicopter, ship and shore base station	Yes	Yes	No (requires moving platform or multiple shore stations)
Major equipment development required	No	Yes	Yes
Technical Risk	Low; modify existing equipment	High; may not be feasible to overcome Loran-C pulse distortion problem	Medium; sophisticated computer processing software needed. also requires development of complete ranging system if CW ranging is used.

position error accuracy is significantly less sensitive to Loran-C geometry Furthermore, the sensitivity can be reduced by taking additional fixes and/or constraining the helicopter trajectory.

Position errors for the Pulse Retransmission configuration are expected to be greater than for TD Transmission due to the adverse effect of Loran-C pulse modulation/demodulation on phase-tracking accuracy. However, detailed analyses of the modulation/demodulation process were not performed during this study because of the clear disadvantages of the Pulse Retransmission configuration with respect to cost and technical risk. As a result, a decision was made by the U.S. Coast Guard at an interim project briefing on 31 July 1979 to discontinue study of the Pulse Retransmission configuration.

Buoy position-fix errors for the Variable Geometry BPAS configuration can be reduced to less than 10 m without unduly constraining the helicopter flight pattern and Loran/ranging fix-taking strategies. Accuracy of the Variable Geometry configuration is less sensitive to buoy-to-pattern monitor separation than is the TD Transmission configuration (the maximum rate of increase is 0.8 m error per km of separation). Sensitivity can be further reduced by placing minor restrictions on the helicopter flight pattern or increasing the number of Loran/ranging fixes. It is important to recognize that the Variable Geometry BPAS configuration accuracy is not influenced by helicopter accelerations in the same manner as is a Loran-C airborne navigation system (e.g., see Ref. 28). This results because the phase-tracking loops in the Loran-C receiver for the Variable Geometry application are assumed to be designed to minimize acceleration-induced errors at the expense of increased measurement noise. Increased measurement noise can be tolerated in the BPAS application, in contrast to the airborne navigation application, because of the redundant information provided by ranging.

1.5 CONCLUSIONS AND RECOMMENDATIONS

Results of analyses of accuracy, cost, complexity, and technical risk presented in this report have demonstrated the feasibility of an electronic Buoy Position Auditing System based on differential Loran-C. The TD Transmission and Variable Geometry BPAS configurations are both feasible. The TD Transmission BPAS configuration exhibits less than half the estimated cost per buoy unit than

the Variable Geometry configuration, but is expected to be less accurate (Table 1.4-1). The Pulse Retransmission configuration exhibits greater technical risk, higher cost, and larger errors than the TD Transmission configuration, and therefore has been eliminated from further consideration.

Based on its lower cost per buoy unit and relatively simple implementation requirements, the TD Transmission configuration is recommended over the Variable Geometry configuration for experimental verification. An appropriate TD Transmission BPAS experiment is outlined in Section 5.2. Data from this experiment will provide a basis for validation of the predicted accuracy of the TD Transmission BPAS configuration in particular and differential Loran-C in general. Data analysis results from the experiment can be combined with the error analysis results presented in this report, to determine the utility of the BPAS concept in the U.S. Coast Guard buoy audit mission.

If the experimentally-derived accuracy of the TD Transmission configuration is found to be insufficient for the buoy audit mission, the Variable Geometry configuration could be tested. The Loran-C data base from the TD Transmission experiment would be useful for refining the Variable Geometry error model employed in this report, and would aid in defining a comprehensive Variable Geometry experiment.

2. SYSTEM COMPONENT DESIGN AND COST ANALYSIS

2.1 INTRODUCTION

This section presents the system component design and cost analysis for all buoy position location schemes under consideration. In evaluating both systems, the following conditions were assumed:

o A maximum telemetry range of 40 km

o The availability of a wideband telemetry channel assignment at 1500 MHz

o The availability of a narrow band telemetry link assignment at 150 MHz

o The availability of a narrow band command and control telemetry link at 150 MHz

o The Loran-C signal environment listed in Table 2.1-1.

The specification and availability of the major system components along with component costs were developed following discussions with various manufacturers. The costs assumed for the telemetry equipment was extrapolated from costs currently being paid by various government agencies for similar equipment procured under competitive bid. In cases where exemplary equipment was identified, data sheets were obtained and included in Appendix G to give the reader an idea of off-the-shelf equipment that could be applied to an experiment.

The costing procedure used for the Loran-C equipment requires special comments. A large number of automatic Loran-C receivers designed for commercial marine applications are presently available. These vary in price from approximately $1700 to $3000. Because of the commercial retailing and distribution activity of the manufacturers, they are reluctant to talk about proposed competitive bid pricing for modifications of their standard equipment in reasonably large volume. For this reason, the dollars listed here were determined

STRONGEST SIGNAL @40 km	104 dBμ	
WEAKEST SIGNAL @1480 km	60 dBμ	
PEAK-TO-PEAK DYNAMIC RANGE		44 dB
DYNAMIC RANGE OF PULSE -		
10% AMPLITUDE TO PEAK		20 dB
**TOTAL DYNAMIC RANGE.		64 dB
DAYTIME SKYWAVE -		
500 km DELAY	90 μsec	
AMPLITUDE	-30 dB	
1480 km DELAY	54 μsec	
AMPLITUDE	+8 dB	

Table 2.1-1   Assumed Loran-C Signal Environment

after:

   o   Examining the dealer retail price for the equipment and taking into
       account normal dealer markups and manufacturer warranty provisions

   o   Examining the physical equipment itself and estimating the dollars
       required to assemble that level of equipment complexity.

An exception to this is the Pulse Retransmission buoy direct/derived pulse
processor. In this case, a company presently not manufacturing equipment for the
Loran-C market had recently completed a design and pricing exercise for the
analog portion of a Loran-C receiver, which they were willing to disclose.

   A final comment is necessary regarding the system parameters used in the
component design for cost analysis and tradeoff purposes. Transmission powers,
telemetry bandwidths, frequencies and digital message formats are all preliminary
and do not represent final system design values, but are felt to be typical and
suitable for the purposes intended.

2.2 TD TRANSMISSION SYSTEM

2.2.1 TD Transmission Buoy

   A block diagram of TD Transmission buoy electronics is shown in Figure
2.2-1. A common antenna is assumed for the reception of the LF Loran-C signals,
the VHF command signals and the transmission of the digital Loran-C data. The
use of a single antenna for all these functions was assumed for two reasons:

   o   first, the space available for mounting antennas on the buoy is limited,
       therefore the use of a single antenna will simplify the mechanical
       installation

   o   second, placed in such close proximity, problems of interference between
       the various elements (e.g. jamming of the command receiver by the VHF
       transmitter or pattern alteration) must be considered even if multiple
       antennas are used. By employing a single antenna and a properly

2-3
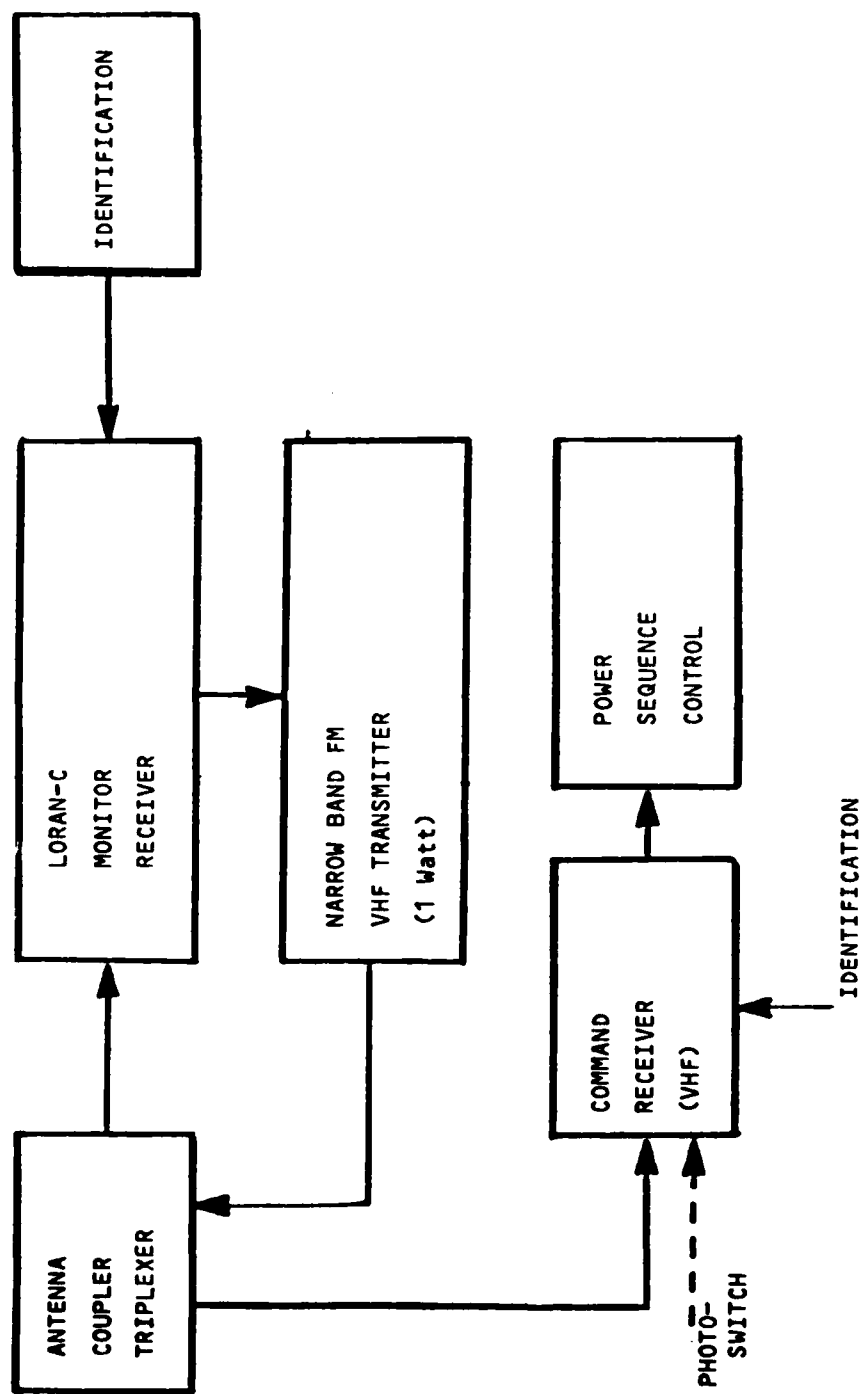
Figure 2.2-1   Block Diagram - TD Transmission Buoy Electronics

designed triplexer, these problems can be solved during the equipment design phase, reducing the potential for electronic problems at the time of installation.

The received Loran-C signals are directed to a Loran-C monitor receiver. This receiver is similar in design concept to an automatic Loran-C receiver, but differs in that:

o   The front end of the receiver and the resolution in the timing logic have been increased to provide additional accuracy and resolution of measurement

o   There is no need for front panel display and control electronics.

The Loran-C monitor receiver produces information regarding the time differences between the various received Loran-C stations, the envelope-to-cycle differences for each station, the signal quality for each station and the Master station/receiver oscillator offset. It is assumed that the receiver design selected will be capable of tracking all received Loran-C signals in a given operating area. Therefore, provisions will be made in the digital message for the retransmission of data from up to five stations (Master plus 4 Secondaries). It is further assumed that the Loran-C receiver will be based on microprocessor technology and therefore will be capable of integrating buoy identification data with the Loran-C data. The output of the Loran-C monitor receiver is a formatted message ready for modulation on a narrowband FM VHF transmitter.

The operation of the TD Transmission buoy electronics is controlled by a VHF command receiver. Upon receipt of a suitable coded command from the base station, the command receiver initiates a power control sequence. This sequence allows time for the automatic lockup and settling of the Loran-C monitor receiver, followed by the transmission of the digitized Loran-C and buoy identification data.

A typical TD Transmission buoy message is shown in Table 2.2-1. A total transmission time of approximately 700 msec/buoy is projected, of which 300 msec is 'dead' time provided for link capture and data demodulator synchronization. The message provides for the retransmission of 16 bits of identification data and

2-5

```
Link Capture & Front Porch                                              300 msec

Identification                      16 Bits              =  16

Loran-C TD's (7 digits)            28 Bits (BCD) x 4 = 112

Envelope Numbers (2 digits)         8 Bits (BCD) x 5 =  40

SNR Numbers (2 digits)              8 Bits (BCD) x 5 =  40

Master/Oscillator Offset           28 Bits (BCD)      =  28
                                                         (236)

Bits for Error Detection/Correction                      236

                                                       472 Bits


                                   472 Bits @1200 Bits/Sec = 393 msec

                                                             693 msec
```

Table 2.2-1   A Typical TD Transmission Buoy Message

complete time difference and signal quality data from the stations. In addition, a bit sequence equal in length to the message is provided for error correction/detection bits.

The TD Transmission data can be transmitted back to the base station using a narrow band VHF communication channel at a data transmission rate of 1200 bits/second. A typical telemetry budget for such a channel is shown in Table 2.2-2. Assuming a transmitter power output of 1 Watt, and a buoy antenna gain of 2dB, a total received signal strength of -93dBm is calculated. The major received noise sources are thermal noise and man-made noise. The available signal and noise combine to yield an IF signal-to-noise ratio of 31dB and a post-demodulation signal-to-noise ratio of 43dB assuring proper data demodulation even under conditions of severe multipath fading.

In order to establish the buoy power requirements, it is necessary to assume an operating cycle for the system. In the standby state, only the buoy command receiver is powered. At the start of an audit, the Loran-C receiver is turned on. The time required for lockup varies with receiver design and signal quality, however times ranging from 4-6 minutes are typical. Following lockup, it is further necessary for the receiver to smooth or integrate the time difference data to provide a single output value representing a statistical average over a period of several minutes. These two steps require a total time of 8 minutes from system turn on to the availability of data. Once smoothed time difference data is computed, the receiver is put in a standby mode in which only the time difference and signal quality data are kept in active storage pending readout of the data by the base station. During the receiver acquisition and settling time, there is no need for a buoy to transmit to the base station, and hence no competition for the telemetry link. Therefore, all buoys within radio range can be commanded to obtain Loran-C data simultaneously.

A typical TD Transmission operating cycle is shown in Figure 2.2-2. The command transmitter issues an ALL call which is received and processed by all buoys in radio range. This causes each buoy to power up the onboard Loran-C receiver.

SIGNAL

TRANSMITTER POWER (1 Watt)	+30 dBm
BUOY ANTENNA GAIN (net with duplexer)	2 dB
FREE SPACE PATH ATTENUATION 40 km - 150 MHz	-109 dB
MULTIPATH FADING MARGIN	20
RECEIVER ANTENNA GAIN	3 dB
TOTAL SIGNAL	-93 dBm

POST-DEMODULATION SNR

INPUT SNR	31 dB
FM IMPROVEMENT	26 dB - - - - -
LOSS FOR M=1	-14 dB - - 20 log(B)
SNR TO DATA DEMODULATOR	43 dB

IF NOISE

THERMAL NOISE (1 Hz)	-174 dBm
BANDWIDTH FACTOR (30 kHz)	+ 45 dB
MANMADE NOISE	0 dB*
GALACTIC NOISE	0 dB
RECEIVER NOISE FIGURE (Typical - reflects presence of manmade noise, 1.5 dB is possible)	5 dB
IF SNR	-124 dBm
	31 dB

$$3 \left[\frac{BW_{in}}{2\, BW_{out}} \right]^3 = 3(B)^3$$

*included in noise figure

Table 2.2-2   TD Transmission Telemetry Budget
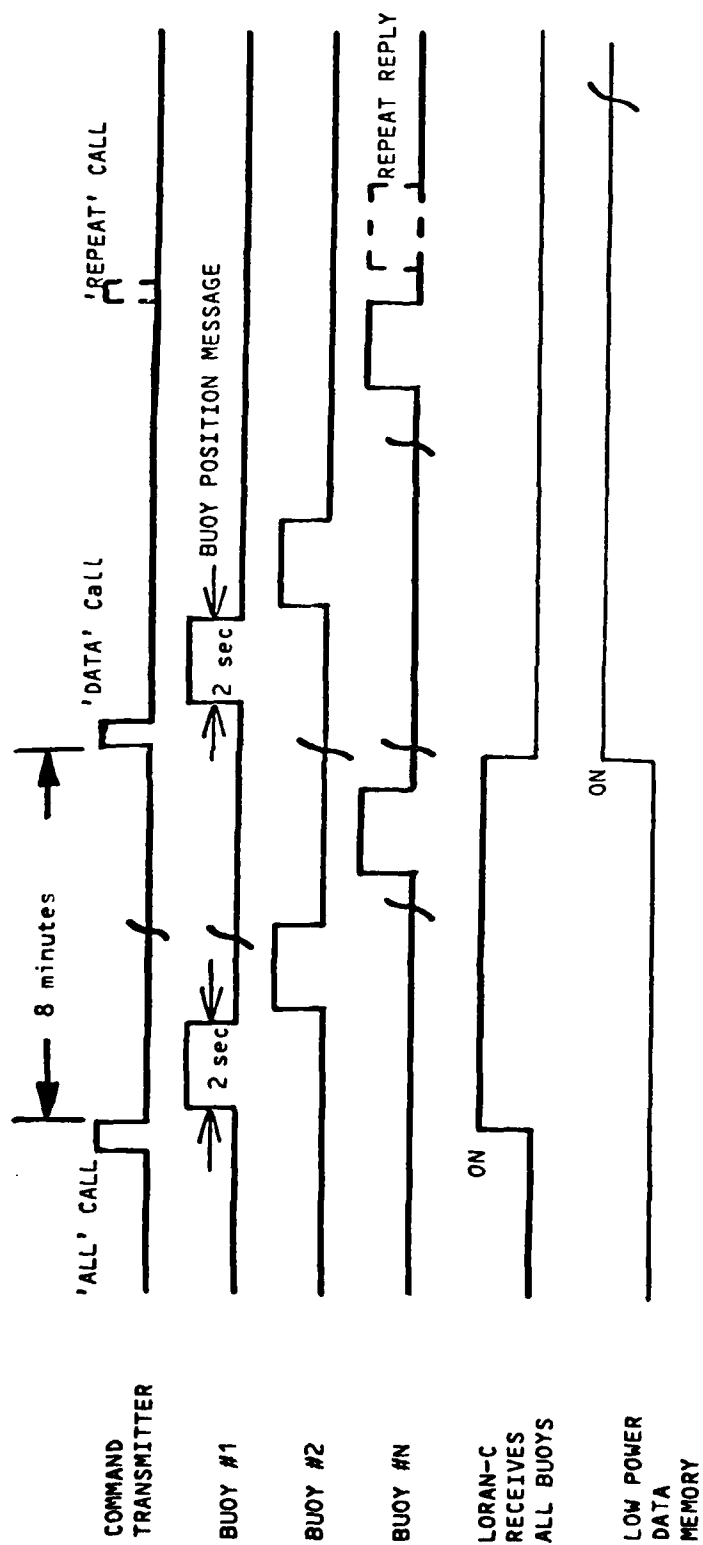
Figure 2.2-2   A Typical TD Transmission Operating Cycle

Immediately following the ALL call, it is possible, and perhaps desirable, to have each buoy acknowledge the receipt of the ALL call. This is accomplished sequentially, with each buoy allowed a 2-second transmission window.* The ALL call acknowledgement could be used to identify buoys out of radio range at the time of data call and to advise the base station electronics to issue an additional call at a more advantageous position.

Following acknowledgement, which takes approximately 2 minutes for 60 buoys, all buoys maintain radio silence. When buoy data are available, one of two schemes could be followed:

1. The buoys could be programmed to sequentially transmit data starting 8 minutes after the ALL call. This transmission sequence would be similar to the acknowledgement sequence and would require 2 minutes for 60 buoys.

2. The base station issues a DATA call to all or selected buoys, causing each buoy to respond with the Loran-C data stored in its low power memory. Because the data can be stored at negligible power consumption, this memory could be kept alive for an extended period of time (e.g. 1 hour, or perhaps until a daylight sensor causes the entire buoy electronics to be powered down). This scheme would permit a helicopter to issue an ALL call during the initial portion of a Search and Rescue (SAR) flight and to acquire data on return. Note also with this system that a relatively simple polling scheme could be implemented in the base station to acquire data from all buoys which answered the original acknowledge, and further to continuously try to activate buoys which did not receive the initial ALL call.

---

*The responses from the buoys could be staggered by using the last digits of the buoy identification number as the appropriate buoy transmission time delay.

A buoy power budget for a TD Transmission scheme employing the operating cycle depicted in Figure 2.2-2 is shown in Table 2.2-3. The power consumptions listed for the command receiver, the Loran-C receiver and the transmitter are taken from devices presently available or under development. The major power consumer on the buoy is the command receiver. Although its current consumption is quite low, 15 mA, it is operated continuously. One obvious technique of reducing power consumption from the command receiver is to employ a daylight photo switch. This will reduce the power by approximately 50% averaged over the year. Other schemes could employ micropower clocking schemes which would only enable the command receiver during specific periods of the day. The Loran-C receiver requires the largest amount of operational power, 10 Watts, however its relatively short duty cycle of 8 minutes keeps its total contribution to the power budget low. The power requirements for the control logic and the transmitter are negligible. The control logic power is minimized through the use of CMOS logic, while the transmitter power requirement reflects its very low transmission duty cycle. Average ampere-hours/day numbers are presented for both a 1 read-cycle/day and a 1 read-cycle/week situation. In addition, these numbers are computed assuming both the use of a plot switch and a continuous operating receiver. The worst case power consumption is .5 ampere-hours/day for daily readings; and the minimum, with photo switch and 1 read-cycle/week is .225 ampere hours/day average.

2.2.2 **TD Transmission Base Station**

The functions required of the TD Transmission base station are:

o   The generation and transmission of audit control signals

o   The reception and demodulation of buoy data

o   The recording of data for reduction to position.

A block diagram of the TD Transmission base station electronics is shown in Figure 2.2-3. The audit control electronics generate audit signals. The process starts with the issue of a CALL to an individual buoy or an ALL call to the field of buoys. This digital message is transmitted to the buoys by the transmitter. Data from the buoys are received by a narrow band VHF FM receiver.

	AMPERE-HOURS	WITH PHOTO-SWITCH
(1) COMMAND RECEIVER .015 Amps (12 V)	.36	.18
(Power Requirement reduced ≈50% with photo switch)		
(2) CMOS CONTROL LOGIC (1 mA)	.03	.03
(3) LORAN-C RECEIVER 10 W, 12 V, 8 min	.11	.11
(4) TRANSMITTER 1 Watt output power	< .01	<.01
35% effeciency; 2.9 Watts, 12 V, 4 sec.		
POWER REQUIRED AT ONE READ CYCLE/DAY...............	.51 A-H/Day	.33
POWER REQUIRED AT ONE READ CYCLE/WEEK...............	0.41 A-H/Day	0.23

Table 2.2-3   TD Transmission Buoy Power Budget
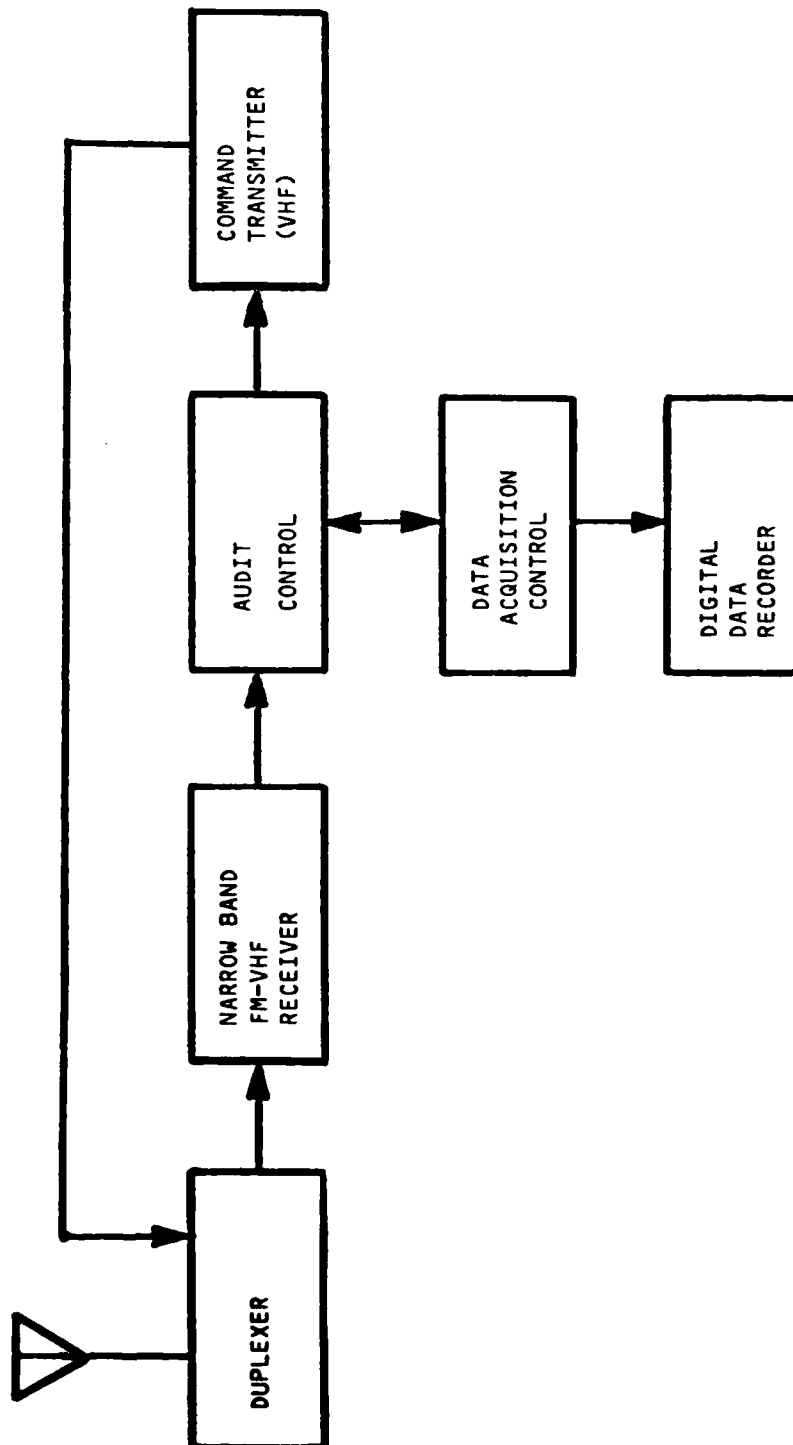
Figure 2.2-3   TD Transmission – Base Station Electronics

The demodulated data from the buoys are processed by the audit control electronics; position data is then recorded under the control of data acquisition electronics. A common antenna is used for both transmission to and data reception from the buoys. As described under the discussion of the typical operating cycle, the audit control electronics can be extremely simple (i.e. control the transmission of a single ALL call and then record the receipt of data which is returned from the buoys) or more complex (i.e. it can monitor which buoys have acknowledged the call, compare this to the buoys from which position data has been received, and use this information to continue to try to audit buoys which have not responded.). Further, the reception of known bad data (e.g. bad parity) could be used to issue a second data call to the buoy until the message was received correctly. A burst data message system possessing similar capabilities is presently being marketed by Aerotron Corporation of North Carolina, for use in low-cost taxicab radio systems.

2.2.3 TD Transmission Cost Estimates

The cost for the various elements of the TD Transmission system are tabulated in Table 2.2-4. The pricing assumes a single lot purchase of 1,000 buoy systems and 10 base stations.

The major cost item in the buoy is the Loran-C monitor receiver. The cost is estimated at $700 to $1,000. It is interesting to note that the uncertainty in the cost of the monitor receiver is very nearly equal to the estimated cost for the remaining buoy electronic components. Presently, Loran-C receivers are available through normal marine dealers at prices as low as $1,700. It is these dealer prices, combined with the 1,000-piece quantity and OEM procurement terms which led to the $1,000 estimate. The $700 range on the estimate was derived by examining various receivers and assigning a dollar value to the difficulty of constructing an equivalent amount of electronics. One item which does not explicitly appear on the table could have a significant cost impact on the electronics. This item is packaging. In developing the proposed prices and system integration/testing costs, it was assumed that the electronics would be packaged internal to the buoy in a compartment which is weatherproof and waterproof.

The base station electronics pricing has assumed the availability of a suitable VHF receiver, transmitters and data recorders. The use of VHF telemetry

BUOY ELECTRONICS (1000-pc Lot)

ANTENNA, COUPLER, DUPLEXER	$ 40
LORAN-C MONITOR RECEIVER	$ 700 - $1,000
COMMAND RECEIVER	$ 70
POWER CONTROLLER	$ 10
TRANSMITTER	$ 90
SYSTEM INTEGRATION & TESTING	$ 150
TOTAL ESTIMATED COSTING......$1,060 - $1,360	

BASE STATION (10-pc Lot)

VHF RECEIVER/DEMODULATOR	$2,000
DATA RECORDER	$1,000
COMMAND TRANSMITTER	$1,000
AUDIT & DATA ACQUISITION CONTROL UNIT	$2,000
SYSTEM INTEGRATION & TESTING	$1,000
TOTAL ESTIMATED COSTING......$7,000	

*Assumes Specification and Initial Development during Experimental Phases.

Does not include non-recurring post-experiment costs.

Does not include system documentation beyond that provided with standard commercial equipment.

Table 2.2-4   TD Transmission Estimated Costing*

equipment separate and apart from the VHF radios presently installed in the helicopter was proposed to minimize integration costs and to maintain a 'roll-on roll-off' disposition for the base station equipment, allowing it to be quickly installed in a helicopter which has a suitable antenna system. As the VHF communication equipment represents about 40% of the estimated base station equipment cost, the use of the on-board communications equipment should be explored prior to system procurement. The audit and data acquisition control unit is assumed to be custom built for the base station.

Both the buoy and base station cost estimates assume that detailed equipment specifications and initial development costs have been borne during the experimental phases and, where necessary, in a post-experimental development program. Further, the cost of the system documentation beyond that typical of the manuals provided with standard commercial equipment has not been included.

2.3 ANALOG PULSE RETRANSMISSION

2.3.1 Pulse Retransmission Concept

Analog pulse retransmission schemes process the received Loran-C pulses and noise to a point where the processed signal is suitable for transmission to the base station in analog fashion. Typically, such systems maintain the 100 kHz carrier frequency of the Loran-C pulses and therefore require bandwidths of about 1 MHz for FM telemetry retransmission of the analog signal.* The major consideration for the Pulse Retransmission buoy electronics are:

---

*Single sideband techniques are rejected based on the need to maintain a highly stable (short term stability) local oscillator and the transmission of noise-free pilot tone to assure accurate reconstruction of the pulse frequency and phase. AM techniques, which could reduce the bandwidth required down to approximately 300 kHz, present a problem in that RF signal detection by the input Loran-C processing electronics can cause instability of the entire package and further, AM lacks the required dynamic range.

o   Preservation of the pulse envelope fidelity to assure accurate cycle selection at the base station

o   Preservation of Loran-C pulse fidelity at the tracking point to assure position accuracy

o   The. need to provide a telemetry signal-to-noise ratio which does not degrade the overall quality of the Loran-C signal

o   The requirement to preprocess the Loran-C signal to assure that the dynamic range of the signal does not exceed the capability of the telemetry link.

A block diagram of the Pulse Retransmission buoy electronics is shown in Figure 2.3-1. As in the case of the TD Transmission electronics, a common antenna is used for both telemetry transmission and reception as well as Loran-C signal reception.

The Loran-C signals are processed by a Loran-C analog pulse amplifier/processor. Several variations of this amplifier/processor have been considered and are discussed in Section 2.3.2. For the present, it is only necessary to assume that the processor prepares the signals for transmission back to the base station in such a manner that they may be processed at the base station to obtain the required time difference information. The output of the amplifier/processor and data encoder are directed by a wideband telemetry transmitter. Due to the fidelity with which the pulse information is to be retransmitted, a 1 MHz bandwidth has been assumed for the modulated signal.* A transmitter power of 5 Watts has been selected for the purposes of this analysis.

---

*While slightly narrower bandwidths may be possible, they are not felt to alter substantially the proposed system design presented.
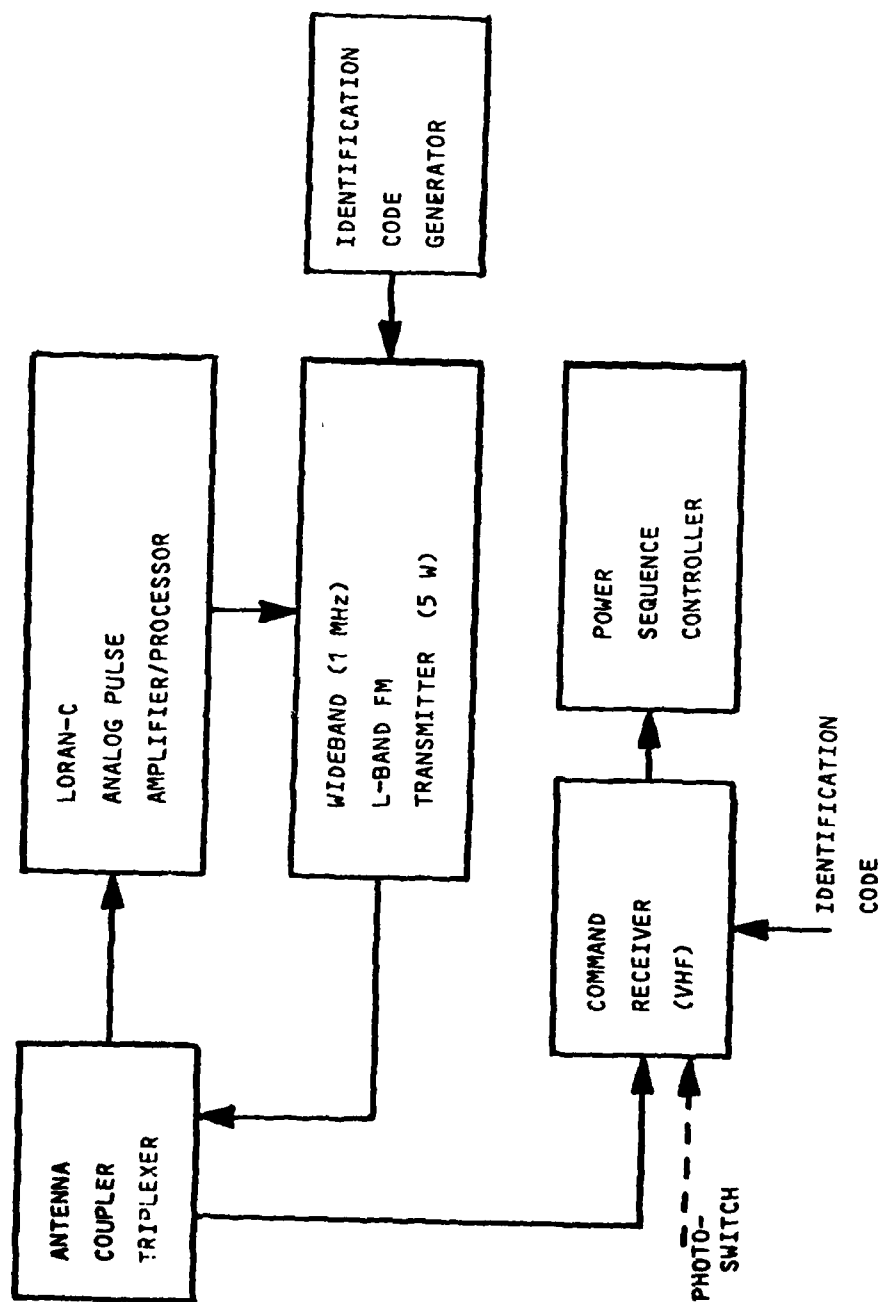
Figure 2.3-1 Block Diagram – Pulse Retransmission Buoy Electronics

The operation of the buoy electronics is controlled by a VHF command receiver. A system command simply turns the buoy on and for selected pulse processing techniques, selects a processing mode. Note that because the Pulse Retransmission approach does not reduce the data to storable time difference, sequencing of the power, first to the Loran-C amplifier/processor and then to the transmitter, is not possible.

Table 2.3-1 shows the telemetry budget for the Pulse Retransmission system. A telemetry frequency of 1500 MHz has been assumed consistent with the desire to obtain authorization for a 1 MHz bandwidth. Despite the increase in transmitter power from 1 Watt to 5 Watts, the IF signal-to-noise ratio is only 12 dB compared to 31 dB for the TD Transmission system. This reduction is attributable to the increased path loss at 1500 MHz and the increased noise due to the 1 MHz IF bandwidth. The 12 dB IF signal to noise ratio yields an anticipated dynamic range of 32 dB from the point at which a pulse will be contaminated by -10 dB of telemetry noise to a signal level which provides the maximum telemetry carrier frequency deviation. The anticipated 32 dB dynamic range is 32 dB less than the 64 dB range required to transmit the anticipated Loran-C signals. This implies that it is not possible to simply amplify the received Loran-C pulses and use them to modulate the transmitter directly and therefore further pulse processing is required.

At this point the reader can assess the reasonableness of the 5 Watt power level selected. First, 5 Watts is a convenient power level to produce with combinations of power transistor devices available in this frequency range. Secondly, to increase the projected dynamic range by 10 dB would require a 10 dB increase in transmitter power, or a transmitter output of 50 Watts. Assuming that the transmitter efficiency stays relatively constant as the power is increased, this 10-fold increase in power would require increases in the prime power well beyond the 1 ampere-hour/day specified, and the cost of such a transmitter would be an order of magnitude more than a 5 Watt unit.

SIGNAL

TRANSMITTER POWER (5 Watts)	+37 dBm
BUOY ANTENNA GAIN (net with duplexer)	2 dB
FREE SPACE PATH ATTENUATION	
40 km – 1500 MHz	-129 dB
MULTIPATH FADING MARGIN*	- 10 dB
RECEIVER ANTENNA GAIN	3 dB
TOTAL SIGNAL.............	-97 dBm

IF NOISE

THERMAL NOISE (1 Hz)	-174 dBm
BANDWIDTH FACTOR (1 Hz)	+60 dB
MANMADE NOISE	0 dB
RECEIVER NOISE FIGURE & ANTENNA TEMPERATURE	5 dB
TOTAL NOISE.............	-109 dBm

IF SIGNAL-TO-NOISE RATIO.......... 12 dB

*An accurate assessment of this number is beyond the scope of this report.

Table 2.3-1   Pulse Retransmission – Assumed Telemetry Budget at 1500 MHz

POST-DEMODULATION SNR

INPUT SNR (1 MHz BW)   12 dB

FM IMPROVEMENT   24 dB - - - - - - $-3\left[\dfrac{BW}{2\ BW_0}\right]^3$

OUTPUT SNR AT FULL DEVIATION   36 dB

SNR IMPROVEMENT FOR
85-115 kHz FILTER   6 dB - - - - - - - 10 $\log_{10}\left[1-\left(\dfrac{f_i}{f_n}\right)^3\right]$

DESIRED TELEMETRY NOISE
TO LORAN-C SIGNAL RATIO $\underline{-10\ dB}$

DYNAMIC RANGE..................... 32 dB

Table 2.3-1 Pulse Retransmission - Assumed
Telemetry Budget at 1500 MHz (continued)

2-21

2.3.2 Pulse Retransmission Pulse Processing Approaches

Three pulse processing approaches have been considered. These are:

o   Pulse compression using logarithmic functions

o   Stepped gain pulse amplifiers

o   Time multiplexed transmission of direct and derived pulses.

2.3.2.1 Pulse Compression Using Logarithmic Functions

A block diagram of a pulse compressor is shown in Figure 2.3-2. The input Loran-C signal is first preamplified, then directed through an amplifier which has a logarithmic amplitude response. The output of this logarithmic compressor is a signal containing all the information of the original input signal but with a reduced amplitude dynamic range. This signal is used to modulate the telemetry transmitter. In effect, the logarithmic compression can be thought of as a continuously variable gain adjustment performed on the input signal. At the base station, the telemetry signal is first demodulated and then amplitude expanded by an amplifier with an inverse logarithmic characteristic. To be sure that accurate Loran-C cycle identification and tracking can be performed, it is necessary that the compression and decompression of the Loran-C pulses occur without distortion. The major drawback to this type of system is the difficulty of producing an accurately calibrated logarithmic compression function in the buoy. This is not simply a matter of 'tweaking' the buoy compressor to match the expander in the base station, but rather of providing identical compression functions in all buoys so that they can be accurately expanded by a single base station expander. In addition to the accuracy of the compression/expansion process, error is also introduced into a pulse compression scheme by uncalibrated gain errors in the telemetry link. Consider the compressed signal log L(t) . If the link from the compressor output to the expander input has a gain error of 'a', the input to the expander will be:

$$(1 \pm a) \log L(t) = \log L(t)^{(1 \pm a)}$$
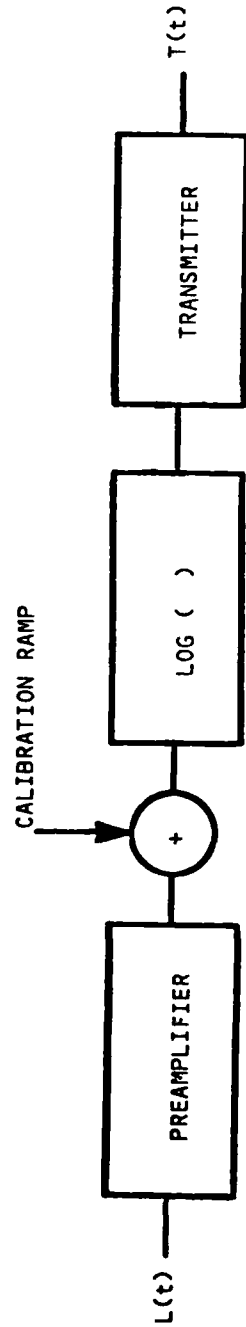
Figure 2.3-2   Pulse Retransmission - Pulse Compression

and the expander output will be:

$$L(t)^{(1 \pm a)}$$

Thus gain error, due to variations in transmitter modulation index or receiver discriminator sensitivities, will produce exponential pulse distortion.

To compensate for some of these errors, it is possible to introduce a calibration ramp as shown in the block diagram. This would provide for the periodic replacement of the Loran-C signal with a 100 kHz pulse of known characteristics at the input to the log amplifier. This pulse would then be processed by the base station to determine the errors existing in the link and the compression/expansion modules.

2.3.2.2 Pulse Retransmission Stepped Gain Amplification

One method for avoiding the calibration problems inherent in the logarithmic compression technique is the stepped gain amplification technique. A block diagram of the stepped gain amplifier is shown in Figure 2.3-3. In this scheme, the Loran-C signal is first preamplified and then passed through a step attenuator prior to amplification by an amplifier which provides linear amplification over a dynamic range compatible with the telemetry link, and which will clip or limit the peaks of signals which exceed that dynamic range. The technique used here is to periodically step or adjust the gain of the attenuator. This assures that the Loran-C pulses of different amplitudes will be amplified linearly by the amplifier for at least one value of attenuation. Notice that small signals will be attenuated below the point of usefulness during periods when high amplitude signals are being properly processed by the attenuator, and further, that during the minimum attenuation steps, large amplitude Loran-C signals will be limited by the amplifier. To process signals which have been step gain amplified, the base station must synchronize to the gain stepping signal in the buoy. For this reason, an output from the gain step control block is shown going into the transmitter.

A drawback to this type of system is that the throughput of the system is reduced by a factor proportional to the number of attenuation steps selected. For example, if four steps are employed, the system designer must assume that any
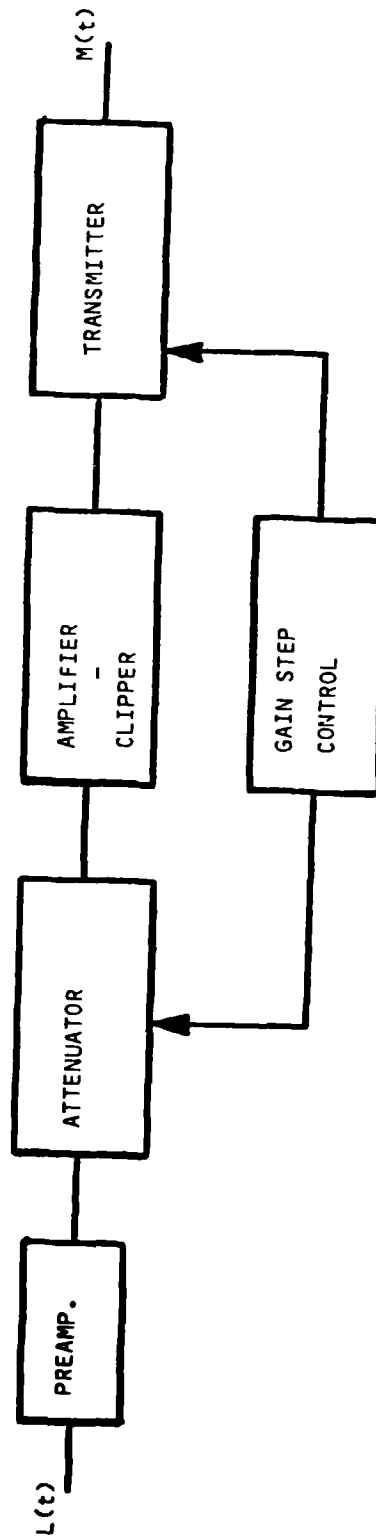
Figure 2.3-3   Pulse Retransmission - Stepped Gain Amplification

given Loran-C pulse will only be properly amplified during one of those steps, thus increasing the time required to do cycle selection by a factor of 4:1. During signal tracking, the effect of the gain attenuation is minimized as it is possible to phase track on a signal which has been limited in the buoy, thus permitting the signal to be tracked for several values of attenuation. It is reasonable to expect, however, that the weaker signals, which require the longest integration time, will only be satisfactorily tracked during the step providing minimum attenuation.

The minimization of hardware error requires that the attenuator provide a constant phase delay at all values of attenuation, as phase variation can introduce time difference error. This is distinctly different from the case in a Loran-C receiver, where propagation delay through the electronics is unimportant because all signals suffer the same delay prior to time difference measurement.

2.3.2.3 Direct and Derived Pulse Retransmission

Figure 2.3-4 is a block diagram of a direct and derived pulse processor. Direct and derived pulse retransmission places an envelope deriver in the analog pulse processor to provide for the retransmission of a derived pulse as well as a direct or simply amplified pulse. The transmission of a derived pulse during the cycle selection period of signal acquisition reduces the requirement to transmit the Loran-C pulse without amplitude distortion as derivation maps the pulse amplitude information into phase space. This permits the derived pulse to be amplified by a limiting amplifier prior to transmission. To provide both a derived pulse for signal acquisition and a direct pulse for signal tracking, a signal selection capability is required, along with a selection scheme. For example, the direct pulse could be transmitted for 1 minute, followed by 5 minutes of derived pulse transmission which was again followed by 2 minutes of direct pulse transmission. This would allow the base station electronics to first orient itself on the direct pulse then perform cycle selection on the derived pulse, and finally to perform tracking on the direct transmitted pulse. Alternately, the command receiver could be used to control the selection process. In either case, base station algorithms which required the presence of only the direct or derived pulse at any specified time would be necessary.

2-26
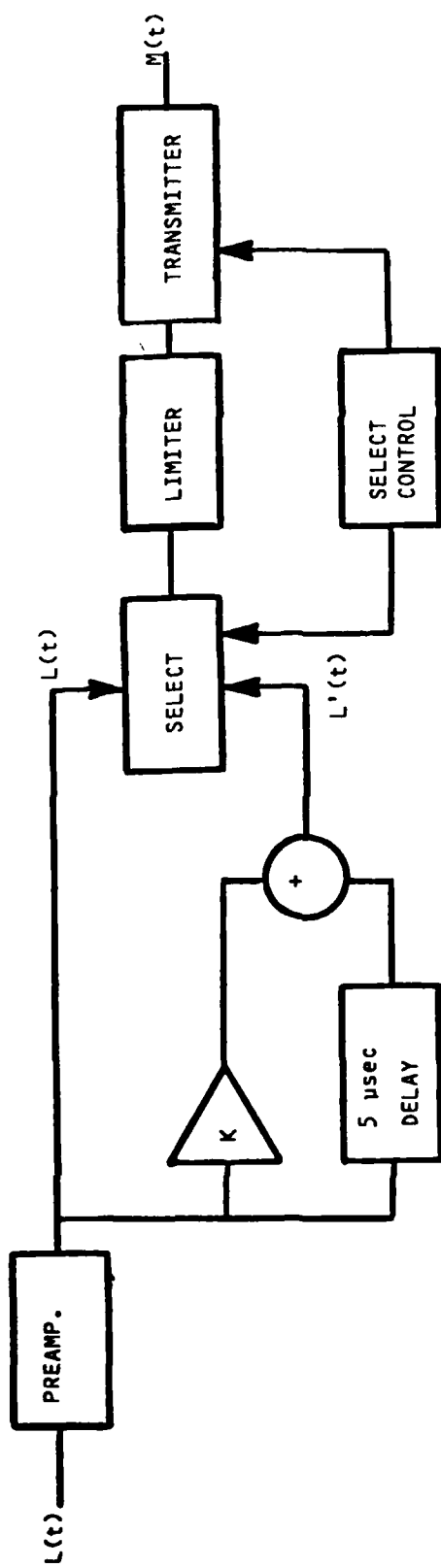
Figure 2.3-4   Pulse Retransmission - Direct and Derived

2.3.3 Pulse Retransmission Cycle and Power Budget

A major disadvantage of analog pulse retransmission is the necessity to continuously transmit the processed Loran-C pulses from the buoy to the base station during the period of time required to acquire and obtain a settled track. This means that the buoys must be audited in sequence and that the base station (e.g. helicopter) must remain within the design telemetry range for the entire audit. The time required to acquire and track the signal is dependent upon the pulse processing selected. In particular, the gain stepping procedure will cause an increase in the tracking and acquisition settling time of somewhere between 2:1 and 4:1 over the times required by either pulse compression or transmission of direct and derived signal. For simplicity, the following discussion assumes continuous availability of usable Loran-C signals (i.e. the use of pulse compression or direct/derived signal retransmission).

The assumed operation cycle is shown in Figure 2.3-5. First, buoy 1 is audited, causing the Loran-C processor and transmitter on buoy 1 to turn on for a period of 6-10 minutes. During this time, the signals are continuously transmitted to the base station, where they are processed to obtain time difference data.* Following the acquisition of data from buoy 1, it is commanded OFF and buoy 2 is commanded ON. Using this technique, an audit capability of 6-10 buoys/hour is possible. The actual time necessary for Loran-C signal acquisition could possibly be less than the time necessarry for a conventional Loran-C receiver, assuming that the Loran-C received directly at the base station could be used to aid in the acquistion of the remote signal.

A power budget for the Pulse Retransmission system is shown in Table 2.3-2. Here again, the command receiver uses a considerable portion of the entire power required, however we now see the effect of requiring the transmitter and the pulse

----

*It is not possible to simultaneously audit other buoys unless complete parallel systems, including alternate telemetry frequencies, telemetry receivers and base station special purpose Loran-C processors are available.
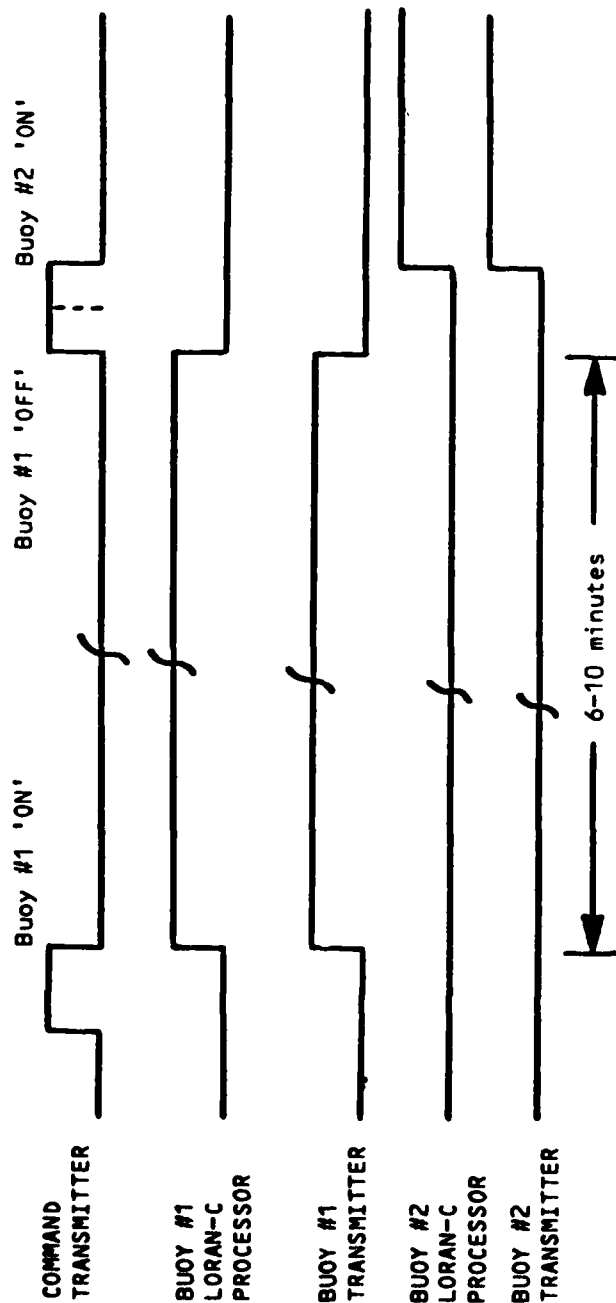
Figure 2.3-5   Pulse Retransmission - Typical Operating Cycle

	AMPERE-HOURS/DAY	WITH PHOTO-SWITCH
(1) COMMAND RECEIVER .015 Amps (12 V) (power requirement reduced ≈50% with photoswitch)	.36	.18
(2) CMOS CONTROL LOGIC (1 mA)	.03	.03
(3) PULSE PROCESSOR 3 Watts @12V, 10 min	.04	.04
(4) TRANSMITTER 5 Watts output power 20% effeciency, 25 Watts @12V, 10 min	.35	.35
POWER REQUIRED ASSUMING ONE READ CYCLE/DAY............... 0.78 A-H/Day		0.60
POWER REQUIRED ASSUMING ONE READ CYCLE/WEEK............... 0.45 A-H/Day		0.27

Table 2.3-2   Pulse Retransmission - Buoy Power Budget

processor to remain on for the duration of the audit period. The transmitter also draws additional power due to the decreased efficiency of transmitters operating at 1500 MHz. In all cases, both 1 read-cycle/day and 1 read-cycle/week, either with or without a command receiver photo-switch, the power is below the required maximum of 1 ampere-hour/day, with the numbers generally running higher than the equivalent cases for the TD Transmission electronics.

2.3.4 Pulse Retransmission Base Station

The Pulse Retransmission base station is much more complicated than the TD Transmission base station. This is due to the requirement for a special purpose Loran-C processor and the desirability of aiding that processor with local Loran-C signals. Both base stations provide the necessary functions of generating and transmitting audit control signals as well as recording the Loran-C time difference data for reduction to buoy position. In addition to these functions, the Pulse Retransmission base station must acquire, perform cycle selection and track the analog pulses transmitted from the buoy. It is also necessary that the special purpose Loran-C processor be capable of monitoring and editing out telemetry fades to prevent false acquistion and/or poor data due to the presence of temporarily noisy conditions. Further, the processor must compensate for helicopter flight dynamics.* A block diagram of the base station is shown in Figure 2.3-6. Here again a common antenna is proposed for the command transmitter, buoy telemetry receiver and base station Loran-C reception. The practicality of using a single antenna for this application on a helicopter will have to be explored further; however, the desirability of only a single antenna is recognized. The buoy telemetry signal is received by an L-band receiver and the output directed to both the audit control electronics for determination of buoy identification and the special purpose Loran-C processor. The output of this special purpose processor is

---

*The velocity of the helicopter is impressed on both the locally received Loran-C signals (due to helicopter-to-Loran-C station Doppler) and on the buoy signals (due to Doppler imposed on the helicopter-to-buoy telemetry path).
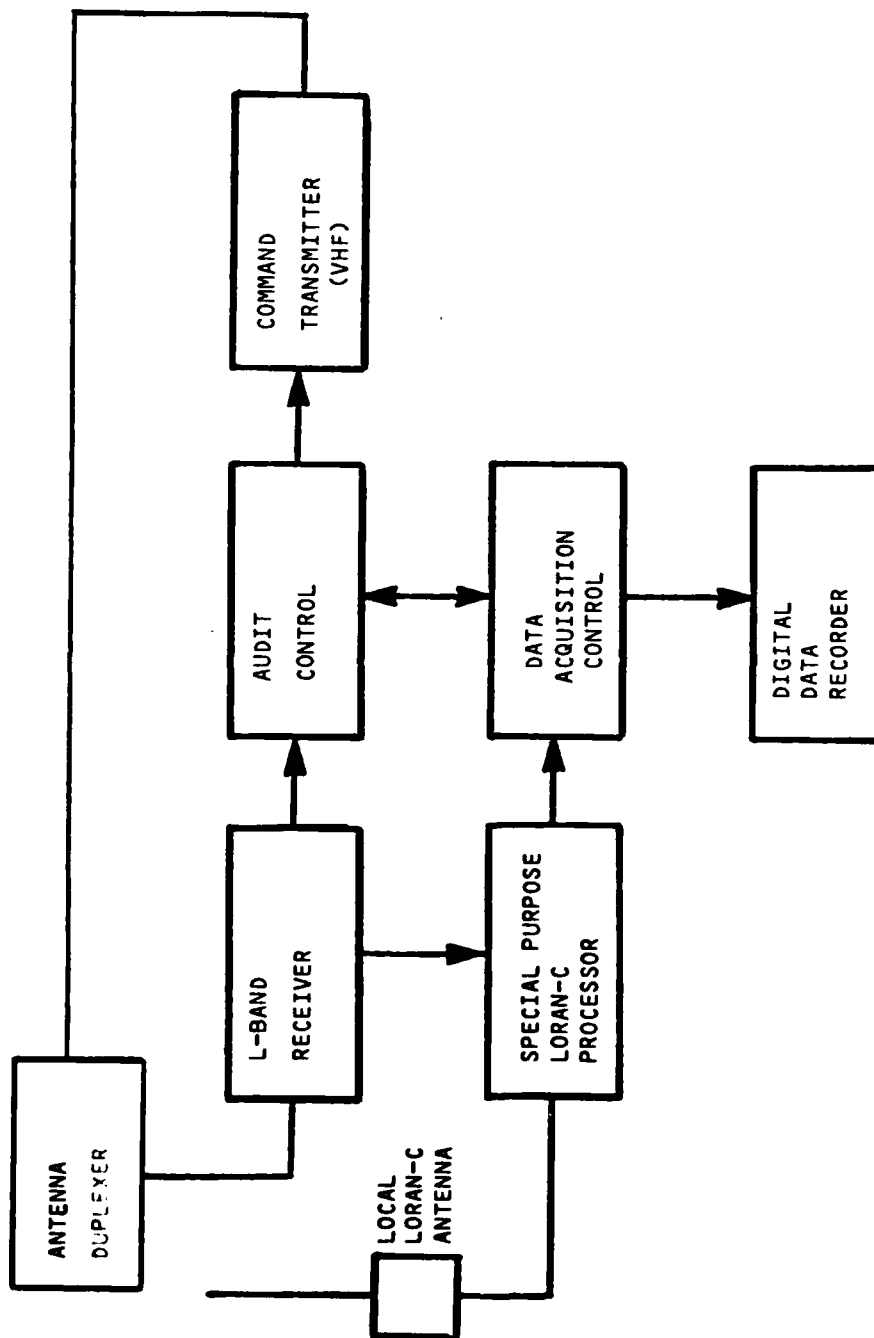
Figure 2.3-6   Pulse Retransmission – Base Station Electronics

Loran-C time difference data, which is recorded on a digital data recorder for reduction to position. The audit control electronics keep track of the time for which a given buoy has been audited and controls the command transmitter which can selectively turn on and off the various buoys being audited.

2.3.5 Estimated Cost of Pulse Retransmission System

Two buoy electronic configurations have been estimated, a pulse-only scheme, assuming a pulse compressor, and a unit which retransmits both the direct and derived pulse. The major expense for both systems is the transmitter. This high cost is due to the necessity of providing the 5 Watt crystal-controlled transmitter at 1500 MHz. The reduction in transmitter price for the direct/derived pulse retransmitter is attibuted to a decrease in the required telemetry link dynamic range. All other items are assumed to be equal, except for the command receiver, where a small additional expense has been allowed to permit the base station to command switching between the direct and derived pulse (Table 2.3-3). These costs are based on a 1000-piece single lot purchase of the buoy electronics and the procurement of 10 base stations.

The base station estimates reflect the increased cost anticipated for a wideband L-band receiver, however this is overshadowed by the cost estimate for the special purpose Loran-C processor. Involved in this cost estimate are:

o   The special nature of the unit (i.e. the design would most likely not find application in other types of systems)

o   The device must be capable of airborne operation and be capable of processing both local and buoy Loran-C signals.

2.4 VARIABLE GEOMETRY TECHNIQUES

Buoy location can also be determined by ranging techniques. The measurement of range or distance from a buoy to a known location establishes the buoy on a fixed line of position which is a circle centered on the known location.

2-33

BUOY ELECTRONICS (1000-pc Lot)

ITEM	RETRANSMITTER TYPE	
	PULSE ONLY	PULSE & DERIVED PULSE
ANTENNA, COUPLER, DUPLEXER	$ 60	$ 60
PULSE PROCESSOR	$ 350	$ 350
COMMAND RECEIVER	$ 80	$ 90
POWER CONTROLLER	$ 10	$ 10
TRANSMITTER	$1,100	$ 880
SYSTEM INTEGRATION & TESTING	$ 150	$ 150

TOTAL COST ESTIMATE...... $1,750 ....$1,540

BASE STATION (10-pc Lot)

L-BAND RECEIVER	$ 5,000
SPECIAL PURPOSE LORAN-C PROCESSOR*	$50,000
DATA RECORDER	$ 1,000
COMMAND TRANSMITTER	$ 1,000
DATA ACQUISITION CONTROL UNIT*	$ 2,000
SYSTEM INTEGRATION & TESTING	$ 4,000

TOTAL COST ESTIMATE......$63,000

*Assumes specification and initial development during experimental phase.
Does not include non-recurring post-experiment costs.
Does not include system documentation beyond that provided with standard commercial equipment.

Table 2.3-3   Pulse Retransmission - Estimated Costing*

Several such measurements from different locations can then fix the buoy position. In principle, a field of buoys about a harbor could be monitored in this way from a network of shore stations. However, in practice multiple sites over a large area will be required to optimize the geometry; such a network will be large, complex and require substantial amounts of real estate.

An alternative technique is to make the range measurements from a moving platform such as a helicopter. The motion of the helicopter generates multiple position lines from a series of range measurements; this is known as a "variable geometry" system. In order to locate the helicopter precisely, differential Loran-C measurements are obtained by making Loran-C TD measurements aboard the helicopter and comparing them, post facto, with those made by a network of pattern monitors. In addition the accuracy of the knowledge of the helicopter's position as derived from the differential Loran-C, can be improved by use of the over-determined solution of buoy position which results from multiple range measurements to multiple buoys. This technique is incorporated into the variable geometry measurements described in this report.

2.4.1 Range Measurement Techniques

Two basically different range measurement techniques are under consideration. They are:

1. Pulse Ranging - In this technique the helicopter emits a stream of pulses of RF energy. These are received by the buoy, and retransmitted to the helicopter. The helicopter receives the return pulse and measures the elapsed time between pulse transmission and pulse reception. An onboard computer multiplies this measurement by the speed of light to calculate the round-trip range.

2. CW Ranging - This technique uses a continuous RF carrier rather than a stream of pulses. The carrier is modulated by a suitable waveform; the helicopter measures the round trip phase shift of this wave form and thus determines the round trip time delay. Since this system allows for both low average and low peak power requirements on the buoy, it can also be used in a one-way range-measurement where the ranging signal

originates on the buoy. In this case, successive measurements are differenced, or subtracted from one another, so as to eliminate a requirement for precise absolute time on the buoy. This results in hyperbolic lines of position.

2.4.2 Pulse Ranging

The conventional pulse ranging system contains a transmitter which emits a series of pulses of RF energy from a helicopter under the control of an internal timing subsystem. The pulses are transponded by the buoy and returned to the helicopter where they are detected by a receiver; range is measured by determining the time interval between the transmitted pulse and the received pulse.

The pulse ranging systems evaluated in this report are commercially available units, or modifications of such units, that were originally designed for precision electronic surveying. In general, the available ranging systems are more sophisticated than required for the BPAS application. The manufacturers of the Trisponder (Del Norte Technology, Inc.) and Mini-Ranger (Motorola) systems were contacted to determine the feasibility of designing a simplified microwave ranging system for application to the Variable Geometry BPAS configuration (correspondence in Appendix D). Del Norte Technology has not expressed an interest in such an endeavor. Motorola has indicated that a system could be designed which uses a modified version of the Mini-Ranger equipment (Appendix D).

The power requirements of the buoy transponder depend on the buoy interrogation schedule. The desired schedule, from the viewpoint of buoy position-fix accuracy, is to command all transponders to "turn on" when first entering the field of buoys and then to range on every buoy at points scattered (equally in time) over the entire round-trip flight path. Each buoy transponder is triggered by a different identification code which is included in the microwave signal. This interrogation schedule results in enough data being collected to guarantee acceptable geometry for the buoy position calculation (Section 3.4 and Appendix C). However, the transponder is active over the entire helicopter flight, causing a potential buoy battery drain of 18 amp-hr per audit (based on a 6 amp current and a 3 hr flight; see specifications for Mini-Ranger transponder in Ref. 29). Adding 6

amp-hr per audit for the command receiver* yields a total drain of 24 amp-hr. The battery drain can be reduced by transponder innovations and/or a different interrogation schedule. For example, data could be collected for only a few segments of the flight pattern and the transponders deactivated between segments.

2.4.3 CW Ranging

The primary difference between CW Ranging and Pulse Ranging lies in the ratio of peak to average RF power. In a CW Ranging system, the peak RF power is equal to the average power; a Pulse Ranging system typically has peak/average ratios of 1000 or greater. A Pulse Ranging system operates by detection of the time of arrival of the leading edge of the pulse. CW Ranging on the other hand, impresses a distinctive wave form on the carrier by phase or frequency modulation. Two wave forms have been investigated in this report. They are pseudo-random codes (PRN Codes), and an ensemble of CW tones known as Stiffler codes (Refs. 35 and 36).

2.4.3.1 PRN Codes

Pseudo-Random Noise (PRN) codes belong to a family of two-level or binary codes. These codes, while completely deterministic, possess certain unique properties which cause them to be extremely recognizable when perturbed or masked by noise. The most important of these is the autocorrelation function. The autocorrelation function of a signal represents its "signature" in time, i.e. the mark, or determining factor, which when comparing two signals tells whether the two are identical or different. Ideally, an autocorrelation function--that is, the correlation function between a received signal, and a synthesized replica of the transmitted signal would have a uniform low value when the two differ, and a single sharp peak when the two are identical. In particular, binary correlation is defined as follows:

---

*Assuming a command receiver drain of .36 amp-hr/day for seven days.

$$\text{Correlation} = \frac{\text{number of agreements} - \text{number of disagreements}}{\text{number of agreements} + \text{number of disagreements}}$$

This means that when two binary signals are compared on a bit by bit basis, their levels will either agree, or disagree, and the correlation represents the relative level of agreement. Stated mathematically,

$$C = \frac{A - D}{A + D}$$

where: C = correlation factor

A = number of agreements

D = number of disagreements

If two pseudo-random sequences, identical except for a time difference (or bit shift) are compared according to the rule that a one is generated whenever a bit of the original and a bit of the shifted sequence are different (exclusive- or, or mod - 2 addition, signified by $\oplus$), the result will always be the same code. (Ref. 37 for a complete example). Since a pseudo-random sequence always has a distribution of 1's and 0's such that there is one more 1 than 0, such a correlation will be:

$$C = 1/N$$

where N = number of bits in the sequence.

On the other hand, when the codes agree, the correlation will be:

$$C = N/N = 1.$$

Therefore the autocorrelation function of a pseudo-random sequence (for reasonably long codes) is essentially zero when the code is not matched and unity when the code is matched.

The "acquisition" of such a code sequence is defined as the process of comparing a received sequence with a locally generated replica and shifting the local reference one bit at a time until the two are determined to be in

synchronism. Obviously to acquire a sequence it is necessary to observe and compare all possible states, or bit positions, for positive identification. A sequence of length P, may require P trials, or correlations, before acquisition is complete. After acquisition, range is determined by measurement of the time shift between transmitted and received codes.

The performance of a typical design is analyzed in Appendix I.

2.4.3.2 Stiffler Codes

A promising waveform for the BPAS application is presented and analyzed in Ref. 36. This waveform can be viewed as a form of tone ranging, which determines range by measurement of the phase shift of a composite set of tones (sine-waves) modulated on an RF carrier (Refs. 35, 38 & 39). The tones are coherent in phase and commensurate in frequency; this is usually achieved by digital division from a common master oscillator. The specific implementation under consideration uses square waves which are submultiples of two from a highest frequency tone of 100 KHz. The implementation details and performance calculations are contained in Appendix I.

It is apparent from the calculations in Appendices H and I that CW ranging systems are strong contenders, in that the measurement standard deviation due to random noise is substantially less than 10 meters rms. The attainment of such a high level of precision is, in practise, extremely difficult due to instrumental biases in the measurement process. However, these are areas under the control of the designer. Careful design will ensure correct system performance.

2.4.4 One-Way Ranging

All Variable Geometry systems considered so far have been two-way techniques; that is, the ranging signal emanates from the same station that makes the final measurement - the buoy merely transponds the ranging signal. In so doing, however, a substantial uncertainty is inserted into the measurement process - not only does the buoy transponder become a major source of noise error, but bias errors due to phase delay changes in the transponder (due to temperature and component drift) also increase the total error. These errors are primarily in the

receiver, because of the amplification and filtering requirements. Conceptually, however, the variable geometry measurement need be only one-way; i.e., the ranging signal could originate at the buoy itself. A typical one-way system is now analyzed.

The flight pattern is shown in Figure 2.4-1. At time T_1, the buoy transmits a pulse. Clock error on the buoy causes the actual transmission time to be:
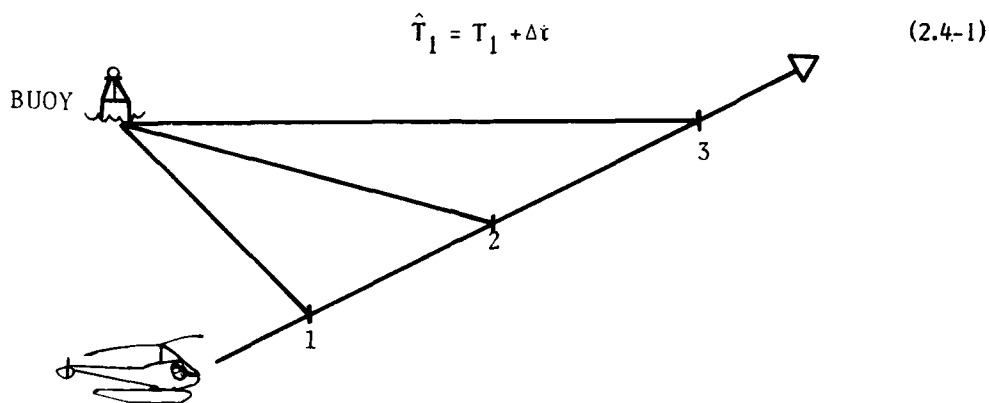
$$\hat{T}_1 = T_1 + \Delta t \qquad (2.4\text{-}1)$$

Figure 2.4-1   Typical Flight Pattern

Δt = accumulated time error (due to oscillator drift) since the clock was last set.

Now the helicopter receives this signal at Position 1, and time T_1'.

$$T_1' = T_1 + \Delta t + \alpha \qquad (2,4\text{-}2)$$

α = Time delay due to distance from buoy to helicopter.

Similarly, the helicopter receives Pulses T_2 and T_3 at positions 2 and 3, resulting in:

$$T_2' = T_2 + \Delta t + \beta \qquad (2.4\text{-}3)$$

$$T_3' = T_3 + \Delta t + \gamma \qquad (2.4\text{-}4)$$

β & γ represent the time delay to positions 2 and 3.

Now form time differences $T_1' - T_2'$ and $T_1' - T_3'$

$$(2.4-2) - (2.4-3) = T_1' - T_2' = (T_1 + \alpha) - (T_2 + \beta) \qquad (2.4-5)$$

$$\text{and } T_1' - T_3' = (T_1 + \alpha) - (T_3 + \gamma) \qquad (2.4-6)$$

Here the assumption is that the timing error Δt is (to a first approximation) common to all three measurements, i.e., the oscillator does not change frequency (drift) during the time period which contains all three measurements. These measurements then locate the buoy on a line of position defined by a hyperbola whose foci are at positions 1 and 2. Position 3 then defines a second hyperbola whose intersection with the first one determines the buoy's position.

a. Oscillator Stability Requirements

The ranging signal is set in time by a clock, whose time stability is determined by a highly stable oscillator. See Figure 2.4-2 below, for a typical design.
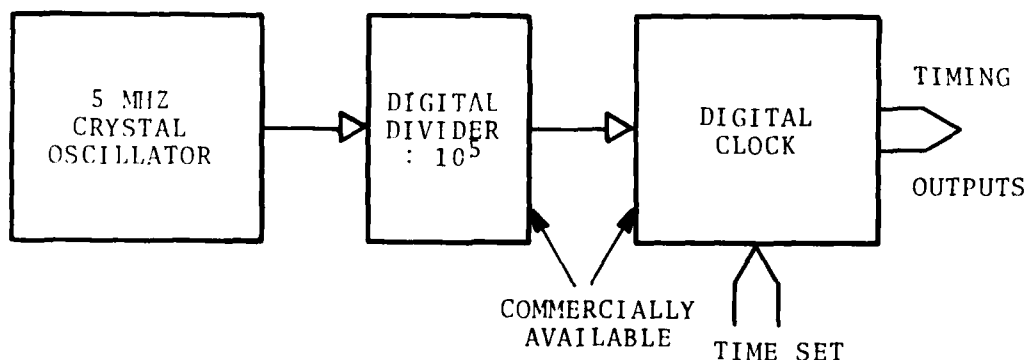
Figure 2.4-2   Typical Digital Clock

If the oscillator drift results in a timing error change of 5 nanoseconds over the course of one buoy position measurement, this will add 5 feet of error to the buoy position (not including GDOP). This timing error analysis applies during the time interval required to do a buoy position fix. Typically, the helicopter will fly at 80 - 120 knots, which is 1.3 - 2.0 miles per minute of flight time. If the buoy is 10 - 20 miles to one side of the flight path, 5 minutes will result in 7 - 10 miles of

flight which will optimize the flight geometry, as in Figure 2.4-3.
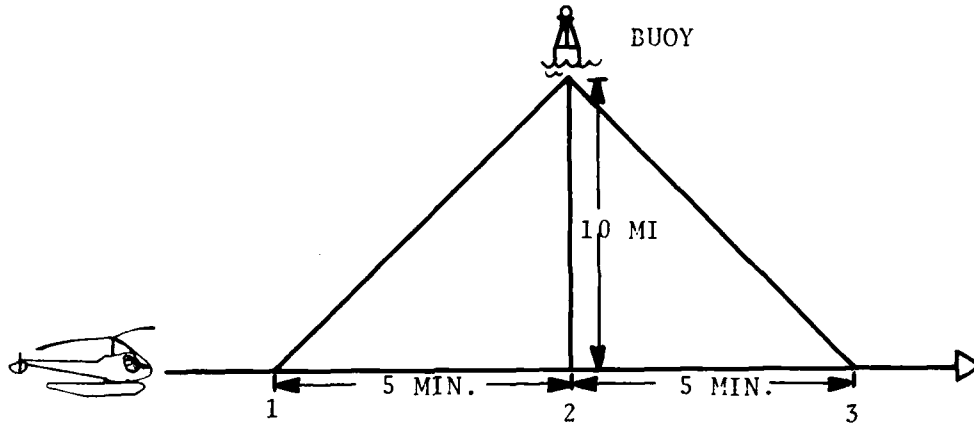
Figure 2.4-3   Flight Geometry

The required oscillator stability is then on the order of 1×10^{-10} over a time period of 1 - 5 minutes. This is a high quality oscillator; however, oscillators of this quality are available for $100 or less. A typical TCXO is specified at 3×10^{-9}/day (constant temperature) for units in the $75 price range. This would result in a 5 minute drift of 2×10^{-11}. Clearly then, this performance can be met by commercial TCXO oscillators, so long as the temperature change within the buoy, over the same 5 minute period is 1°C. Since the buoy is immersed in seawater, it seems reasonable to assume that the temperature will be very constant over short time periods.

b. Timing Stability Requirements

Since the buoy will be visited only once per year, the oscillator drift will determine the tolerance in the buoy timing cycle.   Typical oscillator specs examined during this study ranged from 1×10^{-6} to 1×10^{-7} drift over one year. This would result in a clock error of 3 to 30 seconds over a period of one year. Assume a transmission time per buoy of 10 seconds, and a total of 30 seconds between buoy transmissions, then a typical transmission sequence would be as shown in Figure 2.4-4.
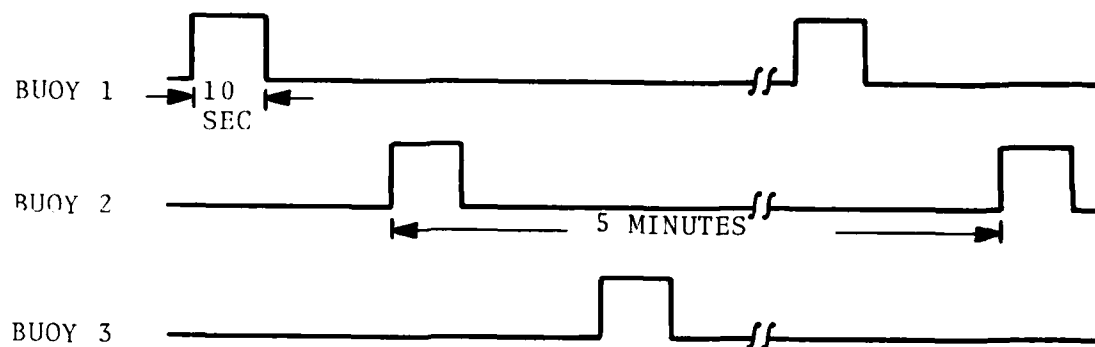
Approximately 5 Minutes

Figure 2.4-4   Typical Buoy Transmission Sequence

In this simplified description, each buoy would transmit a total of 3 times, at 5 minute intervals. Each transmission would provide a burst of 10 seconds of the selected ranging signal, encoded with data for buoy I.D. The helicopter would make three range measurements, and process them to form two sets of range differences. The buoy would then be located at the intersection of the two hyperbolas defined by the two sets of range difference measurements.

In practice, operational and geometrical considerations, as discussed in Section 3.0, would result in multiple measurements for each buoy. This section does not present a complete operational scenario; rather it demonstrates by simple calculation, the feasibility of the one-way ranging approach. Such an approach is very attractive for the following reasons:

(1) The buoy electronics package is greatly simplified, thus resulting in a lower cost operational package. Neither the command receiver, its associated control logic, nor the ranging receiver are required by this system.

(2) A significant (and presently unquantified) system error source, namely bias errors in the buoy transponder receiver, has been removed from the system.

2-43

2.4.5 Ranging System and Power Cost Estimate

The cost and power requirements of a Pulse Ranging system were presented in Section 2.4.3 and Appendix D. This section will concentrate on the CW Ranging system estimates. Tables 2.4-1 and 2.4-2 present the power requirements for two buoy configurations—two-way ranging and one-way ranging. The buoy power requirements are quite modest for either configuration. The primary power drain is either the command receiver (two-way) or the oscillator and clock (one-way). Either configuration easily meets the requirements of one ampere-hour per day. The L-band transmitter generates an RF output of one watt for the one-way system; in the two-way system, this has been boosted to 5 watts to allow for retransmitted noise should the helicopter-to-buoy link encounter significant fading. Although the buoy transmitters could obviously operate (in the absence of fading) with substantially lower power outputs (see link power requirements calculated in Appendices H and I), there is little benefit in further power reduction, because of operational considerations such as:

o There is little or no information at present on the assumed L-band antenna located on the helicopter. Antenna gain and multipath rejection at low elevation angles are critical to this link.

o Because of the low duty cycle, a five watt L-band transmitter contributes only 20% of the total buoy power consumption.

o Lower RF power will not significantly reduce the cost of the L-band transmitter.

The one-way ranging system buoy power requirements are primarily determined by the oscillator and clock. The oscillator and clock must be on continuously in order to maintain system time. However, the quoted current of 10 ma for the oscillator is quite high; units are available with less than half this current drain. Overall, the current drain is still quite modest; indeed all systems examined in this report, except pulse ranging, can easily meet the requirement of no more than one ampere-hour per day current drain.

TABLE 2.4-1

CW RANGING - BUOY POWER BUDGET (TWO-WAY)

	Ampere-Hours
COMMAND RECEIVER	
(0.015 Amp @ 12V) - ON 12 HOURS/DAY AVERAGE	0.180
SYSTEM CONTROL (CMOS LOGIC - 1 MA)	0.024
TRANSPONDER (5 WATT TRANSMITTER, 20% EFFICIENCY)	
RECEIVER POWER DRAIN - 50MA.	
TRANSMITTER POWER DRAIN - 2.08 AMPERES	
TOTAL TRANSPONDER DRAIN - 2.13 AMPERES	
15 SECONDS PER MEASUREMENT, 6 MEASUREMENTS/AUDIT	0.053
FOR ONE AUDIT/DAY -	0.26 A/H per day
FOR ONE AUDIT/WEEK -	0.21 A/H per day

TABLE 2.4-2

CW RANGING - BUOY POWER REQUIREMENTS (ONE-WAY)

SUBSYSTEM	AMPERE-HOURS/DAY
TEMPERATURE-COMPENSATED	
CRYSTAL OSCILLATOR (10 Mz @ 12V)	0.24
TIMING SUBSYSTEM & CONTROL LOGIC (1MA)	0.24
TONE GENERATOR (1MA)	
TRANSMITTER (1 WATT @ 20% EFFICIENCY	.011
15 SEC/MEASUREMENT, 6 MEAS./AUDIT)	
TOTAL FOR 1 AUDIT/DAY	0.275 A-H

The cost estimates, particularly Tables 2.4-3 and 2.4-4, showing cost estimates for the buoy electronics in production quantities, illustrate clearly one basic fact. That is that a two-way ranging system which is tailored to solving the BPAS problem, will be about 5 times as expensive (per buoy) as the TD Transmission system. The primary expense is the transponder which is a special design for this program and has no obvious other function. The cost is primarily due to the receiver requirements--namely, that over the dynamic range of signal level and frequency change and over an unattended operational period of one year, the phase shift (group time delay) must remain constant to within a few nanoseconds. The only easy way to accomplish this is to design the receive portion of the transponder to have a bandwidth of about 40 MHz--however, this will result in a receiver noise power level greater than the signal power. In this event, the transponder will saturate on noise power, suppress the signal energy and the performance will be severely degraded (potentially) by any interference and/or intermodulation problems. Therefore, the design bandwidth can be only slightly wider than the signal RF bandwidth of about 4 MHz, the design effort (and maintenance effort) then becomes a serious problem. From these points of view, two-way CW ranging systems, requiring the development of a dedicated transponder, seem to represent a poor choice, both from system cost and technical risk viewpoints.

However, one-way ranging seems to offer significantly more potential. The design of the electronics package is substantially simpler, as it consists of an oscillator, clock, ranging signal generator and transmitter. The antenna needs to deal with only one signal, thus eliminating the requirement for a diplexer and/or signal combiner. The result of this simplification is a substantially lower cost for the buoy electronics. (Costs for the one-way ranging base station electronics is presented in Table 2.4-5). The overall comparison, however, must note that the helicopter electronics is an order of magnitude more complex for any ranging approach than for TD Transmission. Thus, on balance, TD Transmission appears to be the lowest risk and lowest overall cost approach.

TABLE 2.4-3

BUOY ELECTRONICS - UNIT COSTS (TWO-WAY RANGING)

ANTENNA	60.00
COMMAND RECEIVER	80.00
SYSTEM CONTROL	25.00
TRANSPONDER	$5000.00
ANTENNA SYSTEM	100.00
TOTAL COST PER UNIT (IN PRODUCTION QUANTITIES)	$5265.00

TABLE 2.4-4

BUOY ELECTRONICS - UNIT COSTS

ONE-WAY RANGING - PURCHASE 1000 UNITS

OSCILLATOR	$100.00
TIMING SUBSYSTEM & CONTROL LOGIC	25.00
TONE GENERATOR	50.00
TRANSMITTER	1000.00
ANTENNA	25.00
PACKAGE & TEST	150.00
TOTAL	$1350.00

TABLE 2.4-5

BASE STATION ELECTRONICS - UNIT COSTS

ONE-WAY RANGING - PURCHASE 10 UNITS

L-BAND RECEIVER AND PHASE DEMODULATOR	10,000.00
RANGING SIGNAL PROCESSOR	10,000.00
TIMING SYSTEM	500.00
DATA RECORDING SYSTEM	4,000.00
PACKAGE, INTEGRATE AND TEST	3,000.00
BASE STATION TOTAL -	$27,500.00

3. BUOY POSITION AUDITING SYSTEM ERROR ANALYSIS RESULTS

3.1 INTRODUCTION

Error analysis results for the candidate Buoy Position Auditing System (BPAS) configurations, ie., TD Transmission, Pulse Retransmission, and Variable Geometry -- are presented in this chapter. Boston Harbor has been chosen as the specific scenario for the error analyses, since initial experimental verification of the recommended BPAS configuration is proposed to take place there. Seventeen buoys and three fixed aids (lights) which have been selected for consideration are listed in Table 3.1-1 and indicated on a chart of Boston Harbor in Figure 3.1-1*. Loran-C coverage for Boston Harbor is provided by the master/secondary W/secondary X transmitter triad of the Northeast U.S. Loran-C chain (transmitter locations are indicated in Table 3.1-2 and Figure 3.1-2). A detailed analysis of BPAS errors for other U.S. harbors is beyond the scope of the present study. However, BPAS accuracy for a U.S. harbor which exhibits a different Loran-C geometry or expected pattern monitor-to-buoy spacing than Boston Harbor can be estimated using sensitivity analysis results presented herein. The simulation capability developed for this study is general enough to permit more detailed error analyses for other harbors, if required in the future by the U.S. Coast Guard.

The estimates of buoy position error presented in this chapter are based on error models for the candidate BPAS configurations. The error models for the TD Transmission and Variable Geometry configurations are derived in Appendices A and C, respectively, and are summarized in Section 3.2. Error analysis results for the TD Transmission and Variable Geometry configurations, including the sensitivity of errors to operational and error model parameters, are presented in Sections 3.3 and 3.4, respectively. The error analysis results are used to identify the critical hardware design parameters and operational restrictions for each configuration. After initial investigations, the Pulse Retransmission BPAS configuration was eliminated from further consideration because of high cost and technical risk (Chapter 2). Although a detailed analysis of Pulse Retransmission errors has not been conducted during this study, coarse simulations have been performed to analyze the effect of Pulse Retranmission on Loran-C third-cycle identification. The simulations are detailed in Appendix F, and the initial results are presented in Section 3.5. The candidate BPAS configurations are compared on the basis of buoy position-fix accuracy in Section 3.6.

---

*The charts of Boston Harbor presented in this report are computer-produced.

3-1

TABLE 3.1-1

 TIONS OF SELECTED BUOYS AND FIXED AIDS IN BOSTON HARBOR*

ITEM NUMBER	U S COAST GUARD NUMBER	COMMON NAME	LOCATION	APPROXIMATE LATITUDE (North)	APPROXIMATE LONGITUDE (West)
1	431	Lighted Bell Buoy 2	Boston North Channel	42°22.2'	70°55.2'
2	432	Lighted Buoy 1	Boston North Channel	42°21.9'	70°55.2'
3	437	Lighted Bell Buoy 10	Boston North Channel	42°20.6'	70°56.6'
4	438	Lighted Buoy 9	Boston North Channel	42°20.5'	70°56.2'
5	445	Lighted Buoy 2	Boston Main Channel	42°20.1'	70°59.0'
6	448.50	Light 5 (Fixed Aid)	Boston Main Channel	42°20.0'	71° 0.1'
7	41.52	Lighted Bell Buoy 2	3½ Fathom Ledge	42°21.1'	70°50.5'
8	461	Channel Lighted Bell Buoy 3	Nantasket Roads	42°19.1'	70°52.8'
9	462	Channel Lighted Buoy 4	Nantasket Roads	42°19.2'	70°54.0'
10	463	Channel L. .ted Buoy 7	Nantasket Roads	42°19.0'	70°54.5'
11	464	Channel Lighted Buoy 8	Nantasket Roads	42°18.9'	70°55.0'
12	465	Channel Lighted Buoy 11	Nantasket Roads	42°18.7'	70°55.3'
13	466	Channel Lighted Buoy 12	Nantasket Roads	42°18.3'	70°55.6'
14	479.40	Lighted Buoy 4	Hull Gut Channel	42°17.9'	70°55.5'
15	480	Lighted Buoy 5	Hull Gut Channel	42°17.7'	70°55.4'
16	481	Harrys Rock Light 10 (Fixed Aid)	Hingham Bay Channel	42°17.2'	70°55.9'
17	430	Entrance Lighted Gong Buoy NC	Boston North Channel	42°22.5'	70°54.3'
18	38	The Graves Lighted Whistle Buoy 5	The Graves	42°22.5'	70°51.5'
19	42.10	Boston Lighted Horn Buoy B	Massachusetts Seacoast	42°22.7'	70°47.0'
20	43	Boston Light (Fixed Aid)	Little Brewster Island	42°19.7'	70°53.4'

* From Refs. 33 and 34.
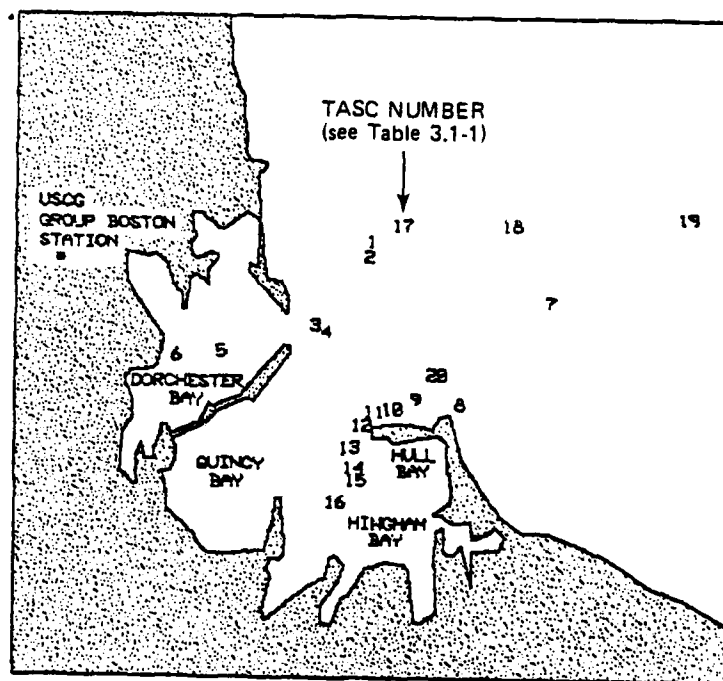
Figure 3.1-1 Locations of Selected Buoys And
Fixed Aids in Boston Harbor

TABLE 3.1-2

NORTHEAST U.S. LORAN-C CHAIN TRANSMITTERS
PROVIDING COVERAGE FOR BOSTON HARBOR*

TRANSMITTER	LOCATION	LATITUDE (North)	LONGITUDE (West)
Master	Seneca, NY	42°42'50.60"	76°49'33.82"
Secondary W	Caribou, ME	46°48'27.20"	67°55'37.71"
Secondary X	Nantucket, MA	41°15'11.93"	69°58'39.09"

* From Ref. 35.
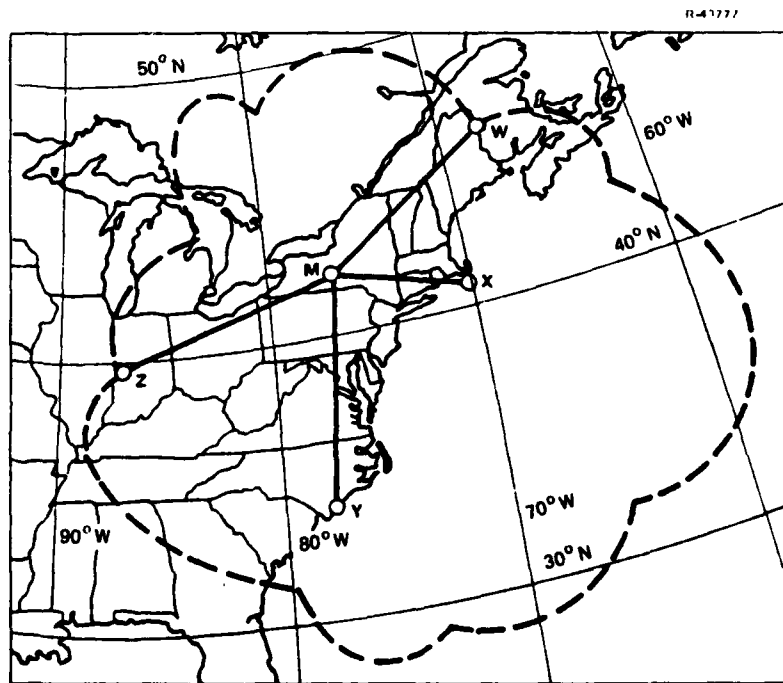
Figure 3.1-2 Northeast U.S. Loran-C Chain Coverage Area

3.2   ERROR MODELING SUMMARY

3.2.1 TD Transmission

The candidate BPAS configurations employ differential Loran-C, either alone (for TD Transmission and Pulse Retransmission) or in combination with a microwave ranging system and altimeter (for Variable Geometry).   The differential Loran-C error model is discussed below, with specific reference to the TD Transmission configuration.   Aspects of the model which differ for the Variable Geometry configuration are discussed in Section 3.2.2.

An adequate data base is not presently available to permit development of an empirical differential Loran-C error model.   Differential Loran-C experiments have been performed, such as the eight-week "Time Stability Study" conducted by the U.S. Coast Guard along the shores of Delaware Bay (Ref. 22). However, development of an empirical differential Loran-C error model for the BPAS application would require a minimum of one year of data, collected in various harbors, at an array of sites within each harbor.   The alternative to an empirical model is a theoretical model, whereby Loran-C propagation theory is employed to establish upper bounds on differential Loran-C errors.   The following attributes of a theoretical error model make it attractive for an initial feasibility study:

o   Applicable assumptions and restrictions can be readily identified
    and clearly stated

o   Model utility is not necessarily limited to a specific geographic
    region or time interval.

The differential Loran-C error model developed for this study is a theoretical model.

Loran-C position errors result from atmospheric noise (which corrupts the Loran-C TD measurements) and from propagation approximations (which are made in converting TDs to geodetic position coordinates i.e. latitude and longitude.*

---

*The TD-to-position transformation is referred to as the "TD grid."

3-5

Errors in the TD-to-position conversion are markedly reduced in differential Loran-C (compared to conventional Loran-C) by referencing the TD's measured at the Loran-C user location (i.e. the buoy) to TDs measured at a pattern monitor. Since the position of the pattern monitor is known precisely, it is only necessary to extrapolate the TD grid from the pattern monitor to the buoy.

Extrapolation of the TD grid from the pattern monitor to the buoy is assumed to be accomplished using the differential Loran-C algorithm detailed in Appendix A (Section A.4.1). It is assumed that TDs are measured by personnel on the buoy tender at the time the TD Transmission equipment is installed on the buoy. These initial TD measurements serve as benchmarks which aid in the extrapolation of the TD grid. The following assumption is necessary in a differential Loran-C algorithm which processes data from a single pattern monitor: TD variations which occur during an audit, or from audit to audit, are exactly the same at the pattern monitor as at the buoy. Differential Loran-C errors result because temporal TD variations are not uniform in space, but rather depend on transmitter-to-receiver ranges (Refs. 11 and 24). These errors cannot be reduced unless TD data from multiple pattern monitors are processed together (or additional information is available, as in the case of the Variable Geometry configuration). Detailed analysis of the utility of multiple pattern monitors is beyond the scope of this study.

Differential Loran-C errors are modeled in Appendix A by assuming that each signal propagation path, from a Loran-C transmitter to a receiver in a harbor*, has the following properties:

o Homogeneous atmosphere (in horizontal direction)-- i.e., surface refractive index and vertical lapse rate are transmitter- and receiver-independent

o Two path segments, each with homogeneous ground conductivity -- i.e., land for the transmitter end of the path and sea water for the receiver end; length and conductivity of the land segment are transmitter-dependent, but are receiver-independent for each transmitter.

---

*The region encompassing the pattern monitor and buoys is referred to as the "harbor".

The assumed propagation medium is simpler than may be encountered in reality but it is expected to describe the important features of the actual medium. Classical Loran-C groundwave propagation theory (Ref. 14) and Millington's method (Ref. 15) are applied to relate the transmitter-to-receiver signal propagation delay (travel time) to the parameters which characterize the propagation medium (i.e. refractive index, vertical lapse rate, and conductivity). The strong correlation between surface refractive index and vertical lapse rate (reported in Ref. 16) permits the atmospheric component of the propagation delay to be expressed by a function of surface refractive index, alone. This delay component is approximated by a linear dependence on transmitter-to-receiver range. However, the propagation delay component associated with conductivity (secondary phase delay (SF), including effects of land and sea water) is nonlinear in range, especially near the land/sea water interface. (See also extensive analysis and calculations concerning this effect in Ref. 24). The nonlinear dependence of SF on the range from the coastline to the receiver (along the transmitter-to-receiver path) is illustrated in Figure 3.2-1, where SF has been referenced to SF at the coastline. It is important to realize that the shape of the nonlinearity depends on the conductivity of the land path segment, even though the path between the coastline and the receiver is all sea water. However, the shape does not depend on the length of the land segment, for lengths greater than 2000 km.* For simplicity, it is assumed that SF is linear for those ranges relevant to a particular transmitter and harbor. It is further assumed that the paths for a particular transmitter and harbor are of one of the following types, where R is the coastline-to-receiver range:

Type I   : R < 15 km

Type II   : 15 km < R < 200 km

Type III   : R > 200 km

The three path types are illustrated in Figure 3.2-2 for a hypothetical harbor. Classification of the path types for an actual harbor may be complicated by an irregular coastline. The slopes of the nonlinear SF curves for the three types of propagation paths are summarized in Table 3.2-1. The slope is termed the "Loran-C scale factor" in this report. Note that the range of scale factor values, corresponding to a particular range of conductivity values, is largest in magnitude for Type I paths and smallest for Type III paths.

---

*The value of SF does depend on land segment length.
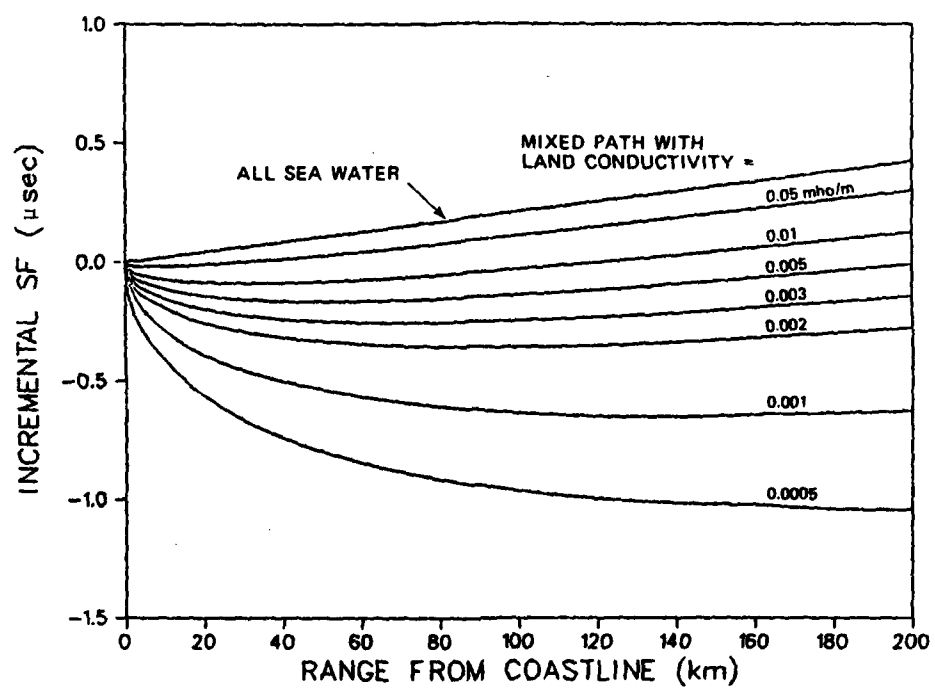
Figure 3.2-1   Incremental SF on Sea Water Path Segment
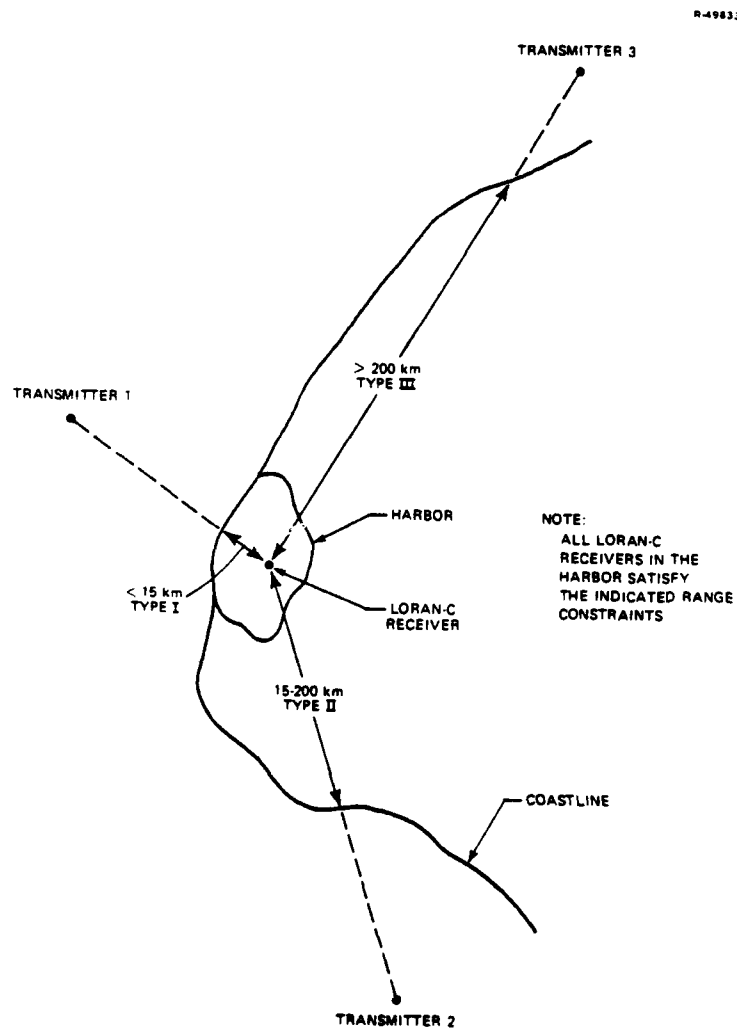
Figure 3.2-2 Definition of Propagation Path Types For
A Hypothetical Harbor

The ideal propagation medium described above is employed in Appendix A to derive the differential Loran-C error model for TD Transmission. The error model includes the following propagation and noise error sources:

o Scale factor error (one per transmitter) -- the difference between scale factors at the equipment installation time and buoy audit time

o Refractive index error -- the difference between refractive index at the installation and audit times

o Buoy measurement noise -- at installation and audit times

o Pattern monitor measurement noise -- at installation and audit times.

TABLE 3.2-1

SLOPES OF SF VERSUS RANGE CURVES

ON SEA WATER PATH SEGMENT (μsec/km)

LAND CONDUCTIVITY (mho/m)	PATH TYPE		
	I	II	III
0.0005	-0.076	-0.0035	
0.001	-0.056	-0.0019	
0.002	-0.041	-0.0006	+0.0021*
0.003	-0.034	-0.0001	
0.005	-0.027	+0.0005	
0.01	-0.020	+0.0010	

*Based on a sea water conductivity of 5 mho/m. Maximum spread assumed to be ±10 percent of the value shown.

It is important to recognize that the scale factor and refractive index errors depend on seasonal variations in the propagation medium. However, since a buoy audit is performed within a 3 hr. time period, it is assumed that the scale factor error and refractive index error are constant during the audit. Buoy and pattern monitor measurement noises are assumed to vary randomly during the audit.

The nominal standard deviations assumed for the error sources are derived in Appendix A and are listed in Table 3.2-2. Scale factor error standard deviation is based on the following assumptions:

o Land conductivity can double between winter and summer (theoretical result from Ref. 11; based on 1-2 m of snow or frozen ground in winter and average ground in summer)

o Seasonal conductivty variations are characterized by a uniform probability distribution between the extreme values

o Buoy Loran-C equipment is installed at the time of a conductivity extreme

o Propagation paths are Type I for all three transmitters.

TABLE 3.2-2

NOMINAL ERROR LEVELS FOR TD TRANSMISSION

ERROR SCALE	VARIABILITY DURING AUDIT	NOMINAL STANDARD DEVIATION
Scale Factor Error	Constant	12×10^{-6} μsec/m
Refractive Index Error	Constant	50×10^{-6}
Buoy Measurement Noise	Random	0.02 μsec
Pattern Monitor Measurement Noise	Random	0.02 μsec

These assumptions are expected to represent a worst case. In particular, note that conductivity would not be expected to double between winter and summer in the Southeast U.S. and West Coast Loran-C chain coverage areas, because winters in these regions are characterized by minimal snow cover. Furthermore, many harbors will have at least one transmitter path which is not

Type I. For example, the secondary W (Caribou, Maine) transmitter path for Boston Harbor is Type III. Refractive index error standard deviation is based on historical meteorological data for Washington D.C. (Ref. 12). This is also expected to be a worst case, since the largest seasonal variations in refractive index encountered in the United States occur in the northeastern region. Buoy and pattern monitor measurement noise standard deviations are both chosen to be 0.02 sec., based on use of the Internav LCM 404 or similar quality Loran-C receiver (Ref.18) and a 5-10 min TD averaging time. The TD Transmission error model can be applied to the Pulse Retransmission BPAS configuration by increasing the buoy measurement noise standard deviation. Analyses needed to estimate the expected increase in noise standard deviation were not included in the present study.

3.2.2 Variable Geometry

Buoy position is estimated in the Variable Geometry configuration from helicopter-to-buoy microwave range measurement and synchronous helicopter Loran-C and altimeter position fixes. In this study, the buoy position is assumed to be estimated with the procedure described in detail in Appendix C. In this procedure, a "coarse" buoy position fix is first calculated by solving for the intersection of circular lines-of-position associated with microwave ranging measurements. An iterative least-squares estimation algorithm, which is a form of Kalman filter (Ref. 17), is then used to compute an estimate of the error in the coarse fix. The error estimate is used to correct the coarse fix to produce a "fine" position fix. The least-squares algorithm relies on linearized equations which apply only when the estimated buoy position is near to the actual position. Several iterations are typically required to achieve the final buoy position estimate, starting from an initial estimate provided by the coarse fix algorithm. The error model described below addressed the steady-state error resulting from multiple iterations of the least-squares algorithm.

The differential Loran-C error model for the Variable Geometry configuration has the same structure as the TD Transmission configuration, but interpretation of the error sources is different. Since the Loran-C user is a helicopter, which is not constrained to fly the same flight pattern every audit, it would require a major data collection effort to establish TD benchmarks, such as can be established for a buoy Loran-C user. It is assumed that a simple TD grid prediction model, consisting of refractive index and a single scale factor, is hypothesized in lieu of benchmarks. The TD grid is extrapolated from the pattern

monitor to the helicopter, using the TD grid prediction model and the differential Loran-C algorithm presented in Apendix A (Section A.4.2.).

In the absence of TD benchmarks, the differential Loran-C error sources for the Variable Geometry configuration are:

o   Scale Factor error (one per transmitter) -- the difference between the scale factor in the hypothesized model and the actual scale factor at the buoy audit time

o   Refractive index error -- the difference between refractive index in the model at the audit time

o   Helicopter measurement noise -- at the audit time

o   Pattern monitor measurement noise -- at the audit time.

The scale factor and refractive index errors depend on the accuracy of the TD grid prediction model.   Note that helicopter and pattern monitor measurement noise only contribute to Loran-C error at the audit time, since no TD measurements are made at an initial (equipment installation) time.

The nominal standard deviations assumed for the Loran-C error sources are listed in Table 3.2-3. The scale factor error standard deviation is based on the following worst-case assumptions:

o   Land conductivity is only known to lie between extreme values of 0.0005 mho/m and 0.01 mho/m

o   Uncertainty in conductivity is characterized by a uniform distribution between the extremes

o   The hypothesized scale factor is based on an extreme conductivity value

o   Propagation paths are Type I for all three transmitters.

3-13

TABLE 3.2-3
NOMINAL ERROR LEVELS FOR VARIABLE GEOMETRY

	ERROR SOURCE	VARIABILITY DURING AUDIT	NOMINAL STANDARD DEVIATION
LORAN-C ERRORS	Scale Factor Errors	Constant	33×10^{-6} μsec/m
	Refractive Index Error	Constant	50×10^{-6}
	Helicopter Measurement Noise	Random	0.02 μsec
	Pattern Monitor Meaurement Noise	Random	0.02 μsec
MICROWAVE ERRORS	Propagation Velocity Error	Constant	0.015 m/μsec
	Common Timing Error	Constant	0.02 μsec
	Independent Timing Errors	Constant	0.02 μsec
	Measurement Noise	Random	0.01 μsec
	Altitude Error	Constant	10 m

The nominal scale factor error standard deviation for the Variable Geometry configuration (33×10^{-6} μsec/m) is significantly larger than for the TD Transmission configuration (12×10^{-6} μsec/m). This results because errors in the hypothesized scale factor for the Variable Geometry configuration are influenced by uncertainty in the spatial characteristics of the land conductivity, as well as by seasonal conductivity variations, while scale factor errors for the TD Transmission configuration are influenced only by seasonal variations. Conductivity varies spatially by at least a factor of 20 (for the United States, from Ref. 13), while seasonal variations at a fixed location are not expected to exceed a factor of two (from Ref. 11). The refractive index error standard deviation for the Variable Geometry configuration is selected to be the same as for the TD Transmission configuration, because spatial variations in refractive index are small compared to

seasonal variations (Ref. 12). Pattern monitor measurement noise standard deviation is the same as in the TD Transmission configuration (0.02 μsec). However, a helicopter Loran-C measurement noise standard deviation of 0.02 μsec is not expected to be achievable, due to the increased bandwidth of the Loran-C phase-locked loops required to compensate for helicopter motion. In the absence of specific data on the required bandwidth, a noise standard deviation of 0.02 μsec has been selected as a nominal value, and sensitivity analyses have been performed to study the effect of increased Loran-C noise standard deviation on Variable Geometry accuracy.

In the Variable Geometry configuration error analyses, the differential Loran-C error model is used in conjunction with microwave ranging system and altimeter error models. The microwave ranging system error model includes the following error sources:

o Propagation velocity error -- the difference between actual
   and assumed microwave signal propagation velocities

o Common timing error (same for all buoys) -- uncompensated bias
   in round-trip signal travel time; could arise from helicopter
   receiver bias or common temperature -- dependent transponder
   delay

o Independent timing errors (one per buoy) -- uncompensated
   bias in round-trip travel time; could arise from differences
   in transponder delays from buoy to buoy, caused by manufacturing
   tolerances

o Measurement noise -- includes all random timing errors.

Note that the microwave propagation velocity error and the common and independent timing errors are assumed to be constant during the audit. All random errors are included in the microwave measurement noise.

Nominal standard deviations for the microwave error sources are listed in Table 3.2-3. Propagation velocity error standard deviation is based on seasonal variations in refractive index at Washington, D.C. Standard deviations for the

MICROCOPY RESOLUTION TEST CHART

NATIONAL BUREAU OF STANDARDS 1963 A

common and independent timing errors and measurement noise are based on use of
a C-band or X-band microwave ranging system. Although the assumed values are
consistent with the ranging errors reported for existing systems (i.e., less than 10
m rms; Ref. 29), the contribution of each of the three error source components
cannot be readily deduced from manufacturer specifications.

The altimeter error is assumed to be constant during the audit. The
nominal altitude error standard deviation listed in Table 3.2-3 (i.e., 10 m) is based
on the APN-171 radar altimeter presently used on U.S. Coast Guard helicopters.
This altimeter is reported to exhibit an error equal to three percent of altitude.
The 10 m rms altitude error standard deviation was selected for a typical 300 m
helicopter altitude.

3.2.3 Measures of Buoy Position-Fix Accuracy

The BPAS error models are emloyed to estimate buoy position-fix
accuracy in the manner described in Appendices A and C. Two measures of buoy
position-fix accuracy are employed in this study. The error ellipse is a contour of
constant probability density corresponding to a probability of 0.39 (under the
assumption of Gaussian error statistics). That is, given a buoy position fix at the
center of the ellipse, the probability that the actual buoy position is within the
ellipse is 0.39. The error ellipse has the advantage of showing not only the size of
the error but also the orientation in space of the axes of maximum and minimum
error. It is often convenient, however, to use a scalar measure of accuracy, even
though such a measure does not contain any informatin about the directionality of
the position error. In this study, rms error is the scalar figure-of-merit used to
characterize buoy position-fix accuracy:

$$\text{rms error} = (\text{var}(\delta N) + \text{var}(\delta E))^{\frac{1}{2}} \qquad (3.2\text{-}1)$$

where

δN = north buoy position error

δE = east buoy position error

var( ) = variance of indicated error

It can be shown that the rms error is nearly proportional to the circumference of
the error ellipse.

3.3 TD TRANSMISSION ERROR ANALYSIS RESULTS

3.3.1 Sensitivity to Pattern Monitor Location

The error ellipses for the 17 buoys in Boston Harbor (fixed aids are excluded) are shown in Figure 3.3-1 for a pattern monitor located at Boston Light (fixed aid 20 in Table 3.1-1). Note that the major axis of each error ellipse is oriented in the direction of the pattern monitor. Table 3.3-1 lists the rms error for each buoy. Buoy position error increases with increasing distance from the pattern monitor, from approximately 10 m rms for the closest buoys (8 and 9) to over 30 m rms for the farthest buoy (19).

Buoy position error is a function of the geometry of the Loran-C stations as well as the location of the pattern monitor with respect to the buoy. However, in the case that the Loran-C lines-of-position cross nearly at right angles, as in Boston Harbor, rms buoy position error is a function only of the range to the pattern monitor, in the manner shown in Figure 3.3-2. The 10 m rms position error for a buoy coincident with the pattern monitor is contributed by measurement noise. It should be noted that averaging the TDs for longer than 5-10 min. is not justified, because of the existence of other error sources (unmodeled) such as buoy motion (during the audit) and TD receiver biases.

The above results show the importance of locating the pattern monitor as near as possible to all buoys. For large harbors, multiple pattern monitors could be used. If a U.S. Coast Guard facility near the center of the buoy network is not available, buoy position error will degrade accordingly. For example, if the pattern monitor is located at the U.S. Coast Guard Group Boston Station (Figure 3.1-1), the maximum rms buoy position error (buoy 19) increases from 31.5 m to 60 m.

3.3.2 Nominal Error Budget

Buoy position error is caused by the following Loran-C error sources:

o Scale factor error

o Refractive index error

LORAN-C LINES-OF-POSITION (HYPERBOLAS)

SCALE: ELLIPSES |——————| 50 m

MAP |——————| 5 km
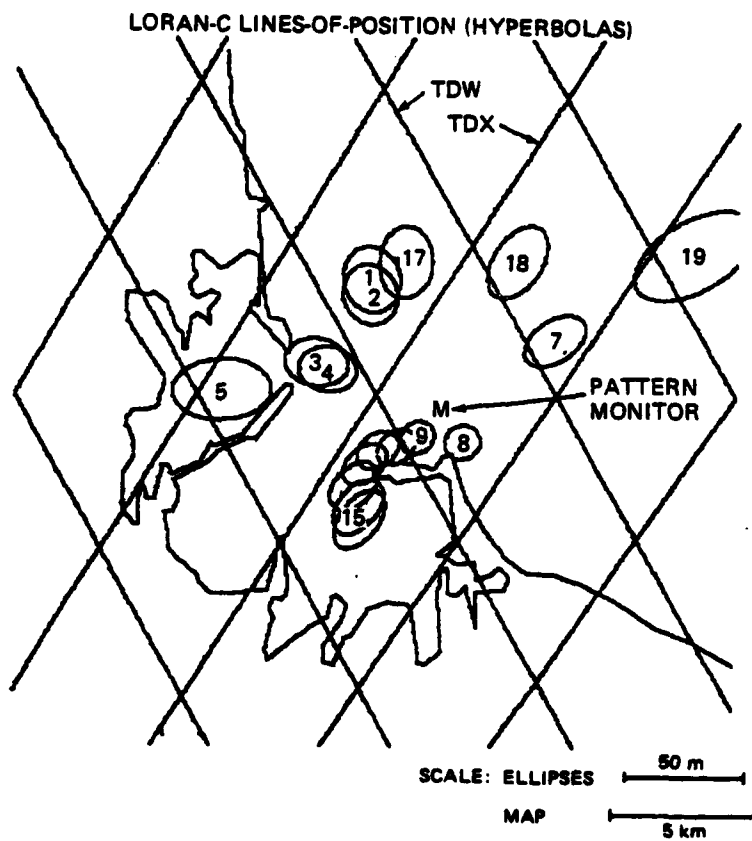
Figure 3.3-1   Nominal Error Ellipses
                  (TD Transmission)

TABLE 3.3-1

NOMINAL RMS BUOY POSITION ERROR
FOR TD TRANSMISSION

BUOY NUMBER	RMS POSITION ERROR (m)
1	18.9
2	17.8
3	17.1
4	16.0
5	24.6
7	16.8
8	10.7
9	10.5
10	11.3
11	12.2
12	13.4
13	15.0
14	16.0
15	16.8
17	19.2
18	19.9
19	31.5

3-18
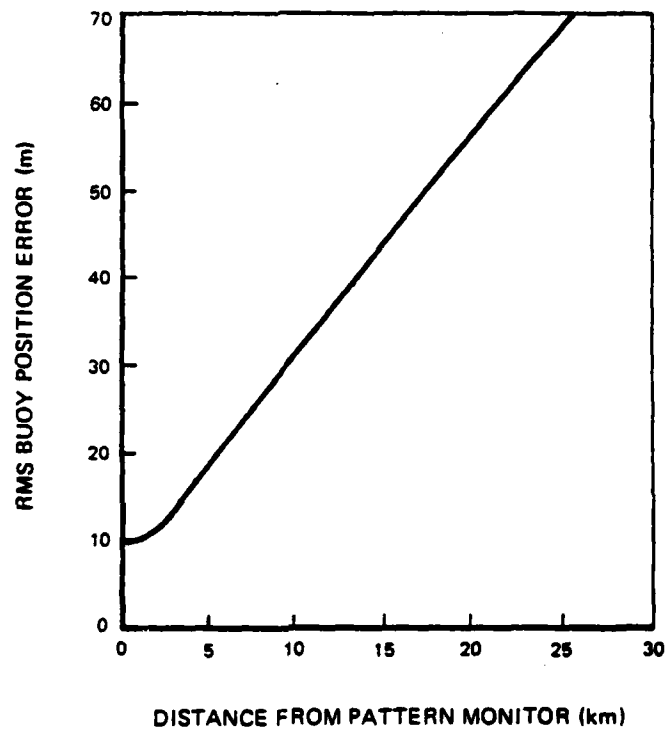
Figure 3.3-2   Dependence of Buoy Position Error on Distance
from Pattern Monitor (TD Transmission)

o Buoy and pattern monitor measurement noises.

The individual contribution of each of these sources to buoy position error is shown in Table 3.3-2 and Figure 3.3-3 for four selected buoys. Measurement noise is the same for all buoys and is composed of equal contributions for the buoy receiver and the pattern monitor receiver. The contribution of scale factor error to buoy position error increases with increasing buoy-to-pattern monitor range, starting from zero when the buoy is coincident with the pattern monitor. At a range of approximately 3 km from the pattern monitor, measurement noise and scale factor error contribute equally to rms buoy position error. Nominal refractive index error makes a negligible contribution to buoy position error.

TABLE 3.3-2

NOMINAL ERROR BUDGET FOR TD TRANSMISSION

ERROR SOURCE	CONTRIBUTION TO RMS BUOY POSITION ERROR (m)			
	BUOY 5	BUOY 15	BUOY 17	BUOY 19
Scale Factor Error	22.5	13.5	16.5	29.9
Measurement Noise	9.9	9.9	9.9	9.9
Refractive Noise Error	0.3	0.2	0.2	0.5
Total Error	24.6	16.8	19.2	31.5

3.3.3 Sensitivity to Error Parameter Values

It is important in a feasibility study to evaluate and compare not only the nominal accuracy of competing systems, but also the sensitivity of accuracy to changes in the assumed error model. Sensitivity study results can be used to address the following topics:

o How does accuracy change if an error source
   is mismodeled
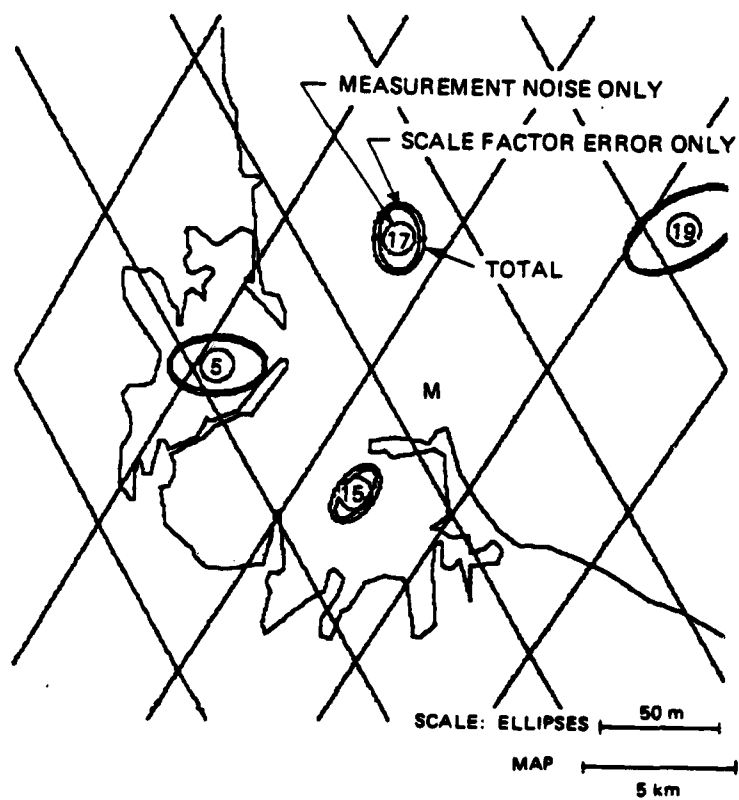
Figure 3.3-3   Measurement Noise and Scale Factor Error
Contributions to Buoy Position Error
(TD Transmission)

o   Which error source(s) must be reduced (by improved
    hardware design, improved calibration procedures, etc.)
    in order to improve accuracy

o   Which error source(s), if any, can be allowed to increase
    (providing a consequent cost savings in hardware,
    operational procedures, etc.) without significantly
    affecting system accuracy.

Sensitivity curves are presented below to show total rms buoy position error under the condition that one error parameter takes on a range of values about its nominal value, and all other error parameters remain at their nominal values.

Accuracy is very sensitive to an increase or decrease in scale factor error, relative to the assumed nominal value (Figure 3.3-4).* The nominal scale factor error standard deviation is computed based on Type I propagation paths for all three transmitters and a factor of two seasonal change in land conductivity (Section 3.2). A theoretical upper bound on scale factor error standard deviation may be computed based on spatial variations in land conductivity over the range of value expected in the entire U.S. (0.0005 to 0.01 mho/m). This corresponds to a scale factor error standard deviation of 33×10^{-6} μsec/m. Figure 3.3-4 demonstrates that buoy position error can exceed 100 m rms in this extreme case. Note that the actual variation in scale factor for the TD transmission configuration depends only on seasonal variations in land conductivity, because of the initial calibration. Therefore, a scale factor error based on the spatial variation in conductivity over the entire U.S. is probably an unrealistic upper bound. If scale factor error is reduced to the value associated with Type II or Type III propagation paths, the residual buoy position error is contributed almost entirely by measurement noise (Figure 3.3-4).

---

*The sensitivity curves in this report have logarithmic abscissa scales, offset by the nominal value of the error source.
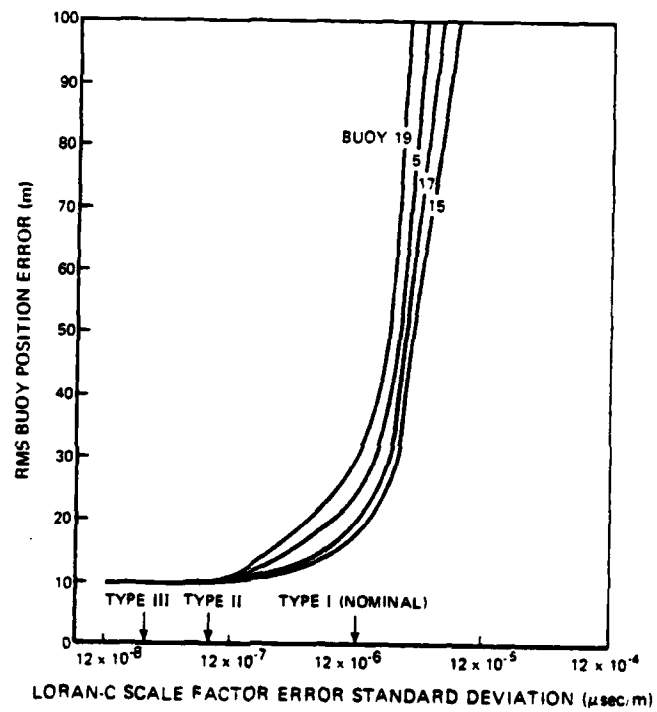
Figure 3.3-4   Buoy Position Error Sensitivity
to Loran-C Scale Factor Error
(TD Transmission)

The effect on buoy position error of changing buoy and pattern monitor Loran-C measurement noise standard deviations is graphed in Figure 3.3-5. The effect on buoy position error of changing buoy or pattern monitor measurement noise is graphed in Figure 3.3-6. A decrease in measurement noise below nominal does not improve performance significantly because of the dominance of the nominal scale factor error. Although accuracy is relatively sensitive to increases in measurement noise, the nominal value is expected to be achievable. Some degradation could result from a requirement to cut the cost of buoy equipment or from exposure to extreme environmental conditions on the buoy. Figure 3.3-6 indicates that a factor of two increase in buoy measurement noise standard deviation results in a relatively small increase in rms buoy position error.

Figure 3.3-7 suggests that an increase in refractive index error of almost two orders of magnitude is required to impact buoy position error. A refractive index error this large is not encountered in practice.

3.3.4 Effect of Loran-C Geometry

The impact of Loran-C transmitter geometry on buoy position accuracy at harbors other than Boston Harbor is evaluated using the scalar index Geometric Dilution of Precision (GDOP). For the TD Transmission configuration, GDOP can be considered as the index by which buoy position error is scaled to determine BPAS accuracy for other harbor locations, subject to the conditions and assumptions enumerated in Appendix A (Section A.2). GDOP is displayed for each location along the U.S. coastline in Figure 3.3-8. The Loran-C secondary pair which gives the minimum GDOP is selected for each point on the coastline, after selecting the Loran-C chain which provides the maximum signal levels. Figure 3.3-8 shows that GDOP is nearly a minimum at Boston Harbor (1.17) and for most of the East Coast. The position errors reported in the previous sections should be scaled by GDOP (for example, the position errors for San Francisco Harbor are approximately 4 times the position errors for Boston Harbor).

3.3.5 Summary of TD Transmission Error Analyses

Buoy position error in the TD Transmission configuration is caused primarily by two error sources:
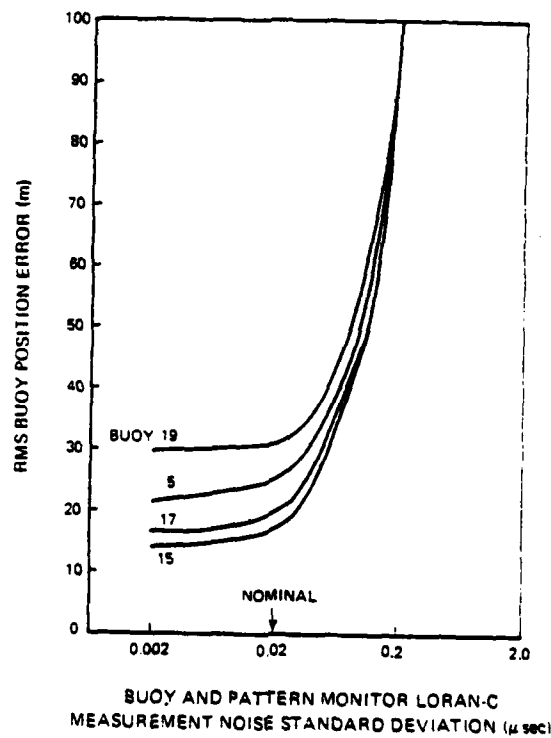
Figure 3.3-5   Buoy Position Error Sensitivity to Buoy <u>and</u> Pattern Monitor Loran-C Measurement Noise (TD Transmission)
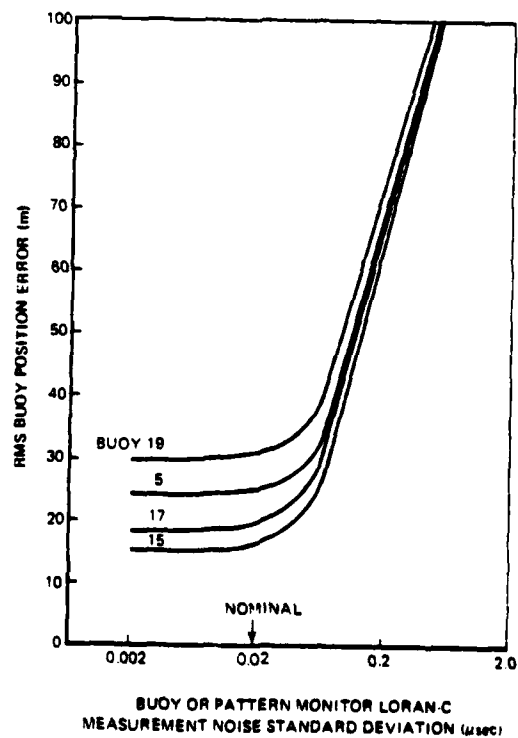
Figure 3.3-6   Buoy Position Error Sensitivity to Buoy <u>or</u> Pattern Monitor Loran-C Measurement Noise (TD Transmission)

3-25
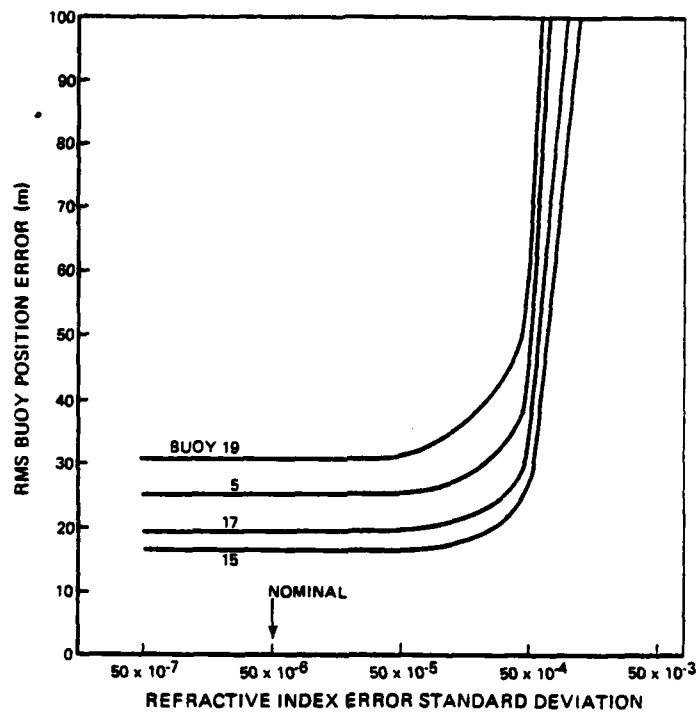
Figure 3.3-7   Buoy Position Error Sensitivity to
                Refractive Index Error (TD Transmission)
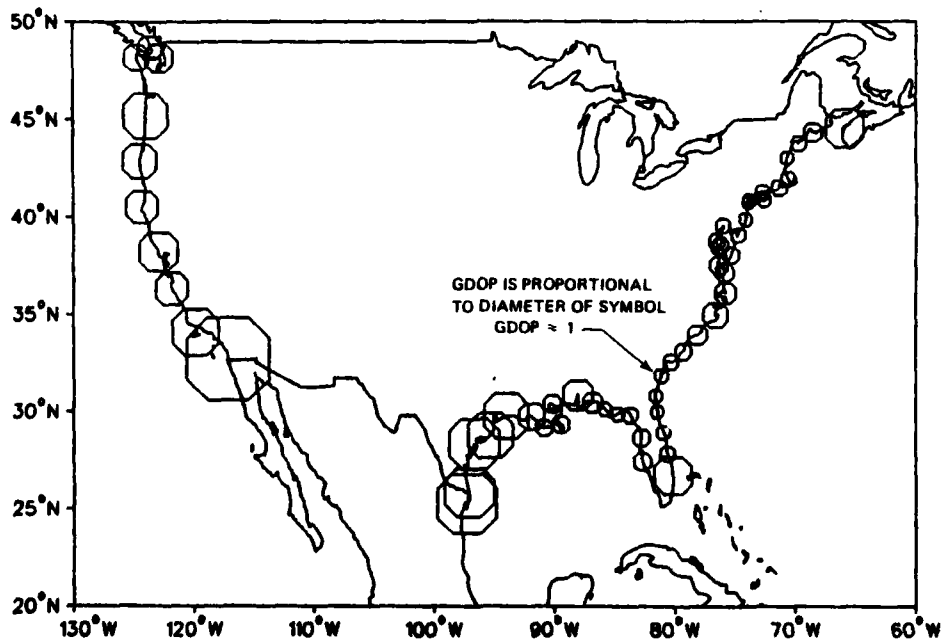
Figure 3.3-8   Loran-C GDOP Along U.S. Coastline

o Loran-C scale factor error

o Measurement noise.

Nominal measurement noise contributes 10 m rms to buoy position error for all buoys. The contribution of scale factor error to buoy position error increases with increasing buoy-to-pattern monitor range, starting from zero when the buoy is coincident with the pattern monitor. At ranges beyond approximately 3 km, scale factor dominates measurement noise. The position errors for the TD Transmission errors are particularly sensitive to the Loran-C geometry.

3.4 VARIABLE GEOMETRY ERROR ANALYSIS RESULTS

3.4.1 Introduction

Processing of redundant measurements by the least-squares algorithm in the Variable Geometry configuration produces an estimate of constant error source parameters as well as buoy position error (Appendix C). The standard deviation of each error is reduced in accordance with the relative "observability" of the error source. Observability depends on the helicopter-to-buoy geometry and the a priori standard deviation of each error source. While the standard devation of noise error sources cannot be reduced by the algorithm, the impact of noise is reduced by averaging as more measurements are processed. It is the combination of calibration of observable constant error sources and noise averaging that produces a reduction in buoy position error in the least-squares algorithm.

Accuracy of the Variable Geometry configuration is a function of:

o   Loran-C transmitter geometry and pattern monitor location

o   Helicopter trajectory

o   Loran-C error levels

o   Microwave ranging system and altimeter error levels.

3-27

The Loran-C error model for the Variable Geometry configuration is very similar to the model for the TD Transmission configuration. However, the impact of some error sources (e.g., Loran-C scale factor error) on accuracy is markedly different, because of calibration of constant errors and averaging of noise errors afforded by the least-squares algorithm.

In Section 3.4.2, accuracy of the Variable Geometry configuration is assessed under nominal error conditions, as a function of helicopter trajectory (flight pattern) and pattern monitor location. Sensitivity of accuracy to Loran-C, microwave ranging and altimeter error levels is presented in Section 3.4.3 for a nominal helicopter trajectory and pattern monitor location. Nominal parameter values for the sensitivity studies are given in Table 3.2-2 unless stated otherwise. Each sensitivity curve shows total system error with all error parameters at their nominal values except the parameter under study. An "optimal" sensitivity study was performed, which assumes the least-squares algorithm to be optimally designed for each assumed set of error parameter values. The optimal sensitivity study provides a lower bound on total system error. A "filter" sensitivity study, on the other hand, shows system accuracy as error model parameters are varied but the filter design is not changed. A filter sensitivity study is more appropriate after a filter design has been finalized.

3.4.2 Sensitivity to Operational Variables

Peripheral Trajectory - Figure 3.4-1 shows the significant effect that helicopter trajectory geometry can have on buoy position error. Fixes 1 through 4 are taken along a straight-line path. Note that after the first fix, no estimate of buoy position can be computed from the least-squares algorithm, because at least two fixes are required to solve for the two components (north and east) of buoy position error. Position error for buoy 17 is reduced from 135 m rms after fix 2 (error ellipse not shown) to 87.0 m rms after fix 3, but additional fixes along the path are not effective. For example, fix 4 only reduces the error to 85.1 m rms. A deviation from the straight-line trajectory (fix 5), however, results in a substantial reduction to 20.4 m rms, and the final fix reduces the error to 6.3 m rms. A straight-line trajectory is ineffective in reducing buoy position error because of limited observabilty of constant error sources by the least-squares algorithm. This

3-28
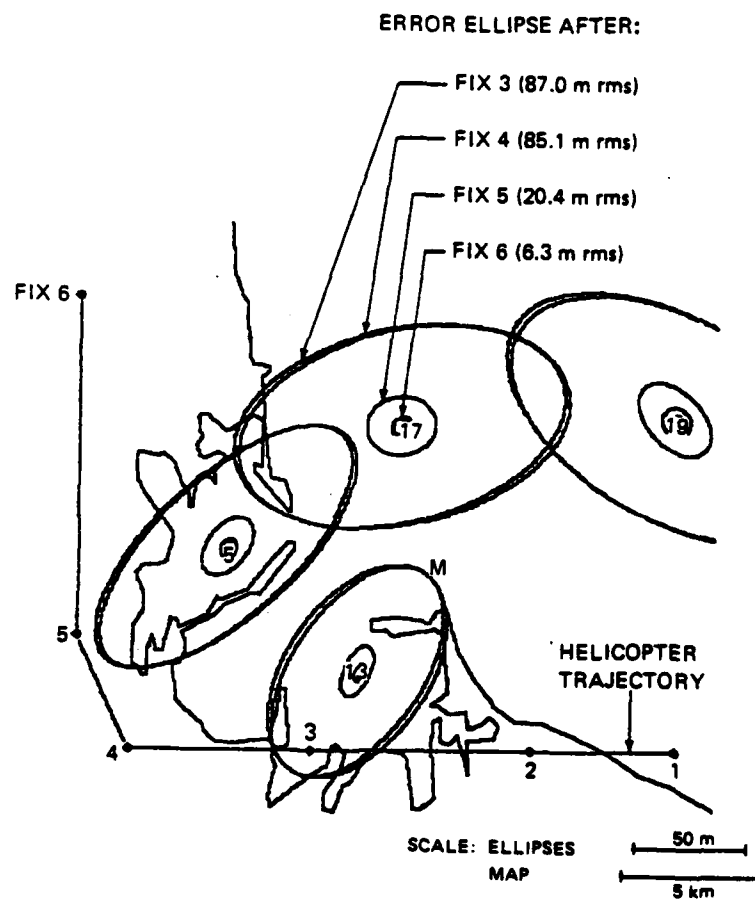
Figure 3.4-1   Buoy Position Error Ellipses For a
                 Peripheral Trajectory (Variable Geometry)

phenomenon is distinct from a similar phenomenon observed with the "coarse" fix solution, whereby a coarse fix cannot be computed from a straight-line helicopter trajectory (Appendix C).

Round-Trip Trajectory - The effect of trajectory shape is studied using the rectangular trajectory shown in Figure 3.4-2, which represents a round trip over the center of the buoy network. The rms error is reduced after 6 fixes to nearly the same level as with the peripheral trajectory (Figure 3.4-1). Sensitivity of trajectory shape is studied using the rectangular trajectory shown in Figure 3.4-2, which represents a round trip over the center of the buoy network. The rms error is reduced after 6 fixes to nearly the same level as with the peripheral trajectory (Figure 3.4-1). Sensitivity of buoy position error to the one-way length (l) and the outbound-to-inbound path separation(s) of the round-trip trajectory is shown in Figure 3.4-3 and Figure 3.4-4. Position errors for the four buoys range from 25 m rms to 47 m rms for a straight line trajectory (s=0) through the center of the buoy network (Figure 3.4-3). The rms error is reduced to less than 10 m for all buoys when the trajectory separation is 3 km or wider. Figure 3.4-4 illustrates (for the four buoys) buoy position error is large for small trajectory lengths, however, for trajectory of lengths greater than 10 km, the error is reduced below 10 m rms. These results imply that relatively minor restrictions on the helicopter trajectory are required to perform a buoy audit using the Variable Geometry configuration. An excursion of a helicopter approximately 10 km into the buoy field, and a return path only 3 km from the original path, are sufficient to perform a successful audit. Furthermore, the audit can be performed with only six microwave ranging (and Loran-C) fixes, thereby requiring little buoy battery power (Chapter 2).

Pattern Monitor Location - The relation of buoy position error to pattern monitor location is somewhat more complex in the Variable Geometry configuration than in the TD Transmission configuration. The position of the helicopter trajectory with respect to both the buoys and the pattern monitor must be considered, because of its relationship to observability of Loran-C errors in the least-squares algorithm. Since the helicopter would fly within the line of sight of the buoys to make microwave range measurements, a pattern monitor located in the center of the buoy network is preferred. Figure 3.4-5 indicates that moving the pattern monitor 94 km east of Boston Light (its nominal location) results in an increase in rms buoy position error from approximately 10 m to 80 m (the helicopter trajectory is the central one depicted in Figure 3.4-6). This increase is
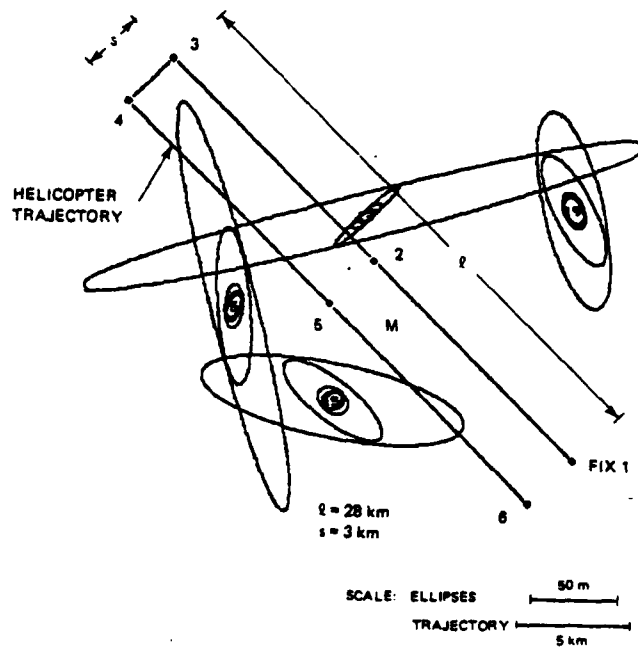
Figure 3.4-2   Buoy Position Error Ellipses for a
Round-Trip Trajectory (Variable Geometry)
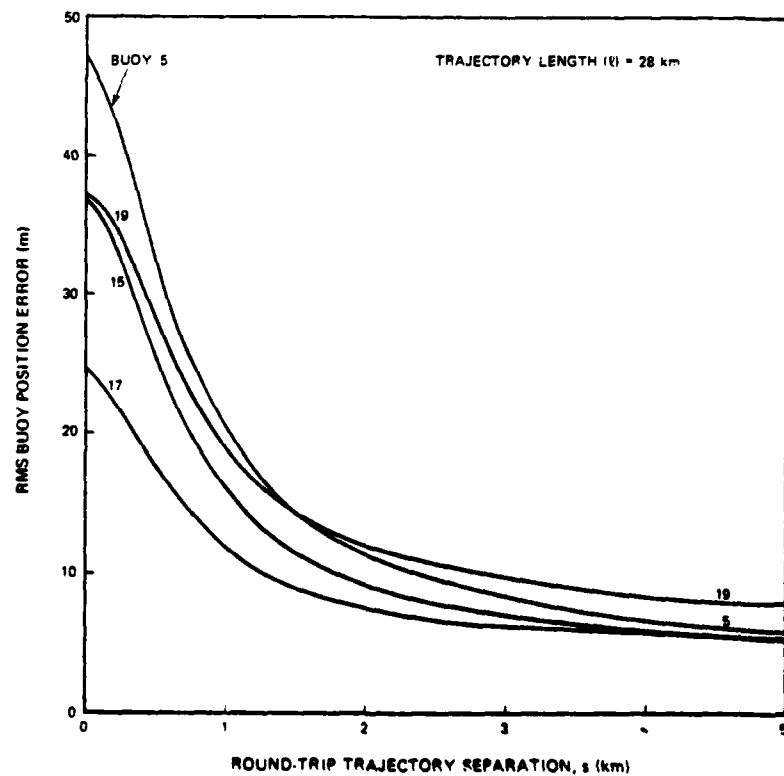
Figure 3.4-3   Buoy Position Error Sensitivity to Separation
of Round-Trip Trajectory (Variable Geometry)

3-31
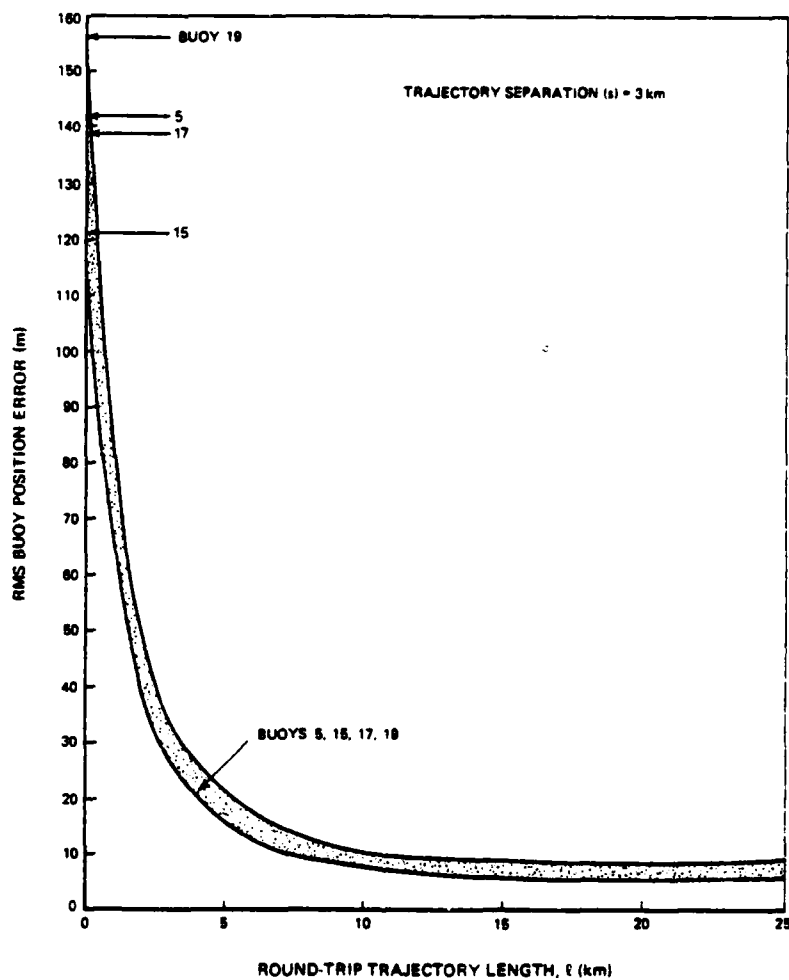
Figure 3.4-4 Buoy Position Error Sensitivity to Length
of Round-Trip Trajectory (Variable Geometry)
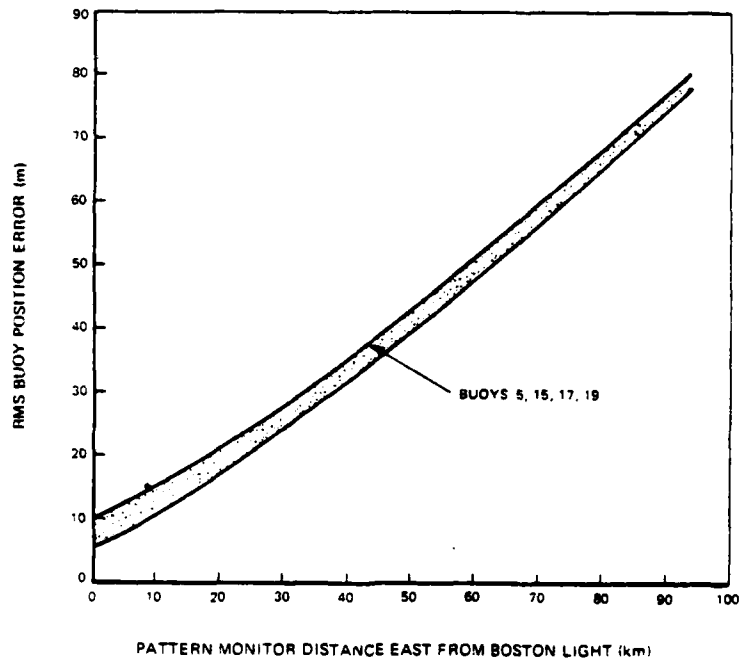
Figure 3.4-5   Buoy Position Error Sensitivity to Pattern
Monitor Location (Variable Geometry)
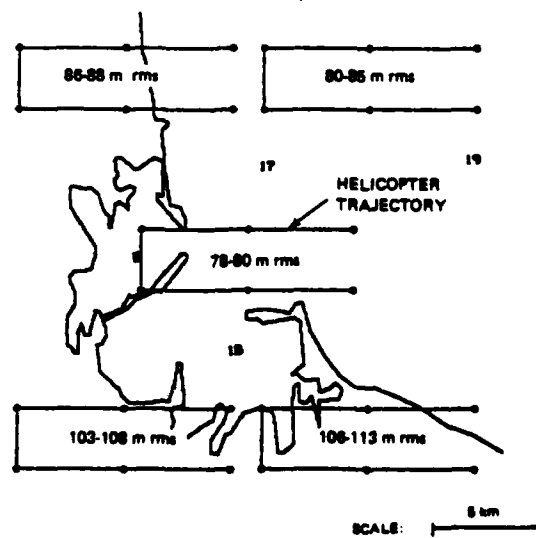
PATTERN MONITOR 94 km EAST OF BOSTON LIGHT; NUMBERS
WITHIN TRAJECTORY SHOW RANGE OF RMS POSITION ERROR
FOR BUOYS 5, 15, 17, 19

Figure 3.4-6   Buoy Position Error Sensitivity to Trajec-
tory Location With Remote Pattern Monitor
(Variable Geometry)

3-33
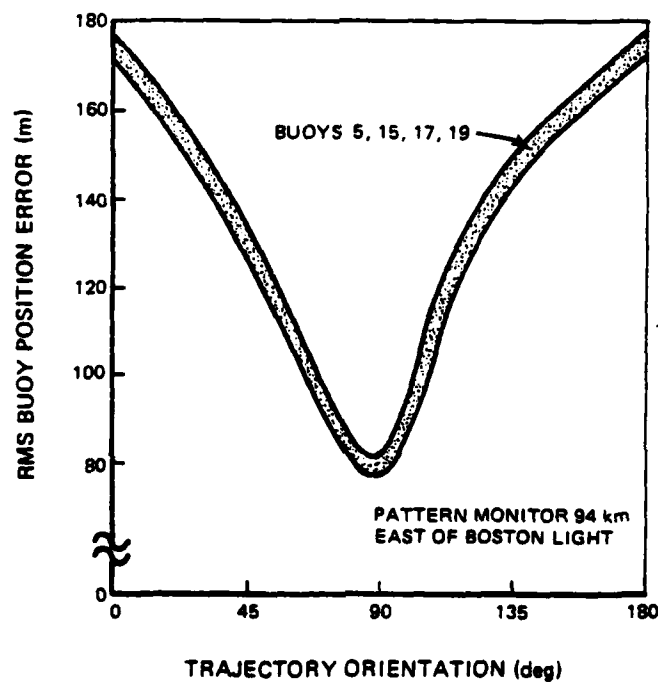
Figure 3.4-7 Buoy Position Error Sensitivity to
Trajectory Orientation with Remote
Pattern Monitor (Variable Geometry)

much less than in the TD Transmission configuration (Figure 3.3-2) because of error calibration by the least-squares algorithm. Note that when the pattern monitor is far from the buoys, the Loran-C transmitter-to-receiver paths for the pattern monitor and buoys may not all be of the same type, in violation of the modeling assumptions made in Section 3.2 and Appendix A. Modeling the entire harbor as Type I in this case provides a worst-case scale factor error.

Helicopter Trajectory with Remote Pattern Monitor - As the pattern monitor is moved from its nominal central location, accuracy not only degrades, as shown in Figure 3.4-5, but accuracy becomes more sensitive to helicopter trajectory. Figure 3.4-6 and Figure 3.4-7 illustrate the sensitivity of buoy position error to helicopter trajectory when the pattern monitor is at a remote location (94 km east of Boston Light). Maximum rms buoy position error over the four buoys increases from 80 m for the central trajectory shown in Figure 3.4-6, to a maximum of 113 m for the southeastern trajectory. When the pattern monitor is at its nominal location, the corresponding range of rms buoy position errors is 10 to 25 m. Figure 3.4-7 indicates that buoy position error is somewhat more sensitive to the orientation of the trajectory when the pattern monitor is remotely located. (Orientation angle is measured to the long axis of the trajectory, clockwise from north; the orientation of the trajectories in Figure 3.4-6 is 90 deg.) When the orientation of the central trajectory is rotated by 90 deg. rms buoy position error increases from 80 m to 175 m. There is little sensitivity to trajectory orientation for the nominal pattern monitor location.

The sensitivity to the helicopter trajectory with a remote pattern monitor is caused by the ability or inability of the least-squares algorithm to calibrate the Loran-C scale factor error. As discussed in Section 3.3, scale factor error causes a position error which is larger along the direction from the Loran-C user to the pattern monitor. The scale factor error is more observable to the least-squares algorithm when the helicopter trajectory exhibits large changes in position along this direction, as is the case for trajectories oriented at 90 deg. (east/west). This explanation of the sensitivity can be seen clearly in Figure 3.4-8, which shows the error ellipses after 6 fixes for the best-case (90 deg) and worst-case (0 deg) trajectories. Buoy position errors for the two trajectories are significantly different along the direction from the helicopter to the pattern monitor (east/west) because of the difference in observability, but nearly equal in the orthogonal direction (north/south).

SCALE: ELLIPSES |———| 50 m
MAP |———| 5 km

PATTERN MONITOR 94 km EAST OF BOSTON LIGHT
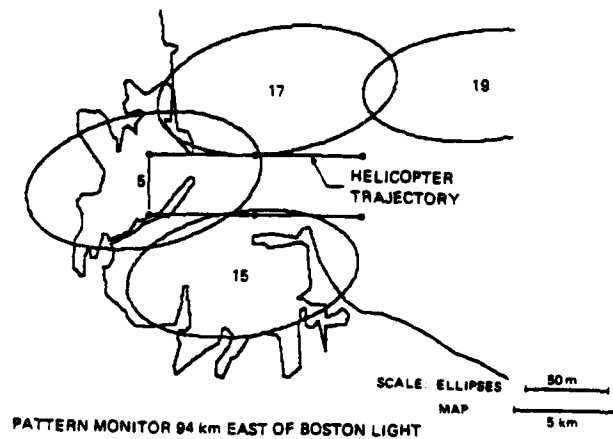
(a)   Best Case Trajectory Oriented Along the
      Halicopter-to-Pattern Monitor Direction

(b)   Worst-Cast Trajectory Oriented Across the
      Helicopter-to-Pattern Monitor Direction

Figure 3.4-8   Error Ellipses For Remote Pattern Monitor
               (Variable Geometry)

3-36

Number of Fixes - Note that the sensitivity studies detailed above were performed with six fixes. Under nominal conditions, buoy position error is not reduced significantly by taking more than six fixes. This is shown by the lower curve in Figure 3.4-9. When the pattern monitor is located remotely, however, six fixes are not sufficient to calibrate the Loran-C scale factor error to its steady-state value, because the helicopter-to-pattern monitor geometry does not vary sufficiently. If more fixes are taken, the restricted geometry effect can be partially offset by the effect of measurement noise averaging. The upper curve in Figure 3.4-9 shows rms buoy position error to be reduced from 80 m to 27 m with 80 fixes; more fixes further reduce the error. While buoy position error can be significantly reduced by taking a large number of fixes, practical limications on the number of fixes must be considered. Limitations are imposed by available buoy battery power, shore station computer capacity and line-of-sight ranging requirement.

Number of Buoys Audited - In the least-squares algorithm, range measurements to all buoys are processed together. The algorithm is thus able to obtain information about the position of a given buoy from measurements to other buoys, and the error is smaller than it would be if measurements to the buoy were processed alone. Figure 3.4-10 demonstates how rms position error for buoy 17 increases as fewer buoys are audited (using a 3 km by 10 km trajectory with 6 fixes); the rms error is more than doubled when buoy 17 is audited alone.

3.4.3 Sensitivity to Error Model Parameter Values

Non-Sensitive Error Parameters - Buoy position error sensitivity to error model parameters was performed with a 3 km by 10 km trajectory oriented as the trajectory shown in Figure 3.4-2. Buoy position error is not sensitive to the following parameters over a factor of 1,000 on either side of nominal:

    o   Loran-C scale factor error

    o   Loran-C refractive index error

    o   Helicopter altitude error

    o   Microwave common timing error.
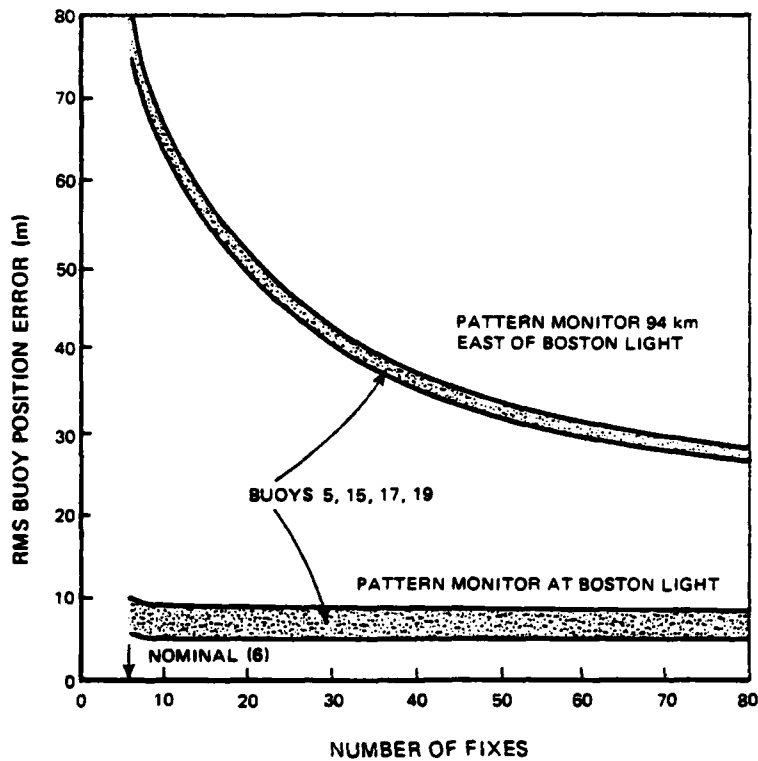
Figure 3.4-9 Buoy Position Error Sensitivity To
Number of Fixes for Remote and Local
Pattern Monitors (Variable Geometry)
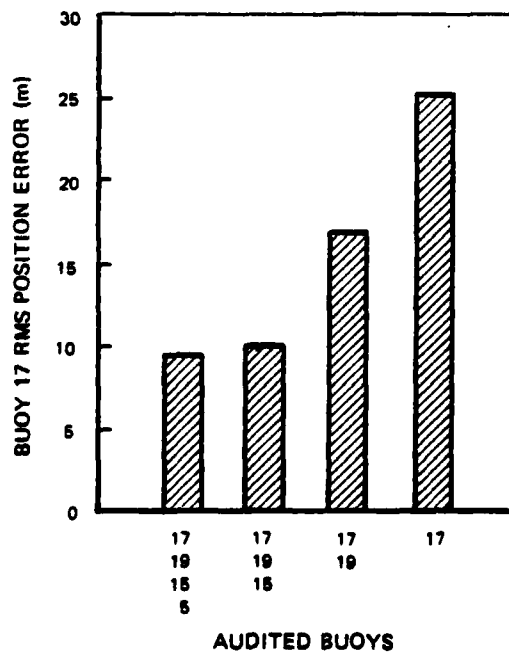
Figure 3.4-10 Buoy Position Error Sensitivity to Number
of Buoys Audited (Variable Geometry)

3-38

The least-squares algorithm can effectively calibrate each of these error sources even from very large initial values.

Sensitive Error Parameters - Buoy position error is sensitive to the following error sources:

o   Microwave propagation velocity error

o   Microwave independent timing error

o   Microwave measurement noise

o   Loran-C measurement noise

An increase in microwave propagation velocity error by more than a factor of 10 is required to affect accuracy (Figure 3.4-11). It is not likely that a significant increase in propagation velocity error would be cuased by refractive index variations. Figure 3.4-11 may also be used, however, to assess the impact of propagation velocity errors caused by other phenomena, such as multipath interference, which were not addressed specifically in this study. Sensitivity to the independent component of the microwave timing error (Figure 3.4-12) is moderate for a factor of 10 increase in the error source. Larger microwave timing errors cause buoy errors to increase rapidly and then level off; the filter can calibrate the independent timing errors when they are large with respect to other error sources. Recall that sensitivity to the common microwave timing error is small; an error which is common to all buoys is more observable to the least-squares algorithm. Although the nominal values for the common and independent microwave timing errors were chosen conservatively, the likelihood of either parameter exceeding its nominal value cannot be readily estimated. Note, however, that the sensitivity to the microwave independent timing error can be reduced by taking more fixes. Figure 3.4-13 shows that when microwave independent timing error is a factor of 100 above nominal (an extremely) unlikely value chosen to better illustrate the point), rms buoy position error for each of the four buoys can be reduced by a factor of 3 by processing 100 fixes.

3-39
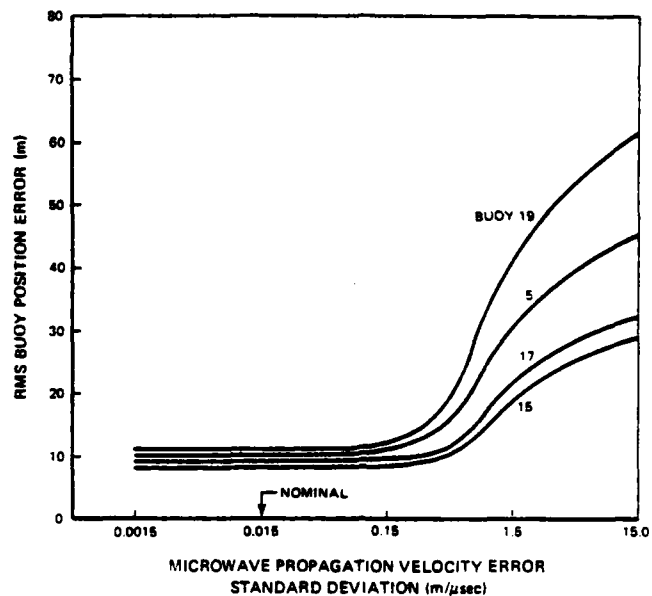
Figure 3.4-11 Buoy Position Error Sensitivity to
Microwave Propagation Velocity Error
(Variable Geometry)
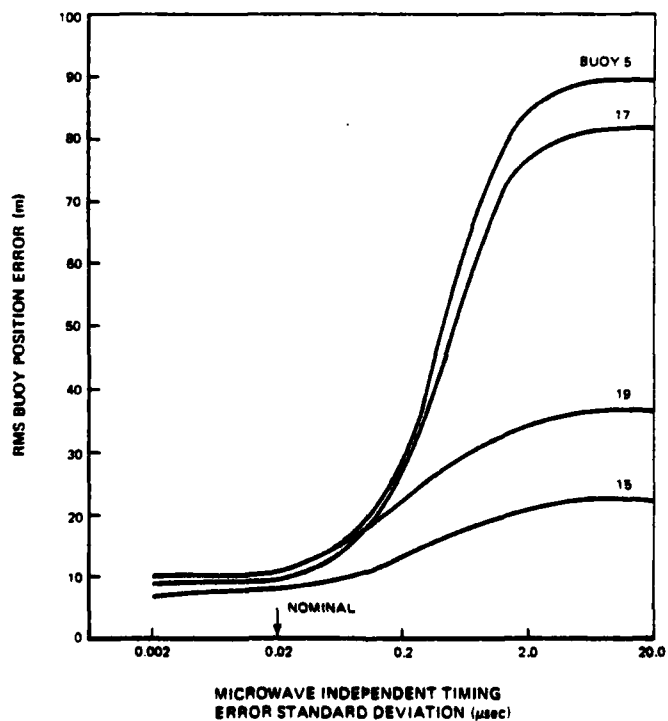
Figure 3.4-12 Buoy Position Error Sensitivity to
Microwave Independent Timing Error
(Variable Geometry)

3-40
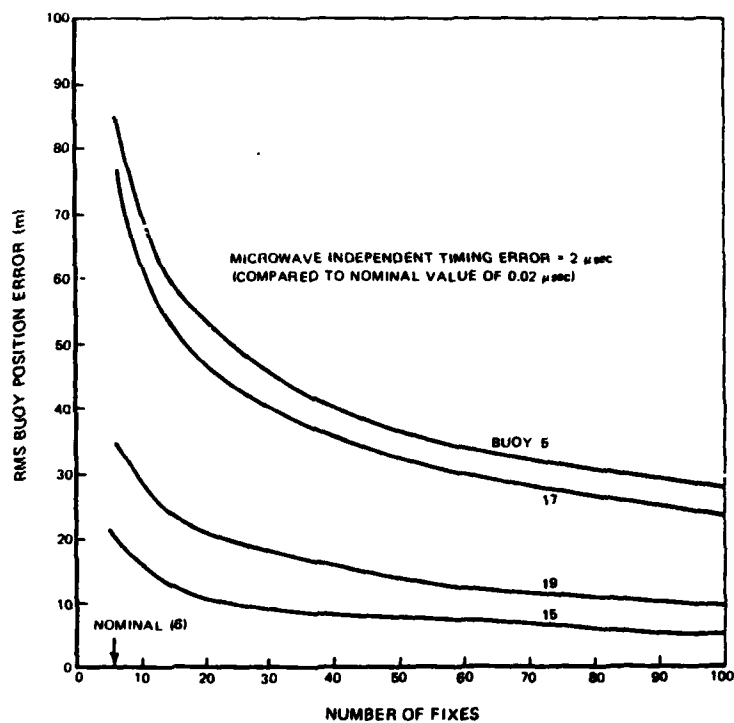
Figure 3.4-13 Buoy Position Error Sensitivity to Number
of Fixes With Large Microwave Independent
Timing Error (Variable Geometry)

Buoy position error exhibits a large sensitivity to measurement noise, in both the microwave ranging (Figure 3.4-14) and Loran-C systems (Figure 3.4-15 and Figure 3.4-16). This large sensitivity is expected since measurement noise impedes the ability of the least-squares algorithm to calibrate the constant error sources. Sensitivity to helicopter Loran-C measurement noise (Figure 3.4-16) is especially important because of the dynamic environment of the helicopter. The nominal standard deviation of the helicopter Loran-C noise was chosen to be the same as for the pattern monitor. However, the increased bandwidth of the Loran-C phase-locked loops, required to compensate for helicopter motion, increases the measurement noise. For example, the phase-locked loop described in Ref. 19 exhibits a factor of four increase in measurement noise standard deviation, when loop gains are adjusted to reduce the acceleration-induced phase error by a factor of 256. While Figure 3.4-16 shows performance to be quite sensitive to an increase in noise relative to the assumed nominal value, this sensitivity may be reduced by processing additional measurements. When helicopter Loran-C measurement noise is a factor of 10 above nominal, Figure 3.4-17 shows that rms buoy position error can be reduced to 10 to 20 m by processing 100 measurements.

3.4.4 Summary of Variable Geometry Error Analyses

Table 3.4-1 provides a summary of the Variable Geometry error analyses detailed in Sections 3.4.2 and 3.4.3. The following parameters are important in the assessment of the Variable Geometry configuration:

- o Shape of helicopter trajectory

- o Pattern monitor location

- o Standard deviation of certain constant microwave error sources

- o Standard deviation of noise error sources

- o Number of fixes.
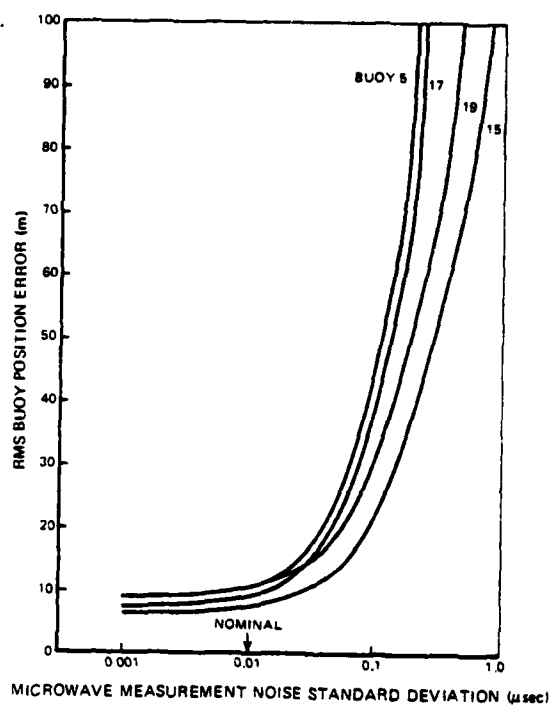
Figure 3.4-14　Buoy Position Error Sensitivity to Microwave
Measurement Noise (Variable Geometry)
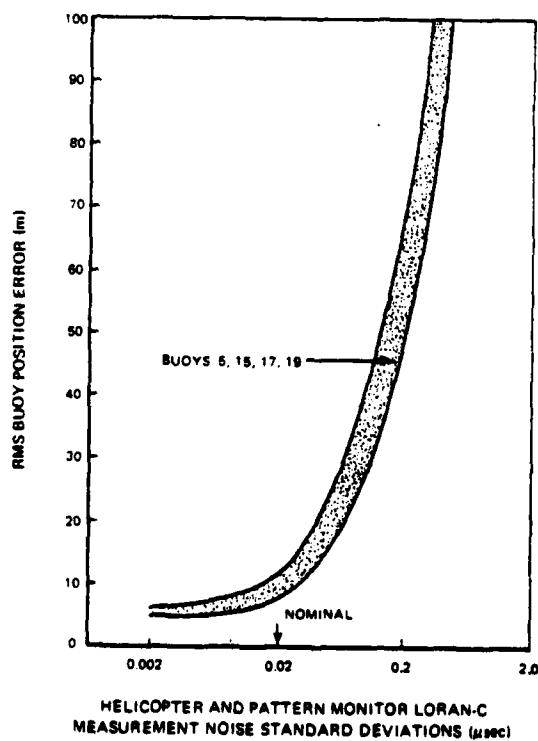
Figure 3.4-15　Buoy Position Error Sensitivity to
Pattern Monitor and Helicopter Loran-C
Measurement Noise (Variable Geometry)

3-43
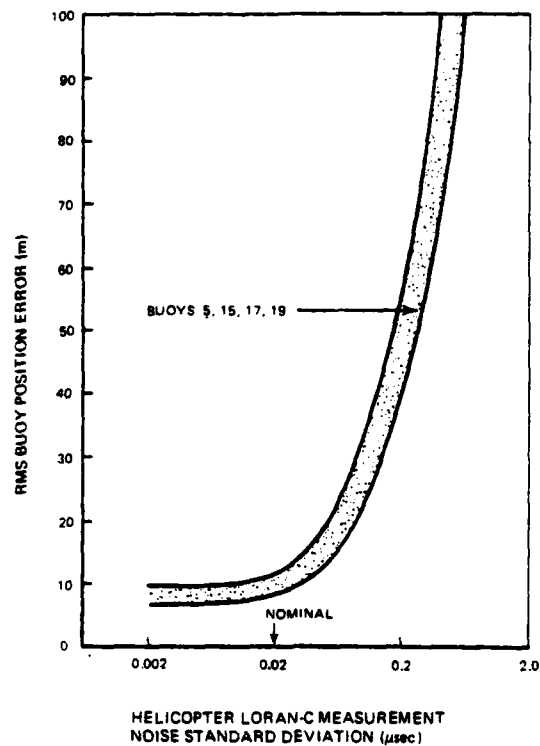
Figure 3.4-16 Buoy Position Error Sensitivity to Helicopter or Pattern Monitor Loran-C Measurement Noise (Variable Geometry)
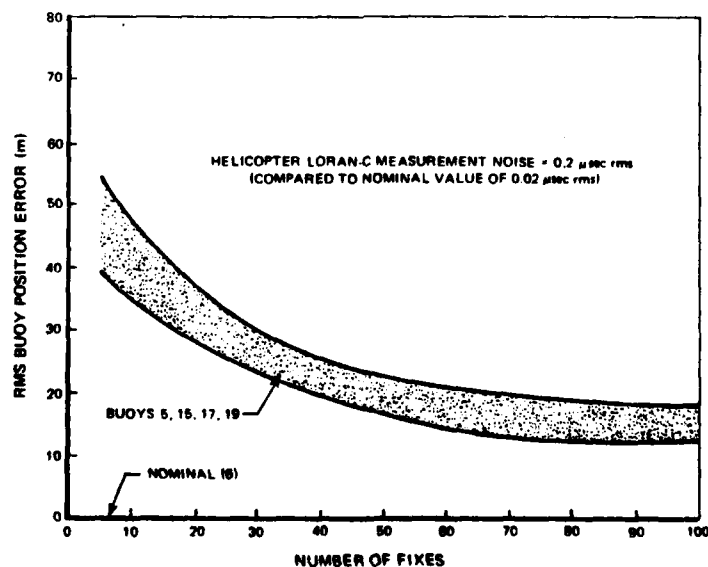
Figure 3.4-17 Buoy Position Error Sensitivity to Number of Fixes With Large Helicopter Loran-C Measurement Noise (Variable Geometry)

3-44

TABLE 3.4-1
SUMMARY OF VARIABLE GEOMETRY ERROR ANALYSES

	PARAMETER	FIGURES	COMMENTS ON BPAS ERRORS
OPERATIONAL PARAMETERS	Helicopter Trajectory	3.4-1 to 3.4-4	Moderate Constraints On Trajectory To Achieve Small Errors
	Straight-Line	3.4-1, 3.4-3	Large Errors
	Peripheral	3.4-1	Small Errors
	Round-Trip	3.4-2, 3.4-3, 3.4-4	Relatively Insensitive To Increases In Round-Trip Separation > 3 km Or Length > 10 km
	Pattern Monitor Location	3.4-5	Increased Errors With Increased Distance From Buoy Network
	Remote Pattern Monitor	3.4-6 to 3.4-9	More Sensitive To Trajectory And Number Of Fixes With Remote Than With Local Pattern Monitor
	Trajectory Location	3.4-6	Smallest Errors With Trajectory In Center Of Buoy Network
	Trajectory Orientation	3.4-7, 3.4-8	Smallest Errors When Trajectory Aligned With Radial To Pattern Monitor
	Number Of Fixes	3.4-9	Reduced Errors With More Fixes
	Number Of Buoys Audited	3.4-10	Increased Errors If Only One Or Two Buoys Audited
ERROR MODEL PARAMETERS	Loran-C Scale Factor Error Refractive Index Error Helicopter Altitude Error Microwave Common Timing Error	Not Shown	Insensitive To These Parameters For A Factor Of 1,000 Range On Either Side Of Nominal
	Microwave Propagation Velocity Error	3.4-11	Relatively Insensitive To Changes In Propagation Velocity Error
	Microwave Independent Timing Error	3.4-12	Moderately Sensitive To Increased Independent Timing Error
		3.4-13	Reduced Errors With More Fixes
	Microwave Measurement Noise	3.4-14	Sensitive To Increased Measurement Noise
		3.4-17	Reduced Errors With More Fixes
	Loran-C Measurement Noise	3.4-15, 3.4-16	Sensitive To Increased Measurement Noise; Reduced Errors With More Fixes

A straight-line helicopter trajectory results in poor accuracy under all conditions considered. A moderate deviation from a straight-line trajectory (3 km by 10 km rectangular trajectory) improves accuracy significantly, under otherwise nominal conditions. Accuracy degrades with increasing distance of the pattern monitor from the buoy network, but can be restored by increasing the number of fixes or by increasing the separation of outbound and inbound legs of the helicopter trajectory. Accuracy sensitivity to other error sources can also be reduced by processing additional measurements. The sensitivity of the Variable Geometry accuracy to Loran-C geometry is significantly less than for the TD Transmission configuration.

3.5   PULSE RESTRANSMISSION SIMULATION RESULTS

The Loran-C Pulse Retransmission BPAS configuration is expected to be less accurate than the TD Transmission configuration due to:

  o   Shorter allowable averaging times necessary to satisfy
    buoy power requirements

  o   Pulse distortion and uncompensated phase shifts introduced
    in the modulation/demodulation process

  o   Additional noise in the retransmission frequency band.

Because the Pulse Retransmission configuration was determined to involve more costly equipment and greater technical risk than TD Transmission (Chapter 2), the relationship between the above effects and Pulse Retransmission BPAS accuracy was not analyzed in detail in the present study. However, coarse simulations were performed to analyze the effect of Pulse Retransmission on Loran-C third-cycle identification. Appendix F includes a description of the model employed in these simulations, and a discussion of the effect of bandpass filter design tolerances and a nonlinear modulation/demodulation process on Loran-C third-cycle identification.

It is concluded from the Pulse Retransmission simulations that Loran-C third-cycle identification is not significantly affected by the following parameters:

o   Manufacturing tolerances (from buoy to buoy) on the center frequency and bandwidth of Loran-C bandpass filters employed in the pulse retransmission equipment on the buoy

o   Static (memoryless) nonlinearities in the modulation/demodulation process.

These results are based on a simple model of a complex system and are intended to be used only as a foundation for more detailed analytical studies. In order to estimate TD measurement errors for the Pulse Retransmission BPAS configuration, a detailed nonlinear dynamic model would have to be developed for the modulation/demodulation process. If an estimate of TD measurement errors becomes available, the sensitivity analysis results presented for TD Transmission in Section 3.3 can be applied to estimate buoy position error for the Pulse Retransmission configuration.

4. COMPUTATIONAL AND MANPOWER REQUIREMENTS

4.1 INTRODUCTION

Implementation of a Buoy Position Auditing System (BPAS) by the U.S. Coast Guard would impose certain computational and manpower requirements. The expected requirements for the TD Transmission and Variable Geometry BPAS configurations are discussed in this chapter. For convenience, the buoy audit mission is divided into the following phases:

- o Data Collection phase -- collect and store the necessary data, and determine data validity

- o Position computation phase -- process the data to compute buoy position fixes

- o Decision-making phase -- employ the position fixes to decide whether or not the buoys are "on station".

The three phases are discussed in Sections 4.2 to 4.4, respectively, and summarized in Section 4.5.

4.2 DATA COLLECTION PHASE

The data collection phase of the buoy audit mission requires minimal computation and manpower. Data collection equipment can be designed to operate semi-automatically, only involving manual interfaces for initialization and data validation.

4.2.1 TD Transmission

In the TD Transmission configuration, the buoy audit is conducted either from a U.S. Coast Guard shore station or from a moving platform such as a helicopter. When the audit is conducted from the shore station, the command sequence discussed in Section 2.2 is employed to "turn on" the buoy Loran-C receivers and request time-averaged TD's. In this command sequence, the TD's for all buoys are averaged during a common 5-10 min. time interval. It is desirable to average the pattern monitor TD's during the same

time interval as the buoy TDs, to avoid errors due to "stale" pattern monitor data.*
This can be accomplished by employing the same TD Transmission equipment on
the pattern monitor as is employed on the buoys (the VHF antenna is not necessary
if the pattern monitor is located at the shore station). In this way, pattern monitor
TD's are synchronized with buoy TD's, without the need for time-tagging the data.
After the TD's from the buoys and pattern monitor are received and stored on
magnetic tape, a validity check is performed to

- o Determine whether or not all TD data have been received

- o Compare measured TD's with expected TD's to identify
     suspect data (e.g., due to Loran-C cycle slips).

The validity check can be conducted by one person using a desk-top calculator. If a
valid data base is not obtained, the command sequence is reinitiated. It is
advantageous, from a buoy power consumption viewpoint, to interrogate only those
buoys from which valid data are not received. However, this requires a buoy
identification code on the VHF interrogation signal.

When the TD Transmission configuration is implemented using a
helicopter, the following complications arise:

- o The helicopter must be in the line-of-sight of the buoys
     during the command sequence

- o Data validity must be checked immediately to permit reinitiation
     of the command sequence during the flight, if necessary.

The line-of-sight constraint, together with the constraint that the helicopter not be
dedicated to the buoy audit mission, may require that the buoys be identified by a
code and interrogated individually or in small groups, rather than be staggered to
guarantee line-of-sight transmission to all buoys. If a large number of buoys are
audited with a helicopter, the helicopter crew may be required to perform some
minor tasks to properly schedule the interrogations. Additional tasks may have to
be performed to check for data validity, but these can be minimized by automating
the validity checks in a microprocessor-based control unit.

---

*Synchronous pattern monitor and buoy TD's are especially important due to the
discontinuous nature of Local Phase Adjustments (Ref. 22).

The use of staggered buoy interrogations requires that pattern monitor TD data also be staggered during the flight. Furthermore, if the pattern monitor does not lie in the line-of-sight of the helicopter, it may be necessary to interrogate the pattern monitor continuously from the shore station, during the flight. This approach necessarily requires time-tagging of buoy and pattern monitor TD's.

4.2.2 Variable Geometry

In the Variable Geometry configuration, the buoy audit is always conducted from a helicopter. Since the helicopter is not equipped to interrogate the pattern monitor, the helicopter data (Loran-C, microwave ranging, and altitude) are stored with time-tags. Pattern monitor TD data are received continuously at the shore station (over a telephone or VHF data link) and also stored with time tags for later processing.

The Variable Geometry error analysis results presented in Chapter 3 show that buoy position-fix errors are not reduced sufficiently when the Loran/microwave fixes are taken along a straight-line helicopter path. To obtain maximum variability in helicopter-to-buoy geometry, it is recommended that fixes be taken at points distributed along the entire round-trip flight path. This fix scenario could be accomplished by the following command sequence:

o   Determine when (e.g., at present times) or where (e.g. using Loran-C) the next fix is to be taken

o   "Turn on" the microwave transponders on all buoys

o   Range to the buoys in sequence, triggering each buoy transponder with a different identification code

o   All buoy transponders "turn off" after a preset time interval.

In this command sequence, the transponders are deactivated between fixes to conserve buoy battery power. Some buoys may not be within the line-of-sight of the helicopter when a fix is taken, or the ranges may be greater than the range for which the microwave system is designed. To accommodate this situation, the microwave interrogator ranges to the next buoy in sequence if a buoy response is not received within a certain period of time.

The scheduling of fixes along the helicopter flight path could be performed automatically during the flight based on geometrical considerations and the approximate helicopter position indicated by Loran-C. However, the error analysis results in Chapter 3 indicate that the details of the fix schedule are not critical, as along as the fixes are taken along the entire round-trip flight path. It is expected that a schedule consisting of fixes taken at equal time intervals can satisfy BPAS accuracy requirements. The time interval between fixes will be chosen based on accuracy and buoy battery drain constraints.

The Variable Geometry BPAS configuration imposes few constraints on the helicopter flight pattern. Nevertheless, it is required that each audited buoy be within range and line-of-sight of the helicopter at enough points along the flight path to provide the least-squares algorithm with the necessary data to compute an accurate buoy position fix. Although this can be largely guaranteed by limiting buoy audits to certain categories of flights, it is also desirable to indicate automatically to the helicopter crew whether or not a sufficient number of fixes are obtained. The crew could then alter the flight pattern to obtain additional fixes, if required by the BPAS mission and if consistent with the primary mission objectives.

4.3 POSITION COMPUTATION PHASE

4.3.1 TD Transmission

Computation of a buoy position fix in the TD Transmission configuration involves the following steps:

o Assemble the relevant data -- buoy and pattern monitor
   Loran-C TDs at the equipment installation and audit times,
   buoy position coordinates at the equipment installation
   time, and Loran-C chain transmitter coordinates

o Estimate the buoy Loran-C range-differences associated with
   the measured TD pair, using the differential Loran-C
   algorithm described in Appendix A (Section A.4.1)

o Solve for the buoy position fix as the intersection of
   the two spherical hyperbolas corresponding to the range
   differences.

4-4

The computation and data storage requirements of the above procedure are minimal and can be accommodated with a desk-top calculator.

4.3.2 Variable Geometry

Computation of buoy position fixes in the Variable Geometry configuration involves the following steps:

o   Assemble the relevant data — helicopter and pattern monitor Loran-C TDs, microwave ranging and altitude data, pattern monitor position coordinates, and Loran-C chain transmitter coordinates

o   Estimate helicopter Loran-C range differences at each point on the flight path, using the differential Loran-C algorithm described in Appendix A (Section A.4.2)

o   Solve for helicopter position fixes at each point on the flight path

o   Employ the helicopter position fixes, together with microwave ranging and altitude data, to compute coarse buoy position fixes (Appendix C)

o   Refine the coarse fixes with the least-squares algorithm (Appendix C) to determine fine buoy position fixes.

The first four steps require minimal computation and data storage. Estimates of data-processing time and computer storage for the least-squares algorithm are presented in Table 4.3-1. The estimates are based on direct implementation of the equations detailed in Appendix C, and include only arithmetic operations and floating-point variables. A significant reduction in storage and a moderate reduction in data-processing time should be achievable by designing the computer software for maximum efficiency. It is apparent from Table 4.3-1 that computation requirements increase exponentially with an increase in the number of buoys audited. If a large number of buoys are audited in a harbor, Variable Geometry computation and storage can be reduced significantly by processing the

buoys in groups. For example, if 300 buoys are audited, data-processing time per fix can be reduced from 3000 sec to 48 sec by implementing the least-squares algorithm for 12 buoy groups (25 buoys in each group). On-line storage requirements are reduced from 20 megabytes to 0.1 megabytes. Degradation in buoy position-fix accuracy is expected to be minimal, as long as the buoys are processed in groups of four or more (Chapter 3, Figure 3.4-10).

TABLE 4.3-1

COMPUTATION REQUIREMENTS FOR LEAST-SQUARES ALGORITHM

NUMBER OF BUOYS	DATA-PROCESSING TIME PER FIX* (sec)	STORAGE CAPACITY** (megabytes)
1	0.004	0.002
10	0.4	0.02
25	4.0	0.1
50	20.0	0.5
100	200.0	2.0
300	3000.0	20.0

*Based on 1 μsec per arithmetic operation.

**Based on 4 bytes per floating-point variable.

4.4   DECISION-MAKING PHASE

Irrespective of which candidate BPAS configuration is implemented by the U.S. Coast Guard, an approach is required for using the outputs of the Buoy Position Auditing System to decide whether or not buoys are "on station." Furthermore, it is desirable to obtain an indication of the confidence that the decision is correct. The approach employed in the decision-making phase of the buoy audit mission is referred to as the "decision algorithm." Candidate decision algorithms are discussed in this section.

4.4.1 Definition of Buoy Station Contour

It is convenient to introduce the concept of buoy station contour -- the boundary of the region in which the buoy may wander and still be considered "on station". The buoy station contour can be established by either of the methods described below, although the two methods do not in general result in the same contour.

4-6

In the first method, the buoy station contour is established by identifying all locations for which the buoy serves its intended function as an aid to navigation. For example, a traffic separation buoy may serve its intended function anywhere in a rectangle whose long side is aligned with the direction of traffic flow, while a major obstruction buoy may have to be located to one side of the obstruction (Figure 4.4-1a). This method of establishing the buoy station contour emphasizes the location of the buoy, rather than the buoy anchor, and recognizes that a buoy may drag anchor without necessarily affecting its use as an aid to navigation.

In the second method, the buoy station contour is established by measuring the buoy position with the Buoy Position Auditing System under different tide and wind conditions, prior to implementation of the operational system. If the buoy anchor does not move during the measurement process, an estimate of the buoy watch circle* is obtained and the watch circle may be employed as the buoy station contour (see Figure 4.4-1b). Alternatively, the buoy position measurements can be employed to establish a number of buoy station contours corresponding to different categories of tide and wind conditions.) This method of establishing the buoy station contour emphasizes the location of the buoy anchor since the buoy position measurements are assumed to be obtained when the buoy anchor is in the single location mandated by the U.S. Coast Guard (surveyed by a buoy tender to a stated 1 to 2 m accuracy).

4.4.2 BPAS Decision Algorithms

It is recommended that the decision algorithm in an operational Buoy Position Auditing System provide the following outputs to U.S. Coast Guard personnel:

o Buoy position fix

o Decision that the buoy is on or off station

o Confidence in the decision.

Two decision algorithms are outlined below.

---

*The path followed by the buoy may be elongated, rather than circular (Ref. 23).

4-7
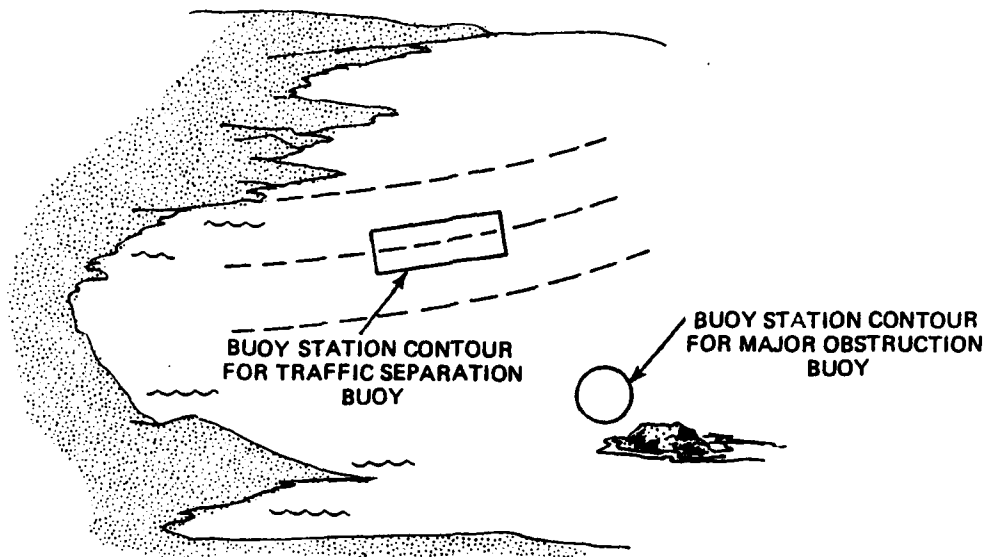
a) Functional Station Contour
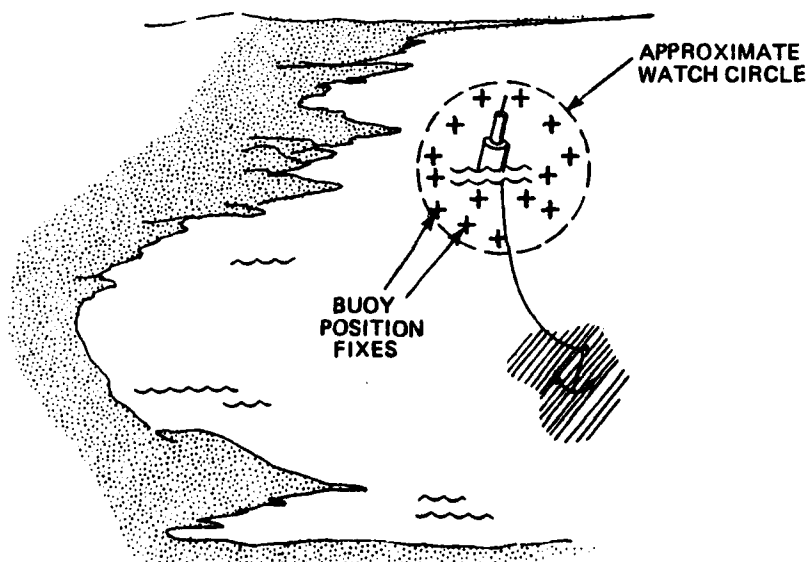
b) BPAS-Indicated Station Contour (Watch Circle)

Figure 4.4-1   Definition of Buoy Station Contour

The first decision algorithm is based on the buoy station contour defined in Section 4.4.1. The buoy position fix is compared to the buoy station contour, preferably on a graphical display. It is decided that the buoy is on station if the fix falls within the station contour, and off station if the fix is outside of the contour (See Figure 4.4-2).

In this approach, the confidence in the decision is based on expected buoy position fix errors. Position-fix error is characterized statistically by a bivariate normal probability density function. Contours of equal probability density are ellipses centered on the position fix (Figure 4.4-2). The probability density function is based on a theoretical error model (validated by experiment) from which an error covariance matrix is computed. The error model includes the various error sources (e.g., Loran-C propagation errors and measurement noise) and the relative geometry of the buoy and helicopter flight path (for Variable Geometry configuration, only), as described in Section 3.2. The probability that the true buoy position is within a particular region can be computed by integrating the probability density function over the region. If the position fix is inside the station contour, the Probability of a Correct Decision (PCD) is the integral of the probability density function inside the station contour; if the position fix is outside the station contour, the PCD is the integral of the probability density function outside the station contour.

If the decision is made that a buoy is off station, the U.S. Coast Guard may, depending on the value of the PCD, choose either to service the buoy immediately or to issue a marine alert pending further verification. The PCD may also be employed to rank off-station buoys to aid in scheduling buoy-tender operations. Similarly, if the decision is made that a buoy is on station, the PCD may aid in the scheduling of future position audits.

In the second decision algorithm, the buoy station contour concept is not used. Instead of defining a specific boundary which encompasses the acceptable buoy locations, a scatter pattern is accumulated for each buoy by measuring its position with the Buoy Position Auditing System over a range of tide and wind conditions, prior to implementing an operational system. (Alternatively, the buoy position measurements can be employed to establish a number of scatter diagrams, corresponding to specific tide and wind conditions.) For a given audit, the buoy position fix is compared to the appropriate scatter diagram. An on-station (or off station) decision is made if the position fix falls near to (or far from) the center of the scatter pattern.

CONTOURS OF POSITION-FIX
ERROR PROBABILITY DENSITY
FUNCTION

BUOY POSITION FIX

BUOY STATION CONTOUR

PCD = Integral of Probability Density Function Inside Station Contour

LONGITUDE

a) Decision: On Station

CONTOURS OF POSITION-FIX
ERROR PROBABILITY DENSITY
FUNCTION

BUOY POSITION FIX

BUOY STATION CONTOUR

PCD = Integral of Probability Density Function Outside Station Contour

LONGITUDE
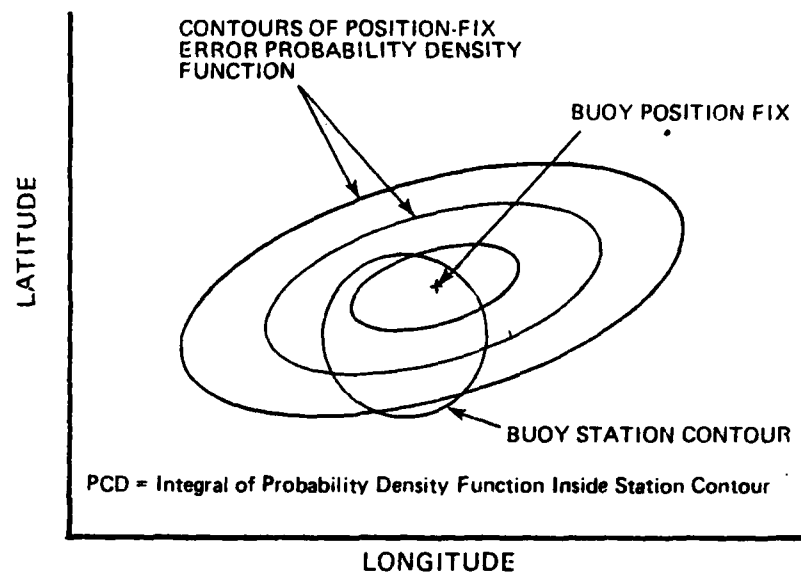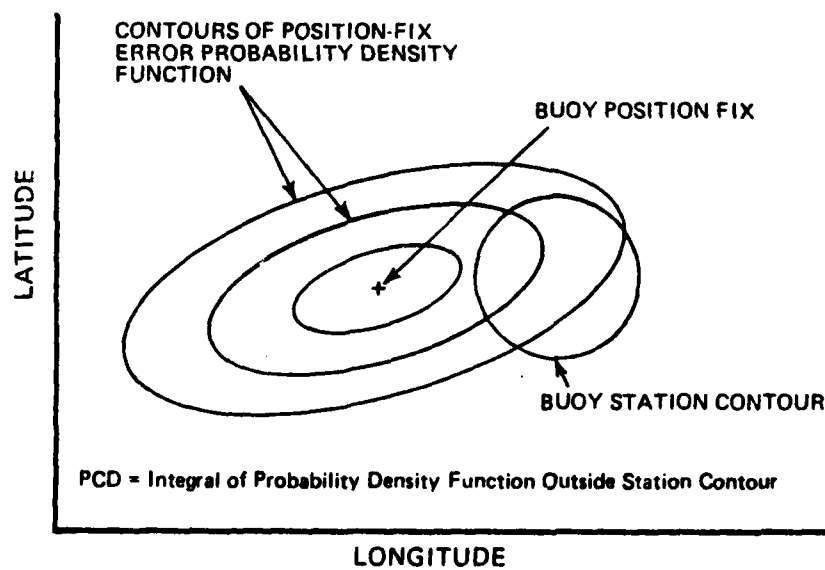
b) Decision: Off Station

Figure 4.4-2   BPAS Decision Algorithm Based on
Buoy Station Contour

4-10

The confidence in a correct decision is a function of the density of the scatter pattern and the distance of the buoy position fix from the center of the pattern. A quantitative algorithm for making the decision and for computing the associated confidence in the decision could be developed based on BPAS experimental data.

The candidate BPAS decision algorithms discussed herein (summarized in Figure 4.4-3) range from the "theoretical" involving a buoy station contour and theoretical probability density function, to the "empirical", relying on a BPAS-generated scatter pattern. The BPAS data required in the empirical decision algorithm (or in the theoretical algorithm with a BPAS-indicated station contour) must be collected prior to implementing the operational system. The data also must cover a range of tide and wind conditions, and, therefore, may require numerous audits to assemble. Acquisition of the necessary data would be more convenient if performed from a shore station rather than from a helicopter. However, this is not considered to be a major advantage of the TD Transmission configuration over the Variable Geometry configuration, since the data collection will require a several month period in either case.

4.5   SUMMARY OF COMPUTATIONAL AND MANPOWER REQUIREMENTS

Consideration of the computational and manpower requirements of the TD Transmission and Variable Geometry BPAS configurations leads to the following conclusions:

o Neither configuration imposes excessive computational
  and manpower requirements during the data collection phase
  of the buoy audit mission

o The position computation phase can be implemented on a desk-top
  calculator for TD Transmission, but requires a mini-computer or
  large-scale computer facility for Variable Geometry

o Both configurations require that trained U.S. Coast Guard
  personnel be available to interpret the results of the buoy
  audit in the decision-making phase.

Further consideration should be given to computational and manpower issues during the BPAS experiment.

4-11

"THEORETICAL"   "EMPIRICAL"

STEP 1 DESIRED
        BUOY
        LOCATION

| FUNCTIONAL STATION CONTOUR | BPAS-INDICATED STATION CONTOUR (WATCH CIRCLE) | BPAS-GENERATED SCATTER DIAGRAM |

STEP 2 DECISION

| DETERMINE IF FIX IS INSIDE OR OUTSIDE OF STATION CONTOUR | DETERMINE HOW CLOSE FIX IS TO CENTER OF SCATTER DIAGRAM* |

STEP 3 CONFIDENCE IN
        DECISION

| COMPUTE PROBABILITY OF A CORRECT DECISION USING PROBABILITY DENSITY FUNCTION | DETERMINE CONFIDENCE FROM SHAPE OF SCATTER DIAGRAM AND RELATIVE LOCATION OF BUOY POSITION FIX* |

*QUANTITATIVE METHODS
SHOULD BE DEVELOPED AFTER
ACTUAL BPAS TEST DATA
ARE AVAILABLE

Figure 4.4-3   Summary of Candidate BPAS
                  Decision Algorithms

5. COMPARISON AND RECOMMENDATIONS

5.1 PERFORMANCE COMPARISON OF BPAS SYSTEM CONFIGURATIONS

A comparison between the TD Transmission, Pulse Retransmission and Variable Geometry approaches is shown in Table 5.1-1 . Position errors for the Pulse Retransmission configuration are expected to be greater than for TD Transmission due to the adverse effect of the Loran-C pulse processing. Since there is also a clear disadvantage of the Pulse Retransmission configuration with respect to cost and technical risk, a decision was made at an interim project briefing on 31 July 1979 to discontinue detailed analysis of the accuracy of the Pulse Retransmission configuration. Therefore, accuracy results for the Pulse Retransmission system are not included in this report. A comparison of the accuracy of the TD Transmission and Variable Geometry BPAS configurations is summarized in Table 5.1-2.

Under the nominal conditions assumed for this study, the Variable Geometry configuration is more accurate than the TD Transmission configuration. Nominal buoy position error is less than 10 m rms in the Variable Geometry configuration, while errors range from 10 m rms to 30 m rms* (with best case GDOP) in the TD Transmission configuration. The TD Transmission configuration has the advantage of minimal impact on U.S. Coast Guard operations, but the requirements of the Variable Geometry configuration are not severe. Only six microwave ranging fixes, taken along a 3 km by 10 km rectangular helicopter trajectory, are required to achieve a 10 m rms buoy position-fix accuracy in the Variable Geometry configuration. The Pulse Retransmission configuration is expected to be less accurate than the TD Transmission configuration because of degradation caused by increased Loran-C measurement noise. Figure 3.3-6 can be used to assess the impact of increased measurement noise on Pulse Retransmission buoy position error.

Loran-C scale factor error impacts the TD Transmission and Variable Geometry configurations differently. The TD Transmission configuration has the advantage of calibrating the Loran TD reading at the time the equipment is installed on the buoy. This calibration reduces the Loran-C scale factor error

---

*Dependent on range from buoy to pattern monitor and GDOP.

Table 5.1-1

Comparison of BPAS Configurations

Consideration	TD Transmission	Pulse Retransmission	Variable Geometry
Cost/Buoy	$1,060 to $1,360	$1,540 to $1,750	$2,500 to $3,500
Cost/Base Station	$7,000	$63,000	$19,000 to $24,000
Audit Capability	10 buoys per 8 min. 20 sec. (60 buoys per 10 min.)	1 buoy per 6-10 min. (6-10 per hour)	7 buoys per 15 min.
Buoy power requirements (A-H = Ampere-Hours) based on 1 audit per week	0.23 A-H/day average	0.27 A-H/day average	0.21 to 0.73 A-H/day average
Max. per day of audit	0.33 A-H/day	0.60 A-H/day	0.26 to 3.36 A-H/day
Frequency Allocation	Standard VHF Communication Channel	Standard VHF Communication Channel and wide band L-band	Wide band L-band or X-band
Ability to work with helicopter, ship and shore base station	Yes	Yes	No (requires moving platform or multiple shore stations)
Major equipment development required	No	Yes	Yes
Technical Risk	Low; modify existing equipment	High; may not be feasible to overcome Loran-C pulse distortion problem	Medium; sophisticated computer processing software needed. also requires development of complete ranging system if CW ranging is used.

TABLE 5.1-2

TD TRANSMISSION AND VARIABLE GEOMETRY ACCURACY COMPARISON

	CONSIDERATION	TD TRANSMISSION	VARIABLE GEOMETRY
	Nominal rms Error	10-30 m	<10 m
	Operational Requirements	Minimal	3 km By 10 km Rectangular Trajectory With Six Fixes
LORAN-C ERRORS	Scale Factor Error	Initial Calibration When Equipment Is Installed; BPAS Errors Sensitive To Scale Factor Error	No Initial Calibration; BPAS Errors Not Sensitive To Scale Factor Error Because Of Calibration By Least-Squares Algorithm
LORAN-C ERRORS	Pattern Monitor Measurement Noise	BPAS Errors For Both Configurations Sensitive To An Increase In Pattern Monitor Measurement Noise; Nominal Should Be Achievable, However	
LORAN-C ERRORS	Buoy Or Helicopter Measurement Noise	Factor Of Five Increase In Measurement Noise Produces 50 m rms BPAS Error; Subject To Extremes In Buoy Environment	Factor Of Five Increase In Measurement Noise Produces 30 m rms BPAS Error; Dependent On Receiver Tracking-Loop Bandwidth
LORAN-C ERRORS	Refractive Index Error	Negligible Impact On BPAS Error For Both Configurations	
MICROWAVE ERRORS	Propagation Velocity Error	The TD Transmission Configuration Is Not Subject To Microwave Ranging And Altimeter Errors	Factor of 10 Increase In Propagation Velocity Error Produces Negligible Increase In BPAS Errors
MICROWAVE ERRORS	Common Timing Error		BPAS Errors Not Sensitive To An Increase In Common Timing Error
MICROWAVE ERRORS	Independent Timing Error		Factor Of 10 Increase In Independent Timing Error Produces 30 m rms Buoy Position Error
MICROWAVE ERRORS	Measurement Noise		Factor Of Five Increase In Measurement Noise Produces 30 m rms Buoy Position Error
	Altimeter Error		BPAS Errors Not Sensitive To Altimeter Error
	Pattern Monitor Location	BPAS Errors Sensitive To Distance Of Pattern Monitor From Buoys	Less Sensitive Than TD Transmission; Sensitivity Can Be Further Reduced By Additional Fixes And/Or Improved Helicopter Trajectory
	Potential For Improved Accuracy	Multiple Pattern Monitors	BPAS Error Estimates Significantly Less Than 10 m rms Are Unrealistic Because Of Potential Impact Of Unmodeled Error Sources
	Loran-C Geometry (GDOP)	Very Sensitive - Proportional to GDOP	Relatively Insensitive

5-3

standard deviation to 12 nanosec/km (from a value of 33 nanosec/km if no initial calibration is made, as in the Variable Geometry configuration). However, in the Variable Geometry configuration, processing of redundant information in the least-squares algorithm results in calibration of the scale factor error at the time of the audit, even from the large initial value. For the round trip trajectory shown in Figure 3.4-2, the least-squares algorithm reduces scale factor error standard deviation from 33 nanosec/km to approximately 5 nanosec/km. This nominal scale factor error standard deviation for TD Transmission is a worst-case value computed by assuming the equipment to be installed when the conductivity is at an extreme of its expected seasonal cycle. If equipment is actually installed when the conductivity is at its average value, rather than at an extreme value, the scale factor error standard deviation is reduced to 6 nanosec/km, and buoy position error is 20 m rms or less for all buoys (Figure 3.3-4).

Buoy position errors for both configurations are sensitive to an increase in Loran-C measurement noise. It is expected, however, that the pattern monitor receiver can meet the 0.02 sec design criterion. Investment in a better quality pattern monitor is not warranted because buoy position error would not be substantially reduced (Figures 3.3-6 and 3.4-16). Helicopter Loran-C measurement noise for the Variable Geometry configuration is expected to be higher than the nominal 0.02 sec because of helicopter motion during the signal averaging time. Buoy position accuracy of 30 m rms can still be achieved, however, even with an increase in helicopter measurement noise from 0.02 sec rms to 0.10 sec rms (Figure 3.4-16). The buoy Loran-C receiver for the TD Transmission configuration does not move significantly during the signal averaging time, but it is possible that exposure to extreme environmental conditions may impact its performance. An increase in buoy Loran-C measurement noise to 0.10 sec rms causes an increase in buoy position error to 50 m rms in the TD Transmission configuration (Figure 3.3-6). A decrease in helicopter or buoy Loran-C measurement noise does not improve the accuracy of either configuration significantly under otherwise nominal conditions.

The most important distinction between the TD Transmission and Variable Geometry configurations affecting accuracy is the availability of redundant information in the Variable Geometry configuration. The Variable Geometry configuration is more accurate than the TD Transmission configuration primarily

because of calibration of the Loran-C scale factor error by the least-squares algorithm at the time of the audit. Redundant information also makes the Variable Geometry configuration more adaptable in the event of adverse system constraints, such as a remote pattern monitor location. Accuracy can normally be improved under adverse conditions by increasing the number of fixes or altering the helicopter trajectory.

Sensitivity of Variable Geometry accuracy to ranging errors is relatively small for most error sources. Propagation velocity and common timing errors are well-calibrated by the least-squares algorithm. Hardware performance requirements relative to these error sources could therefore be relaxed from the assumed nominal requirements, if warranted by cost savings. It is more important to control the source of an independent timing error, but a factor of ten increase in this error beyond the assumed nominal value only causes an increase in buoy position error to 30 m rms (Figure 3.4-12). Measurement noise is the most critical hardware parameter in the ranging system. The nominal value of 0.01 sec rms applies to a Pulse Ranging system operating in C-band or X-band; measurement noise for a CW Ranging system operating at L-band is expected to be higher. An increase in measurement noise to 0.05 sec rms causes an increase in buoy position error to 30 m rms (Figure 3.4-14). However, a decrease in measurement noise achieved with a higher quality system will not improve accuracy substantially.

The nominal accuracy of the Variable Geometry configuration estimated (less than 10 m rms buoy position error) meets the expected accuracy requirements for a Buoy Position Auditing System. A study of methods to further improve the accuracy of the Variable Geometry configuration is therefore not warrented. Note that the influence of unmodeled error sources becomes important for estimated buoy position errors less than 10 m rms. For example, errors introduced by buoy motion, or by a Loran-C receiver TD bias, are not modeled.

Improvement of TD Transmission accuracy to 10 m rms for all buoys requires reduction of Loran-C scale factor error, the primary error contributor. The most straight forward approach is to reduce the buoy-to-pattern monitor separation. It is shown in Section 3.3, however, that a separation of less than 3 km is required to achieve 10 m rms accuracy. In order to obtain a separation of less than 3 km,

several pattern monitors may be required. Coverage of Boston Harbor for example, could be achieved with four pattern monitors. Multiple pattern monitors have one additional advantage; with such a system it is conceptually feasible to calibrate the Loran-C scale factor error at the time of each audit, similar to the calibration achieved in the Variable Geometry configuration. Although detailed analysis of this approach was beyond the approach of the present study, it is expected that significant improvement could be achieved with three or more pattern monitors. For maximum accuracy, the position of each pattern monitor should be fixed and known precisely. Some improvement in TD Transmission accuracy may also be possible, by estimating scale factor error through processing of data from certain buoys known to be near to their correct locations during the audit.

The TD Transmission BPAS configuration is very sensitive to Loran-C geometry. Buoy position fix errors are scaled by the Geometric Dilution of Precision (GDOP) - e.g., the position errors for San Francisco Harbor are approximately 4 times the position errors for Boston Harbor. However, in those locations where GDOP is poor the addition of more pattern monitors can reduce the buoy position errors to within acceptable limits. The Variable Geometry position error accuracy is significantly less sensitive to Loran-C geometry. Furthermore, the sensitivity can be reduced by taking additional fixes and/or constraining the helicopter trajectory.

This study has shown that Pulse Retransmission will be significantly inferior to TD Transmission in both performance and cost. The initial reason for considering the Pulse Retransmission approach was the hope that the simplicity of Loran-C processing at the buoy would permit lower cost buoy electronics. While the costing exercise indicates that the Loran-C processing part of the Pulse Retransmission system will in fact be less expensive than the TD Transmission approach, this is overridden by the marked increase in cost for the telemetry transmitter and base station electronics. While the TD Transmission buoy electronics is conceptually much more complicated due to the processing required in the Loran-C monitor receiver, the cost for that complexity is reduced due to the availability of a stand-alone, fully automatic Loran-C receiver. Essentially, the development costs and the development of production expertise for that device has been shared by a broad base of users.

The base station costs again reflect the expense involved in the design and development of technically sophisticated equipment for limited use. The TD Transmission system can be constructed out of standard hardware components with the majority of the custom system design contained in the software programming for the audit control and data acquisition electronics. Pulse Retransmission, on the other hand, requires the special purpose Loran-C receiver which must be designed, produced and documented solely for this application.

The Loran-C pulse retransmission concept has been successfully applied to the tracking of weather balloons, using equipment manufactured by Beukers Laboratories, Inc. (Ref. 25). In addition, the U.S. Coast Guard has conducted analyses and testing of the concept in support of the Distress Alerting and Locating System (DALS) development effort (Refs. 9 and 21). Experience has shown that the modulation/demodulation process can distort the Loran-C pulse envelope, which contains information needed to identify the third cycle of the 100 kHz Loran-C carrier. Since the third-cycle, positive-going zero crossing must be tracked to meet the requirements of a precision buoy audit,* the pulse distortion issue is critical in the assessment of the Pulse Retransmission BPAS configuration. The following approaches for reducing the effect of pulse distortion are considered in this report:

- o   Logarithmic (or similar) pulse compression
- o   Stepped-gain pulse amplification
- o   Time-multiplexed transmission of direct and derived pulses.

Each approach requires a specialized Loran-C receiver to process the coded pulses. There is considerable technical risk involved in pursuing these approaches since Loran-C equipment for their implementation has not been developed and tested.

The audit capability of the two systems differs markedly. Due to the parallel nature of the processing which is performed on the TD Transmission buoy electronics and the relatively short period of time required to transmit the

---

*Other Loran-C carrier cycles may be tracked for non-precision applications such as DALS.

receiver were to become available (a distinct possibility). The reduced channel bandwidth requirement could force selection of the TD Transmission system even if all other considerations were balanced. Due to the congestion of the radio spectrum, the allocation of a wide bandwidth channel is relatively hard to obtain. This is especially true when there is an alternate and viable technology which does not require the wide bandwidth. This indeed is the case between the TD Transmission and Pulse Retransmission approaches. Both approaches require a command link which can be provided by presently authorized VHF communication channels, however, the authorization of a wideband L-band channel for the Pulse Retransmission approach would be difficult to justify in light of the availability of the TD Transmission concept, which could also transmit return data on existing VHF channels.

The power requirements of the buoy ranging transponder depend on the buoy interrogation schedule. The desired schedule, from the viewpoint of buoy position-fix accuracy, is to command all transponders to "turn on" when first entering the field of buoys and then to range on every buoy at points along the entire round-trip flight path. Each buoy transponder is triggered by a different identification code which is included in the ranging signal. This interrogation schedule results in enough data being collected to guarantee acceptable geometry for the buoy position calculation (Section 3.4 and Appendix C). However, a pulse ranging transponder would be active over the entire helicopter flight, causing a potential buoy battery drain of 18 amp-hr per audit (based on a 6 amp current and a 3 hr flight; see specifications for Mini-Ranger transponder in Ref. 29). Adding 6 amp-hr per audit for the command receiver* yields a total drain of 24 amp-hr. The battery drain can be reduced by transponder innovations and/or a different interrogation schedule. For example, data could be collected for only a few segments of the flight pattern and the transponders deactivated between segments. The CW ranging systems require significantly less power than the pulse ranging system.

---

*Assuming a command receiver drain of 0.36 amp-hr/day for seven days.

Since the pulse ranging system assumed here is a relatively simple modification of an off-the-shelf unit, the power drain is a given from its manufacturer. The CW ranging system, on the other hand, is a new development, whose specifications are tailored to the BPAS application. It is probable that a pulse ranging system design could be developed for this program, with an acceptable power drain; however, the development costs would be similar to those for the CW ranging system and considerably in excess of the total cost of the pulse ranging system assumed in this report.

The decision over which type of ranging system to use will require a careful analysis, including the design requirements of all subsystems and a detailed compilation of all error sources for each system. This is beyond the scope of the present study.

The Variable Geometry BPAS configuration requires a greater data processing capability than the TD Transmission and Pulse Retransmission configurations. The differential Loran-C algorithm is somewhat different than the algorithm used in the other configurations, although its computational burden is still minimal. The algorithm employs helicopter and pattern monitor TDs measured at the audit time, but no TD data are assumed to be available for use as an initial reference (Appendix A, Section A.4.2). The difference between helicopter and pattern monitor TDs is used in a simple TD grid prediction model to estimate the position of the helicopter relative to the pattern monitor. The least-squares algorithm, which combines helicopter Loran-C position fixes with range and altitude data, may require a fairly large-scale computer facility for implementation. The buoy positions are all computed together in the least-squares algorithm, in contrast to separately, as in the TD Transmission and Pulse Retransmission BPAS configurations. The optimal integration of data from all buoys enables calibration of certain error sources and reduction of the effect of others (Section 3.4).

Both the TD Transmission system and the Pulse Retransmission system have the ability to work with the base station located on a rapidly moving platform such as a helicopter, a slowly moving platform such as a ship, or fixed shore base stations. This is contrasted to other approaches employing variable geometries, which require either a moving platform as a part of the position solution, or else a network of multiple shore stations for each harbor area.

The technical risk associated with the TD Transmission system is felt to be rather low, due to the ready availability of all major system components. Again in contrast, the Pulse Retransmission system, which requires major development, is assigned high risk. It is further noted that although this study considered several concepts which could be applied to the analog retransmission of Loran-C signals from the buoys to the base station, none of these techniques have been proven in actual systems.

5.2 RECOMMENDED TD TRANSMISSION BPAS EXPERIMENT

An experiment is outlined below for verification of the TD Transmission Buoy Position Auditing System configuration. The experimental outline is intended to be followed by a detailed test plan. The recommended TD Transmission experiment meets the following objectives:

o   Evaluation of the performance of the TD Transmission equipment required on the buoys and at the shore station

o   Assessment of TD Transmission accuracy in Boston Harbor

o   Validation of the differential Loran-C error model presented in this report, to enable TD Transmission accuracy to be estimated for other harbors

o   Testing of algorithms for use in deciding whether or not buoys are "on station."

These objectives can be met by installing Loran-C receivers on floating buoys, at

fixed sites, and on a U.S. Coast Guard vessel, and by installing VHF interrogation equipment at a shore station. Data are collected periodically from the shore station for one year, and additional data are collected using the vessel, at selected times during the year.

5.2.1 Equipment Evaluation

Although equipment performance will be evaluated during the entire experiment, certain special tests are recommended. Proper operation of the Loran-C receivers on the buoys and fixed aids should be verified for a range of environmental conditions. This can be accomplished by periodically positioning the ship next to each buoy or fixed aid, measuring the TDs with the ship's Loran-C receiver, and comparing the TDs with those transmitted from the buoy or fixed aid to the shore station. The incremental position-fixing resolution of the Loran-C receiver selected for the experiment should be determined by navigating the ship along short radials originating at a fixed aid (pattern monitor). The length of the radials should be at least 100 m and the ship's position relative to the fixed aid should be determined by transit theodolite and a measuring line. Data from this experiment permits an evaluation of the contribution of measurement noise to differential Loran-C errors, since propagation effects are negligible within 100 m of a pattern monitor.

5.2.2 Accuracy Assessment for Boston Harbor

Differential Loran-C accuracy in Boston Harbor is determined from TD data collected at five to ten fixed-sites, equipped with Loran-C receivers and VHF transmitters, and placed such that site-to-site distances vary from 1 km to 20 km (with priority given to distances between 3 km and 12 km). Fixed aids to navigation, as well as island facilities, are candidates for fixed sites. Each fixed site should be automatically interrogated periodically from the shore station (e.g., the TSC facility in Cambridge) and its TDs recorded on magnetic tape. It is important to realize that the fixed-site data must be collected for a year to properly assess differential Loran-C accuracy. The data are analyzed by interpreting one fixed site to be a pattern monitor and all other fixed sites to be

Loran-C users (buoys). Each fixed site is in turn defined to be a pattern monitor, thus providing a substantial data base.

Although the fixed sites provide an excellent data base for studying the temporal character of differential Loran-C errors, it is desirable to collect additional Loran-C data from a ship to provide greater spatial detail. It is recommended that the vessel be equipped with a microwave ranging system (e.g., Motorola Mini-Ranger) for precise positioning. (Alternatively, the vessel could visit stationary landmarks in Boston Harbor.) Once per season, the vessel should circumnavigate (to the extent possible) at least one fixed site, at ranges of 1, 3 and 5 km. These data will permit a detailed analysis of the directionality of differential Loran-C errors.

5.2.3 Refinement of Error Model

The differential Loran-C error model discussed in Section 3.2 and Appendix A accounts for the expected effect of the land/sea water conductivity interface. In particular, the errors due to temporal variations in land conductivity (i.e., scale factor errors) are largest if the buoy being audited is less than 15 km from the coastline in the transmitter direction (Type I propagation paths). The error is smallest if the buoy is greater than 200 km from the coastline (Type III propagation paths). If the Boston Harbor experimental results are to be used to estimate TD Transmission accuracy for other harbors, It is important that the distinction among Type I, Type II, and Type III propagation paths be verified. This is best accomplished by interfacing the vessel's precision Loran-C receiver with a cesium beam or rubidium clock to measure Time-of-Arrival (TOA). TOAs should be measured along 10 km radials to the Northeast U.S. Loran-C transmitters as follows:

o   Type I: master (Seneca, NY); along a radial in Boston Harbor

o   Type II: master; along a radial approximately 50 km east of Boston

o   Type III: secondary W (Caribou, ME); along a radial in Boston Harbor.

By combining the TOA data with precise vessel's track data from a microwave

ranging system, the scale factor can be computed for each radial. A relatively large clock drift can be tolerated because a 10 km radial is navigated in less than an hour; the clock phase offset is not important because the data are only used to measure the change in TOA along the radial. The test should be repeated four times during the year to ascertain the seasonal scale factor variation for each path type.

5.2.4 Testing Decision Algorithms

It is recommended that the TD Transmission equipment be installed on an operational buoy and on an experimental buoy, to provide data for testing BPAS decision algorithms (Section 4.4). Each buoy should be interrogated hourly for a month, and daily, thereafter to develop a history of buoy dynamics. The purpose of the operational buoy is to provide the opportunity to demonstrate the system to U.S. Coast Guard personnel presently charged with maintaining buoys on station. The experimental buoy is used to simulate off-station conditions. The anchor of the experimental buoy should be moved (without informing the data analysts) and the candidate decision algorithms employed in an attempt to detect the motion.

5.2.5 Recommended Experimental Hardware

This section defines the hardware necessary for an experimental program to determine the performance of the TD Transmission system. The experimental buoy system is based on the system block diagram shown in Figure 2.2-1. It is assumed that the experimental buoy system will be used both on floating navigational aids and as a differential Loran-C monitor when placed at a fixed site. The suggested experimental buoy equipment and costs are shown in Table 5.2-1. Also listed in this table are the model numbers of typical commercial equipment meeting the system requirements.

Table 5.2-2 shows the development costs associated with the buoy equipment. These costs include modification of the buoy's Loran-C processor firmware to incorporate buoy identification information and other modifications of the output

	$ Per Unit
Antenna System	$ 200
Loran-C Monitor Receiver (Internav LCM 404)	$6,700
Command Receiver (Communitronics MR-18-FM)	$ 400
Power Control/Command Decide	$ 400
Transmitter (Communitronics T-111)	$ 300
Integration/Testing	$2,000
	$10,000

BUOY SYSTEM TOTAL FOR 4 UNITS.................$40,000

Table 5.2-1

Experiment Electronic Equipment Cost,

Buoy Electronic Systems for Experiment (4 units)

Buoy Loran-C Processor	$ 4,000
Power Sequence and Control Logic	$ 4,000
Antenna System	$ 3,000
Integration/Packaging/Testing	$15,000

BUOY DEVELOPMENT TOTAL.......................$26,000

Table 5.2-2

Experiment Electronic Equipment Cost,

Develop Buoy Electronics

data stream which may be required. The antenna system and power sequence control logic are custom designs. Conceptually, the antenna system is straight forward, with the majority of the development effort involved with the design of the mechanical structure and pattern measurement to assure proper operation. The power sequence control logic is assumed to be microprocessor-based and constructed from standard building blocks. The majority of this effort involves the development of firmware to execute the power sequence specified by the experimental test plan.

The base station electronics are based on the block diagram shown in Figure 2.2-3. The required hardware and typical commercial model numbers are listed in Table 5.2-3. It is assumed here that the development hardware will be the hardware used for the experiment. Therefore, items such as the telemetry receiver, command transmitter and antenna system reflect anticipated procurement costs rather than development costs. Here again, the audit and data acquisition control is a custom designed microprocessor-based system with the majority of the development/procurement costs representing firmware which provides the functions required by the experimental test plan.

The quick-look data capability requires special comment. It is not anticipated that a quick-look capability will be included in the operational system. It is provided in the experimental system to permit on-site analysis of the experimental data and verification of system performance prior to final data analysis. It is possible that this quick-look data capability can be provided by existing capital equipment.

All base station equipment is assumed to conform to high quality commercial construction standards. In particular, it is not envisioned that this equipment will be modified or procured to flightworthy hardware standards. Due to the experimental nature of this program, it is felt that there is little risk in the use of commercial equipment in the helicopter airborne environment and further, that the cost of providing equipment certified for aircraft operation would unreasonably increase the expense of the experimental program.

The hardware equipment costs for the experimental program are summarized in Table 5.2-4. Data sheets for all cited pieces of commercial equipment are

Telemetry Receiver (Communitronics MR-11)	$ 1,100
Command Transmitter (Communitronics MT-11-10 Watts)	$ 1,500
Audit & Data Acquisition Control	$ 8,000
Antenna System	$ 200
QUICK-LOOK DATA CAPABILITY	$20,000
Integrate/Package/Test	$15,000

BASE ELECTRONICS TOTAL......................$45,800

Table 5.2-3
Experiment Electronic Equipment Cost,

Develop Base Electronics

Develop Buoy	$ 26,000
Buoy Systems for Experiment	$ 40,000
Base Electronics	$ 45,800
System Specification & Technical Monitoring	$ 30,000

SYSTEM TOTAL.....................$141,800

Table 5.2-4

Experiment Electronic Equipment Cost,

Total

contained in Appendix G. The quoted costs do not include money for data reduction hardware or software; thus these costs are sufficient to pay for experimental hardware, but not the experiment itself. However, very recent data indicates that some of the quoted costs can be substantially reduced. Hardware being developed for the Suez Canal Vessel Traffic System, which uses differential Loran-C with time differences transmitted to a base station via a digital data link, may be applicable to the BPAS requirement. In this event, it appears that the total in Table 5.2-4 would reduce to about $90,000.

APPENDIX A
DIFFERENTIAL LORAN-C ERROR MODEL

A.1   INTRODUCTION

The candidate Buoy Position Auditing System (BPAS) configurations considered herein employ differential Loran-C, either alone (for TD Transmission and Pulse Retransmission) or in combination with a microwave ranging system (for Variable Geometry). In this appendix, a model is derived which characterizes differential Loran-C position errors in terms of signal propagation parameter variations and measurement noise.

The relationship between position error and range difference error is reviewed in Section A.2. Loran-C signal propagation is discussed in Section A.3, where an equation is derived to express measured time difference (TD) in terms of propagation parameters and measurement noise. The TD equation is employed in Section A.4 to derive the range difference error equations, the structures of which are identical for the three candidate BPAS configurations. In Section A.5, the error statistics applicable to the individual BPAS configurations are discussed.

A.2   RELATIONSHIP BETWEEN POSITION ERROR AND RANGE DIFFERENCE ERROR

The candidate BPAS configurations employ the hyperbolic mode of Loran-C, whereby a position fix for a buoy or helicopter is computed as the intersection of two hyperbolic lines-of-position, each defined by a range difference. The

range differences for a transmitter triad consisting of two
secondary stations (1 and 2) and a master station (m) are

$$RD_1 = R_1 - R_m$$
$$RD_2 = R_2 - R_m$$
$$(A.2-1)$$

where R_i is the range from transmitter i to the Loran-C user
(see Fig. A.2-1). Each range difference is estimated from
time differences measured at the user and a pattern monitor,
in the manner described in Section A.4. North and east posi-
tion errors (δN and δE) are related to errors introduced in
the conversion from time difference to range difference (δRD_1
and δRD_2) by the following equation:

$$\begin{bmatrix} \delta N \\ \delta E \end{bmatrix} = - \overbrace{\begin{bmatrix} (\cos\beta_1 - \cos\beta_m) & (\sin\beta_1 - \sin\beta_m) \\ (\cos\beta_2 - \cos\beta_m) & (\sin\beta_2 - \sin\beta_m) \end{bmatrix}}^{B}{}^{-1} \begin{bmatrix} \delta RD_1 \\ \delta RD_2 \end{bmatrix} \quad (A.2-2)$$

R-46630
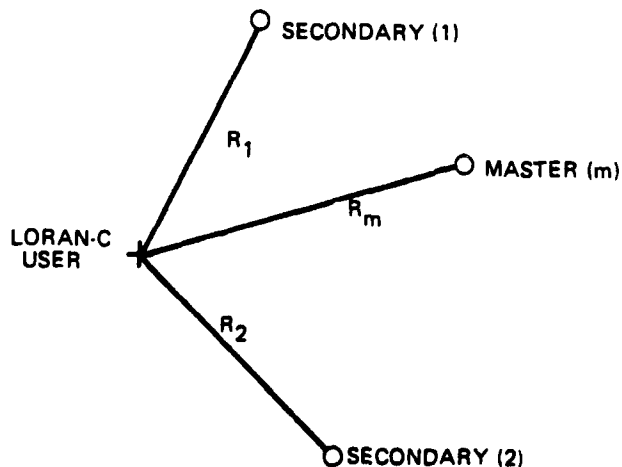
Figure A.2-1 Hyperbolic Loran-C Geometry

A-2

Bearing angles from the user to transmitter i, measured clockwise from north, are denoted by β_i in Eq. A.2-2. The transformation matrix B is very nearly the same for all user locations in a harbor, unless the harbor is located near a Loran-C transmitter. However, range difference errors depend critically on the location of the user <u>within the harbor</u>, specifically his location with respect to the pattern monitor.

Geometric Dilution of Precision (GDOP) is a scalar index which can be used to characterize the transformation matrix B, for the purpose of comparing Loran-C geometries in various U.S. harbors. GDOP is the ratio of radial position error, $(\delta N^2 + \delta E^2)^{\frac{1}{2}}$, to range difference error, under the assumption that the two range difference errors have equal standard deviations and are correlated with correlation coefficient 0.5 (Ref. 10):

$$ GDOP = \frac{a}{2 \sin\theta} \left[\frac{1}{\sin^2\alpha} + \frac{1}{\sin^2\gamma} - \frac{\cos\theta}{\sin\alpha \; \sin\gamma} \right]^{\frac{1}{2}} \qquad (A.2-3) $$

where

$\alpha = (\beta_1 - \beta_m)/2$

$\gamma = (\beta_2 - \beta_m)/2$

$\theta = (\beta_1 - \beta_2)/2$

$a = \sqrt{2}$ (normalizes GDOP to unity for perfect geometry)

Some care must be exercised in employing GDOP as an indicator of Loran-C geometry when one range difference error is expected to be much larger than the other. In this case, the actual transformation matrix B must be considered in comparing Loran-C geometries.

A.3   EQUATION FOR MEASURED TIME DIFFERENCE

In this section, an equation is derived which relates measured time difference to propagation parameters and measurement noise. Although certain simplifying assumptions are made in the derivation of the TD equation, the assumptions do not detract from the utility of the equation for error modeling. Therefore, the equation is assumed to be exact in the derivation of the range difference error equation in Section A.4.

The measured time difference at a Loran-C user location u at time t is denoted by $TD_i(u,t)$, for a transmitter pair consisting of secondary station i and the master station. The measured TD is related to signal propagation delays, emission delay[*] and noise by the equation

$$TD_i(u,t) = \phi_i(u,t) - \phi_m(u,t) + ED_i(t) + v_i(u,t) \quad (A.3-1)$$

where

$$\phi_i(u,t) = \text{propagation delay from i to u}$$
$$\phi_m(u,t) = \text{propagation delay from m to u}$$
$$ED_i(t) = \text{emission delay for secondary i}$$
$$v_i(u,t) = \text{measurement noise}$$

Note that propagation delays and measurement noise depend on the user location and measurement time, whereas the emission delay is the same for all user locations at any particular measurement time. The emission delay varies with time due to variations in transmitter to System Area Monitor propagation delays (see Ref. 11) and the discontinuous nature of Local Phase Adjustments.

---

[*]Emission delay is the time between secondary and master signal transmissions.

Each propagation delay appearing in Eq. A.3-1 can be expressed in terms of three parameters which describe the signal propagation path for the 100 kHz Loran-C groundwave:

- Atmospheric refractive index at the surface (n)

- A parameter (α) related to the vertical lapse rate of atmospheric refractive index

- Effective ground conductivity (σ), including terrain effects.

It is assumed that refractive index and vertical lapse rate are homogeneous for all propagation paths relevant to a harbor. This is a reasonable assumption since seasonal variations in these parameters are significantly greater than the spatial parameter variations which exist in a Loran-C chain coverage area at any one time (see Ref. 12). Conductivity, on the other hand, typically varies more from path to path for widely spaced paths, than it does from season to season for any one path (see Ref. 13). Therefore, conductivity is assumed to be the same for paths from a particular transmitter to all users in a harbor, but different for different transmitters. Note that conductivity is not necessarily homogeneous along a path.

Under the above assumptions, the propagation delay from i to u is given by the equation:

$$\phi_i(u,t) = \frac{n(t)}{c} R_i(u) + SF(\sigma_i(u,t), R_i(u)) + \widetilde{SF}(\alpha(t), R_i(u))$$

(A.3-2)

where

c = speed of light in free space = 0.299792 km/μsec

$n(t)$ = refractive index

A-5

$\alpha(t)$ = vertical lapse rate parameter

$\sigma_i(u,t)$ = conductivity for path i to u (or conductivity profile for mixed path)

$R_i(u)$ = range from i to u

SF = secondary phase delay for actual conductivity but standard atmosphere ($\alpha = 0.75$)

$\hat{SF}$ = contribution of non-standard atmosphere to secondary phase delay

The propagation delay from m to u is given by Eq. A.3-2 with i replaced by m. Equation A.3-2 includes a term for each propagation parameter:

- The first term depends on n and involves the speed of light in free space

- The second term involves SF versus σ and range, as defined by classical propagation theory for a homogeneous path (Ref. 14) or Millington's method for a mixed path (Ref. 15)

- The third term depends on α and is defined by classical theory.

It is shown below that the third term can be approximated by a function of n, thereby reducing the number of parameters needed to characterize the medium, from three to two.

Secondary phase delay is plotted against α in Fig. A.3-1, for various ranges and a conductivity of 0.005 mho/m, indicating a linear dependence (Ref. 14). Furthermore, the **slopes** of the lines in Fig. A.3-1 are very nearly linear **in range** for ranges less than 800 km. Specifically, the contribution of a non-standard atmosphere to secondary phase delay can be approximated by
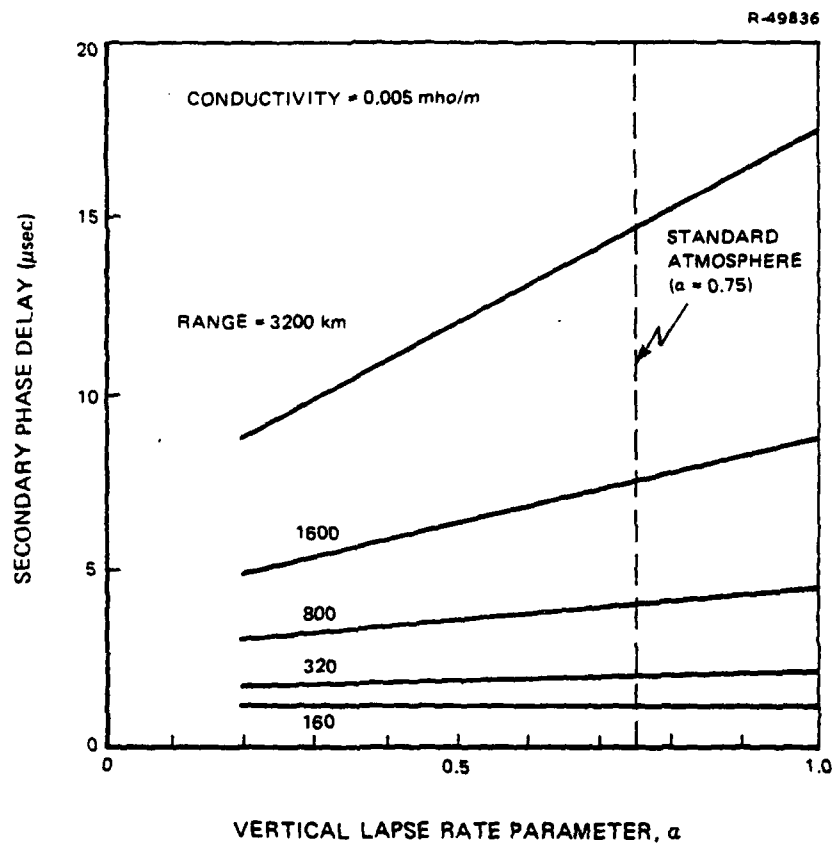
Figure A.3-1   Effect of Non-Standard Atmosphere on
Secondary Phase Delay

$$SF = 0.00373 \ R_i(u) \ [\alpha(t) - 0.75] \qquad (A.3-3)$$

with $R_i(u)$ in km and SF in μsec. It is assumed that there is
no coupling between σ and α, implying that Eq. A.3-3 is appli-
cable for all conductivities.

To relate α and n, consider the definition of α in
terms of the change in refractive index between the surface
and 1.0 km altitude (Δn):

$$\alpha = 1 + 6378 \ \Delta n \qquad (A.3-4)$$

A-7

For most meteorological conditions (excluding temperature inversions), Δn is negative and highly correlated with surface refractive index n. In Ref. 16, the following regression equation is fit to 888 pairs of data from 45 National Weather Service stations, resulting in a correlation coefficient of 0.93:

$$\Delta n = -7.32 \times 10^{-6} e^{5577 (n-1)} \qquad (A.3-5)$$

Substituting Eq. A.3-5 into Eq. A.3-4 and linearizing the resulting equation, yields the approximation

$$\alpha = 0.75 - 1715 (n - 1.0003) \qquad (A.3-6)$$

Employing Eqs. A.3-2, A.3-3, and A.3-6, the propagation delay expressed in terms of n and σ alone is

$$\phi_i(u,t) = [6.42 - 3.06 \ n(t)] \ R_i(u) + SF(\sigma_i(u,t), \ R_i(u)) \qquad (A.3-7)$$

Substitution of Eq. A.3-7 into Eq. A.3-1 yields the TD equation:

$$TD_i(u,t) = [6.42 - 3.06 \ n(t)] \ [R_i(u) - R_m(u)]$$
$$+ \ SF(\sigma_i(u,t), \ R_i(u)) - SF(\sigma_m(u,t), \ R_m(u))$$
$$+ \ ED_i(t) + v_i(u,t) \qquad (A.3-8)$$

A.4   RANGE DIFFERENCE ERROR EQUATION

The time difference equation derived in Section A.3 is assumed to characterize measured Loran-C TDs exactly. In this section, the TD equation is applied to the derivation of a range difference error equation.

Range difference errors are caused by approximations in estimating range differences from TDs measured at the user and pattern monitor locations. In order to derive the range difference error equation, a mechanization for differential Loran-C must be assumed. The assumed mechanization has the following characteristics:

- One pattern monitor is employed in each harbor (utilization of multiple monitors is not considered in the present study)

- TDs are measured simultaneously at the user and pattern monitor locations (requires post-mission data processing in Variable Geometry configuration)

- If the user is a buoy, the user and pattern monitor TDs are measured when the Loran-C equipment is installed on the buoy (ideally, with the buoy located at its correct anchor position)

- If the user is a helicopter, a TD grid prediction model is hypothesized for the harbor.

The assumed mechanizations are different for cases of buoy and helicopter Loran-C users because initial TD measurements are available for buoys but not for helicopters. The range difference error equations are derived separately in Sections A.4.1 and A.4.2, and their common structure is summarized in Section A.4.3.

A.4.1 Buoy Loran-C User (TD Transmission and Pulse Retransmission)

If the user is a buoy, the objective is to determine any change in buoy range difference between the time of equipment installation (t_o) and the time of buoy position audit (t). Four measured TDs are available for this purpose -- $TD_i(u_o, t_o)$,

$TD_i(p,t_o)$, $TD_i(u,t)$, and $TD_i(p,t)$ -- where u_o is the user location at time t_o (surveyed by buoy tender), u is the unknown user location at time t, and p is the surveyed pattern monitor location. It is assumed that the range difference at location u is <u>estimated</u> by the following equation

$$\hat{RD}_i(u) = RD_i(u_o) + c\,[TD_i(u,t) - TD_i(p,t)]$$
$$- c\,[TD_i(u_o,t_o) - TD_i(p,t_o)] \qquad (A.4\text{-}1)$$

where $RD_i(u_o)$ is known. Equation A.4-1 is motivated by the intention to reference user TDs to pattern monitor TDs in order to reduce the effect of Loran-C temporal variations.

The range difference <u>error</u> for the assumed mechanization is

$$\delta RD_i(u) = \hat{RD}_i(u) - RD_i(u)$$
$$= \left\{ c\,[TD_i(u,t) - TD_i(u_o,t)] - [RD_i(u) - RD_i(u_o)] \right\}$$
$$+ \left\{ c\,[TD_i(u_o,t) - TD_i(u_o,t_o)] - c\,[TD_i(p,t) - TD_i(p,t_o)] \right\}$$
$$\qquad (A.4\text{-}2)$$

where the term $TD_i(u_o,t)$ has been added and subtracted in order to partition the error. The first term in the partition is the error for no temporal Loran-C propagation or noise variations, while the second term is the error for no buoy motion ($u=u_o$). Measured TDs appearing in Eq. A.4-2 can be expressed by Eq. A.3-8 (where u_o or p may replace u, and t_o may replace t). The range difference error for no temporal Loran-C variations and modest buoy motion (such that the distance from p to u_o is much larger than the distance from u_o to u) is negligible compared to the error for temporal Loran-C variations and no buoy motion. In the case of no buoy motion, the error is given by the second term in Eq. A.4-2, which can

be expanded in terms of propagation parameters and noise to yield the following equation[*]:

$$\frac{1}{c} \delta RD_i(u) = -3.06 [n(t) - n(t_o)] [RD_i(u) - RD_i(p)]$$
$$+ [SF_i(u,t) - SF_i(p,t)] - [SF_i(u,t_o) - SF_i(p,t_o)]$$
$$- [SF_m(u,t) - SF_m(p,t)] + [SF_m(u,t_o) - SF_m(p,t_o)]$$
$$+ [v_i(u,t) - v_i(u,t_o)]$$
$$- [v_i(p,t) - v_i(p,t_o)] \qquad \text{(A.4-3)}$$

The error equation does not involve the emission delay, whose effect is nullified by the pattern monitor.

Four terms which appear in brackets in Eq. A.4-3 involve the difference between SF at the user and SF at the pattern monitor. It is assumed that the SF versus range curve for a particular time and transmitter is linear <u>over those ranges relevant to the users and pattern monitor in a given harbor</u>. The circumstances under which this assumption holds are discussed in Section A.5. The <u>scale factor</u> (slope of SF curve) for transmitter i at time t_i is denoted by $\zeta_i(t)$ and depends on the conductivity structure of the path between transmitter i and the harbor at time t. The resulting range difference error equation is

$$\frac{1}{c} \delta RD_i(u) = -3.06 [n(t) - n(t_o)] [RD_i(u) - RD_i(p)]$$
$$+ [\zeta_i(t) - \zeta_i(t_o)] [R_i(u) - R_i(p)]$$
$$- [\zeta_m(t) - \zeta_m(t_o)] [R_m(u) - R_m(p)]$$
$$+ [v_i(u,t) - v_i(u,t_o)]$$
$$- [v_i(p,t) - v_i(p,t_o)] \qquad \text{(A.4-4)}$$

---

[*]The more compact notation $SF_i(u,t) = SF(\sigma_i(u,t), R_i(u))$ is used here.

A-11

A.4.2 Helicopter Loran-C User (Variable Geometry)

If the user is a helicopter, the objective is to determine the range difference at a particular location on the helicopter track. In general, no measured TDs are available for this location at an initial time t_o, in contrast to the case of the buoy Loran-C user. Only two measured TDs -- $TD_i(u,t)$ and $TD_i(p,t)$ -- are available to estimate the range difference, requiring a different mechanization of differential Loran-C. In particular, a TD grid prediction model must be hypothesized. It is assumed that the model is characterized by a refractive index $\bar{n}$ and a scale factor ζ and that the range difference is estimated by

$$\overset{\wedge}{RD}_i(u) = RD_i(p) + \frac{TD_i(u,t) - TD_i(p,t)}{6.42 - 3.06\,\bar{n} + \zeta} \qquad (A.4-5)$$

Subtracting $RD_i(u)$ from both sides of Eq. A.4-5 and substituting for measured TDs yields the error equation

$$\begin{aligned}
\frac{1}{c}\,\delta RD_i(u) = &-3.06\,[n(t) - \bar{n}]\,[RD_i(u) - RD_i(p)] \\
&+ [\zeta_i(t) - \zeta]\,[R_i(u) - R_i(p)] \\
&- [\zeta_m(t) - \zeta]\,[R_m(u) - R_m(p)] \\
&+ v_i(u,t) - v_i(p,t)
\end{aligned} \qquad (A.4-6)$$

A.4.3 Error Equation Structure

The range difference error equations for buoy and helicopter Loran-C users (Eqs. A.4-4 and A.4-6, respectively) have identical structures, although the error sources have different interpretations. The error sources are divided into two categories: propagation-related errors which are assumed

to be _biases_ over the time interval of the buoy audit, and measurement noises which are assumed to be _random_ (both in time and space) during the audit. The biases for the buoy Loran-C user are the differences between propagation parameters at the audit time and at the equipment installation time; for the helicopter Loran-C user, the biases are the differences between propagation parameters at the audit time and for the hypothesized model. The Loran-C biases comprise the following _state vectors_:

$$
\begin{array}{cc}
\text{Buoy} & \text{Helicopter} \\[4pt]
\underline{x}_L = \begin{bmatrix} n(t) - n(t_o) \\ \zeta_1(t) - \zeta_1(t_o) \\ \zeta_2(t) - \zeta_2(t_o) \\ \zeta_m(t) - \zeta_m(t_o) \end{bmatrix} & \text{or} \quad \begin{bmatrix} n(t) - \bar{n} \\ \zeta_1(t) - \bar{\zeta} \\ \zeta_2(t) - \bar{\zeta} \\ \zeta_m(t) - \bar{\zeta} \end{bmatrix}
\end{array}
\qquad \text{(A.4-7)}
$$

where scale factor errors for both secondary transmitters (i = 1 and 2) have been included. Measurement noise includes components for TDs measured at the user and pattern monitor. In the case of a buoy Loran-C user, noise is included at both the audit time and the equipment installation time, while noise is only included at the audit time for the helicopter Loran-C user. The Loran-C _measurement noise vectors_ are

$$
\begin{array}{cc}
\text{Buoy} & \text{Helicopter} \\[4pt]
\underline{v}_L = \begin{bmatrix} v_1(u,t) - v_1(u,t_o) \\ v_2(u,t) - v_2(u,t_o) \\ v_1(p,t) - v_1(p,t_o) \\ v_2(p,t) - v_2(p,t_o) \end{bmatrix} & \text{or} \quad \begin{bmatrix} v_1(u,t) \\ v_2(u,t) \\ v_1(p,t) \\ v_2(p,t) \end{bmatrix}
\end{array}
\qquad \text{(A.4-8)}
$$

By substituting the range difference error equation into the position error equation (Eq. A.2-2), north and east position errors can be expressed by the following equation:

$$\underline{z}_L = \begin{bmatrix} \delta N \\ \delta E \end{bmatrix} = BM\ \underline{x}_L + BN\ \underline{v}_L \qquad (A.4-9)$$

Matrix B is defined in Eq. A.2-2 and matrices M and N are defined by

$$M = c \begin{bmatrix} -3.06\ [RD_1(u) - RD_1(p)] & -3.06\ [RD_2(u) - RD_2(p)] \\ R_1(u) - R_1(p) & 0 \\ 0 & R_2(u) - R_2(p) \\ R_m(u) - R_m(p) & R_m(u) - R_m(p) \end{bmatrix}^T$$

$$\qquad (A.4-10)$$

$$N = c \begin{bmatrix} 1 & 0 & -1 & 0 \\ 0 & 1 & 0 & -1 \end{bmatrix}$$

The Loran-C error model is employed alone for the TD Transmission and Pulse Retransmission BPAS configurations, and in combination with microwave ranging system and altimeter error models for the Variable Geometry configuration (see Appendix C).

If the Loran-C position fix is the only information utilized for estimation of buoy position in the TD Transmission and Pulse Retransmission BPAS configurations, the buoy position error covariance matrix (Ref. 17) is computed by

$$\text{cov}\ \underline{z}_L = BM\ (\text{cov}\ \underline{x}_L)\ M^T B^T + BN\ (\text{cov}\ \underline{v}_L)\ N^T B^T \qquad (A.4-11)$$

where cov $\underline{x}_L$ and cov $\underline{v}_L$ are the covariance matrices for the state and noise vectors, respectively. The buoy position error covariance matrix for the Variable Geometry configuration is presented in Appendix C.

A.5   ERROR STATISTICS

A.5.1 State Vector

Each Loran-C bias (Eq. A.4-7) is the difference between the values of a propagation parameter at times t and t_o (for a buoy), or between the value at time t and the value assumed in a hypothesized model (for a helicopter). Standard deviations are assigned to the biases based on available information concerning maximum seasonal and spatial variations in the Loran-C propagation parameters.

Refractive index (n) is assumed to be spatially homogeneous since seasonal variations dominate spatial variations. Seasonal variations differ for different regions of the United States, but are largest for the northeastern region. Maximum, minimum, and mean seasonal cycles in refractive index are plotted from historical data (Ref. 12) in Fig. A.5-1 for Washington, D.C., illustrating a spread of approximately 110 x 10^{-6}. The following worst-case assumptions are made:

- $n(t_o)$ or $\bar{n}$ is at an extreme of the historical data

- $n(t)$ obeys a uniform distribution between the extremes.

These assumptions result in a computed standard deviation of 50 x 10^{-6} for the refractive index error. This value is em-

A-15
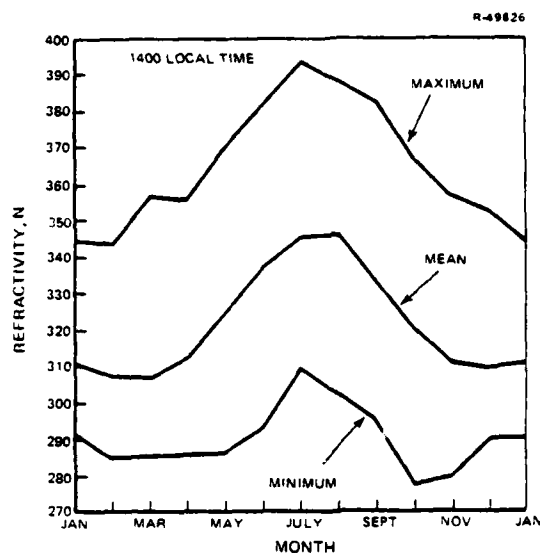
Figure A.5-1 Seasonal Refractive Index Cycle for Washington, D.C. $(n = 1 + 10^{-6}N)$

ployed as the nominal value in the covariance simulations herein. Each scale factor error, $\zeta_i(t) - \zeta_i(t_o)$ or $\zeta_i(t) - \bar{\zeta}$, for $i = 1,2$, or m, is related to the difference in conductivities for the transmitter-to-harbor path at times t and t_o (or between the conductivity at time t and the conductivity in the hypothesized model). The scale factor $\zeta_i(t)$ is the slope of the SF versus range curve at time t, in the region defined by the Loran-C users and pattern monitor. Because the Loran-c users in the BPAS application are located in a harbor, the discontinuity in conductivities at the land/sea water interface plays an important role in determining $\zeta_i(t)$. The interface effect is analyzed below using Millington's method for computing SF along a mixed land and sea water path.

A-16

The following characteristics apply to the trans-
mitter-to-user propagation paths for analysis purposes (see
Fig A.5-2):

- The transmitter is separated from the
  coastline by land of homogeneous conduc-
  tivity σ_L and range R_L

- The harbor is separated from the coastline
  in the transmitter direction by sea water
  with conductivity σ_S and range R_S; R_S
  depends on specific user location

- The harbor itself, covering all Loran-C
  users*, is entirely sea water with con-
  ductivity σ_S.

R-49601

LAND PATH   SEA WATER PATH
(σ_L, R_L) (σ_S, R_S)

TRANSMITTER   HARBOR
                                        (σ_S)
          COASTLINE
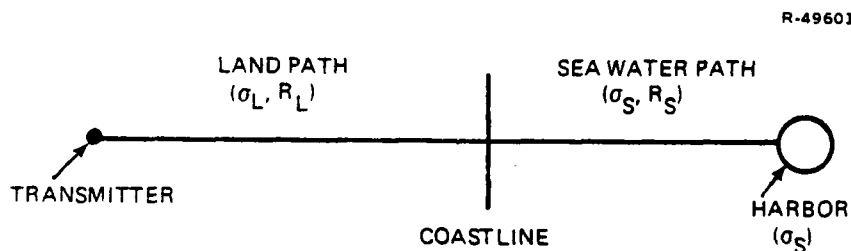
Figure A.5-2 Mixed Land and Sea Water Path

If the harbor is close to the coastline in the transmitter
direction, the range R_L may depend on the bearing angle from
the particular user to the transmitter. The shape of the
coastline is important in this case. For tractability, it is
assumed that R_L is the same for all users in the harbor.

Millington's method of expressing SF for the assumed
mixed path includes six terms (Ref. 15):

---

*Although helicopter tracks or pattern monitor locations may
 be on land, they are assumed to be close to the water.

A-17

$$SF = \tfrac{1}{2}[SF(\sigma_L, R_L) + SF(\sigma_S, R_L + R_S) - SF(\sigma_S, R_L)$$
$$+ SF(\sigma_S, R_S) + SF(\sigma_L, R_L + R_S) - SF(\sigma_L, R_S)]$$

$$(A.5-1)$$

Each term is the SF for a homogeneous path with a particular range and is predicted by classical propagation theory in the manner shown in Fig. A.5-3. Substitution of the classical

R-46631
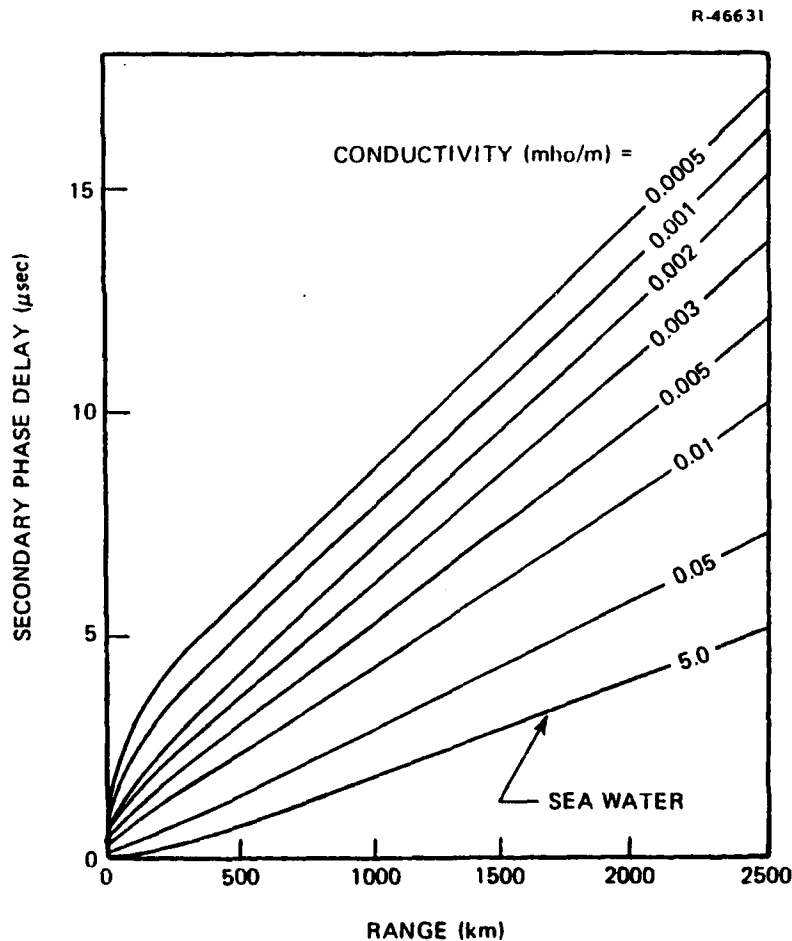
Figure A.5-3 Secondary Phase Delay for a Homogeneous Propagation Path

A-18

theory results into Eq. A.5-1 reveals that SF <u>decreases</u> on crossing the coastline from land to sea water. This phenomenom is illustrated in Fig. A.5-4 for various land conductivity values and land path lengths. Note that the <u>slope</u> of the SF curve on the sea water path segment depends on land conductivity (σ_L) and sea water path length (R_S), but not on land path length (R_L). For R_S less than 200 km, the slopes depend on σ_L in the manner shown in Fig. A.5-5, where the incremental SF (relative to SF at the coastline) is plotted versus R_S. Slope is independent of σ_L for R_S greater than approximately 200 km. It is assumed that <u>all</u> paths for a <u>particular</u> transmitter and harbor fall into one of the following categories:

Type   I: R_S < 15 km
Type   II: 15 km < R_S < 200 km
Type III: R_S > 200 km

Slopes of the SF versus range curves for the three path types are summarized in Table A.5-1 for the spread of land conductivities found in the United States (see Ref. 13).

Interpretation of the slopes listed in Table A.5-1 depends on whether the Loran-C user is a buoy or helicopter. <u>In the case of a helicopter Loran-C user</u>, the scale factor error is $\zeta_i(t) - \zeta$. Note that $\zeta_i(t) - \zeta$ may be large, even if there are no <u>temporal</u> variations in land conductivity. This follows from the fact that <u>spatial</u> variations in land conductivity, which must be known to correctly hypothesize ζ, cannot be mapped reliably at present. Since ζ would be based on a conductivity map which may have significant errors, the following worst-case assumptions are made:
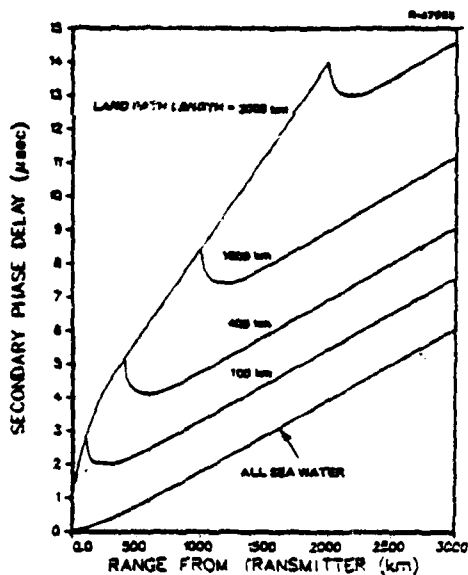
a) Land Conductivity = 0.0005 mho/m
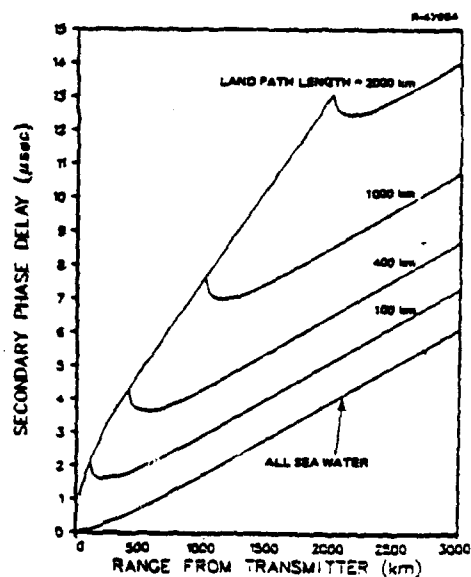
b) Land Conductivity = 0.001 mho/m
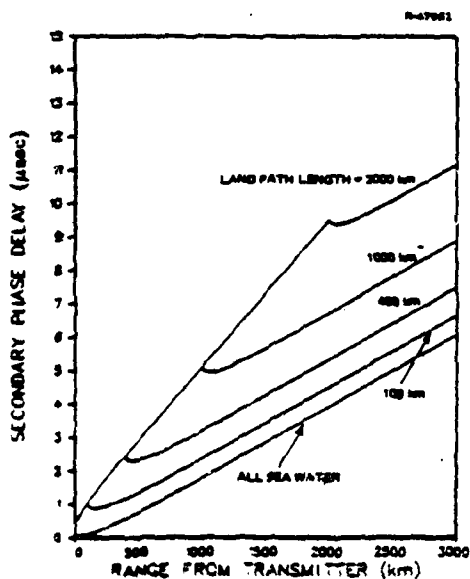
c) Land Conductivity = 0.005 mho/m
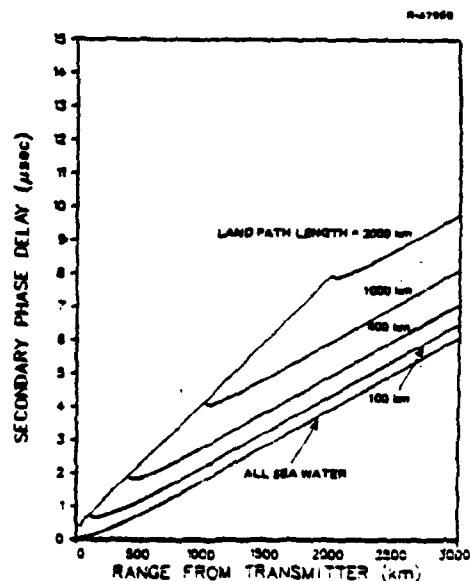
d) Land Conductivity = 0.01 mho/m

Figure A.5-4   Secondary Phase Delay for a Mixed
Land and Sea Water Propagation Path
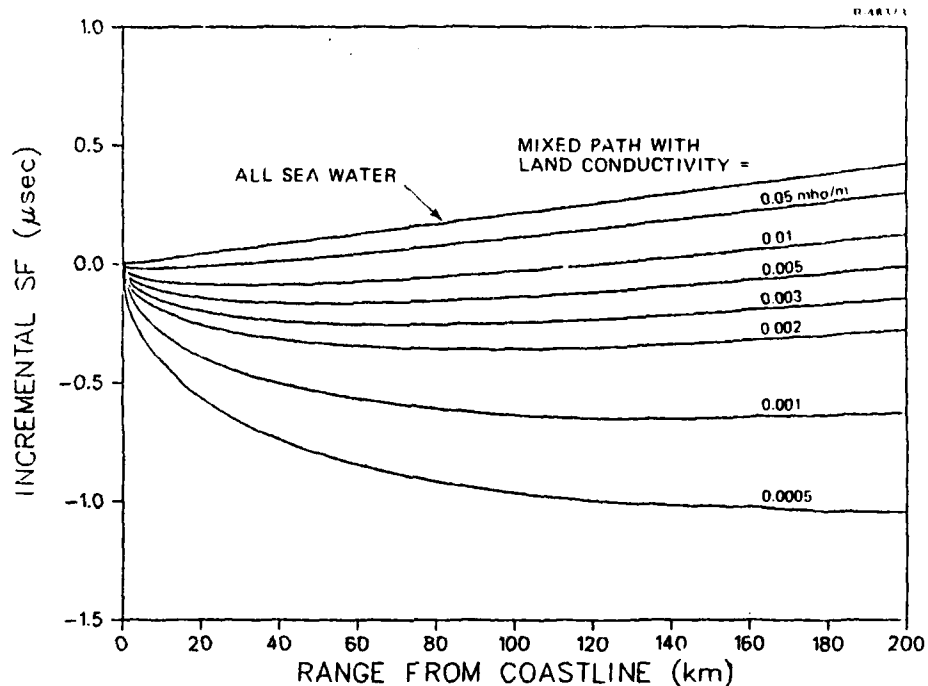
Figure A.5-5   Incremental SF on Sea Water
Propagation Path Segment

TABLE A.5-1

SLOPES OF SF VERSUS RANGE CURVES
ON SEA WATER PATH SEGMENT (μsec/km)

LAND CONDUCTIVITY (mho/m)	PATH TYPE		
	I	II	III
0.0005	-0.076	-0.0035	
0.001	-0.056	-0.0019	
0.002	-0.041	-0.0006	+0.0021*
0.003	-0.034	-0.0001	
0.005	-0.027	+0.0005	
0.01	-0.020	+0.0010	

*Based on a sea water conductivity of 5 mho/m. Maximum
spread assumed to be ±10 percent of value shown.

- ζ is chosen at an extreme of the theoretically possible scale factor values in Table A.5-1 (for the applicable path type)

- The actual scale factor $\zeta_i(t)$ can lie anywhere in the spread of values in Table A.5-1 and is described statistically by a uniform distribution.

The resulting standard deviations for the scale factor errors are summarized in Table A.5-2 (for helicopter).

TABLE A.5-2

STANDARD DEVIATION OF SCALE FACTOR ERROR (μsec/km)

LORAN-C USER	PATH TYPE		
	I	II	III
Helicopter	0.033	0.0026	0.00024
Buoy	0.012	0.0009	0.00024

In the case of a buoy Loran-C user, the scale factor error is $\zeta_i(t) - \zeta_i(t_o)$. Temporal variations in land conductivity are expected to be a small fraction of spatial variations. An increase by a factor of two is expected from winter to summer for conditions of 1-2 m of snow or frozen ground in winter and average ground in summer (theoretical result from Ref. 11). Employing Table A.5-1, it is found that a doubling of conductivity has the greatest effect on the scale factor for low values of conductivity. Assuming, conservatively, that the conductivity is 0.0005 or 0.001 mho/m at time t_o and can take on any value between 0.0005 and 0.001 mho/m at time t, the standard deviations for $\zeta_i(t) - \zeta_i(t_o)$ are those listed in Table A.5-2 (for buoy).

The standard deviations listed for Type I paths are employed as the nominal values in the covariance simulations herein, representing a worst case. The three scale factor errors (for i = 1,2, and m) are assumed to be independent.

A.5.2 Measurement Noise Vector

The measurement noise vector (Eq. A.4-8) includes two noises (corresponding to two measured TDs) for the Loran-C user and two noises for the pattern monitor. In the case of a buoy Loran-C user, each noise includes components at times t and t_o. In the case of a helicopter Loran-C user, each noise involves only a component at time t.

Noise in the Loran-C frequency band (90-110 kHz) is primarily atmospheric, rather than internal to the receiver. Since the distance from p to u and the time between t_o and t are generally large compared to the expected correlation distance and correlation time for atmospheric noise, it is assumed that the noises in all receiver <u>channels</u> are independent. However, the noises associated with two TDs measured at the same location at the same time both involve the master station channel, and are thus correlated with correlation coefficient 0.5. Denoting the standard deviations of user and pattern monitor TDs by σ_u and $\sigma_p{}^*$, the measurement noise covariance matrix for a helicopter Loran-C user is

$$\text{cov } v_L = \begin{bmatrix} \sigma_u^2 \begin{bmatrix} 1 & 0.5 \\ 0.5 & 1 \end{bmatrix} & 0 \\ 0 & \sigma_p^2 \begin{bmatrix} 1 & 0.5 \\ 0.5 & 1 \end{bmatrix} \end{bmatrix} \quad (A.5-2)$$

---

*Not to be confused with conductivities.

The measurement noise covariance matrix for a buoy Loran-C
user is twice that given by Eq. A.5-2, although the user TD
standard deviation σ_u is not necessarily the same as for a
helicopter Loran-C user.

The TD standard deviations, σ_u and σ_p, depend on

- Receiver resolution and signal processing
  techniques

- Signal-to-noise ratio (SNR)

- Averaging time and tracking-loop gains

- Receiver motion during averaging time
  interval.

The assumed nominal values for σ_u and σ_p in the TD Transmis-
sion configuration are 0.02 μsec, based on use of the Internav
LCM 404 or similar quality Loran-C receiver, for an SNR of
0 dB, an averaging time of 2 to 5 min, and no buoy motion
during the averaging time interval (Ref. 18). A nominal value
of 0.02 μsec for σ_p is also assumed in the Pulse Retransmis-
sion and Variable Geometry configurations. However, σ_u for
these configurations is expected to be larger than the nominal
value.

In the Pulse Retransmission configuration, σ_u depends
on the FM telemetry link -- both as it affects the Loran-C
third-cycle zero crossing and the atmospheric noise in the
Loran-C frequency band. Analysis of these effects was not
included in the present study.

In the Variable Geometry configuration, σ_u depends
critically on receiver tracking-loop gains, which are selected
to trade off errors due to helicopter accelerations and atmos-

A-24

pheric noise. The second-order tracking loop for the Micro-logic ML-120 receiver is analyzed in Ref. 19. It is shown that the standard deviation of the tracking error (error in tracking third-cycle zero crossing) is proportional to $\sqrt{G}$, where G is the first-order loop gain (the second-order loop gain is adjusted to keep the damping ratio at a fixed value). On the other hand, the steady-state tracking error due to receiver acceleration is proportional to $1/G^2$. Therefore, the gain G must be small enough to minimize errors due to noise, but large enough to minimize acceleration errors. Loop-gain settings for the helicopter-borne Loran-C receiver in the Variable Geometry BPAS configuration would have to be selected based on flight tests under actual helicopter maneuvers. The error analyses discussed herein are based on a nominal noise standard deviation of $\sigma_u = 0.02$ μsec.

APPENDIX B
BANDPASS FILTER MODEL

The bandpass filter model employed in the Pulse Re-transmission simulations discussed in Appendix F is described by the second-order transfer function

$$\frac{I_o(s)}{I(s)} = G \frac{1 + as + bs^2}{1 + ds + bs^2} \qquad (B-1)$$

where

$I(s)$ = Laplace transform of input current $i(t)$

$I_o(s)$ = Laplace transform of output current $i_o(t)$

s = Laplace transform parameter

G = gain chosen such that maximum of $i_o(t)$ equals maximum of $i(t)$

The bandpass filter frequency spectrum ($s = 2\pi f j$) is characterized by the center frequency (f_p), the -3 dB bandwidth (Δf), and the rejection level (D). These parameters are related to the parameters in Eq. B-1 by

$$f_p = 1/(2\pi\sqrt{b})$$
$$\Delta f = d/(2\pi b) \qquad (B-2)$$
$$D = 20 \log (a/d)$$

It should be noted that the spectrum approaches a constant value (equal to the value at f_p minus the rejection D) at low and high frequencies. Although bandpass filters typically

exhibit a frequency response which decreases at low and high frequencies, the assumed filter model is realistic for large rejection levels and band-limited input signals. The rejection level was set to 40 dB in all simulations. The magnitude and phase angle of the bandpass filter frequency spectrum for a 100 kHz center frequency and 30 kHz bandwidth are illustrated in Fig. B-1.
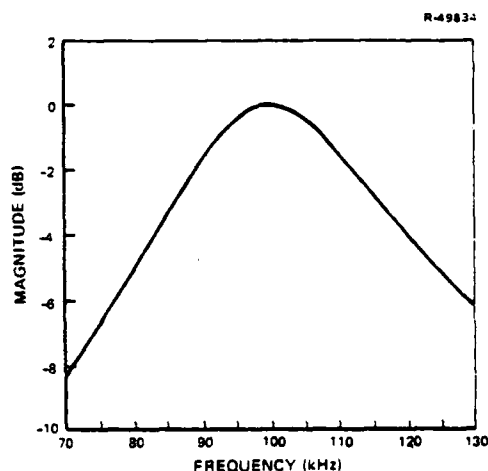
a) Magnitude
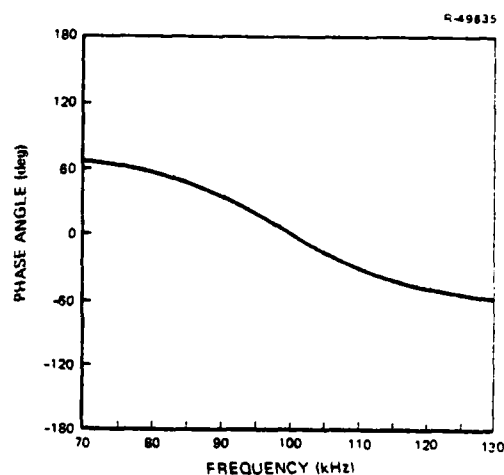
b) Phase Angle

Figure B-1   Bandpass Filter Frequency Spectrum

APPENDIX C

VARIABLE GEOMETRY CONFIGURATION ERROR MODEL

C.1   INTRODUCTION

In the Variable Geometry BPAS configuration, buoy position is estimated from helicopter-to-buoy microwave range data and synchronous helicopter Loran-C and altimeter position data. Measurements from at least two different helicopter positions are required to compute the position of a buoy. Additional information is needed to resolve the position ambiguity inherent in intersecting two circular lines-of-position (LOPs). The ambiguity is typically resolved by making a third measurement at a helicopter position which is not colinear with the first two positions. Fig. C.1-1 illustrates computation of the buoy position, assuming that there are no
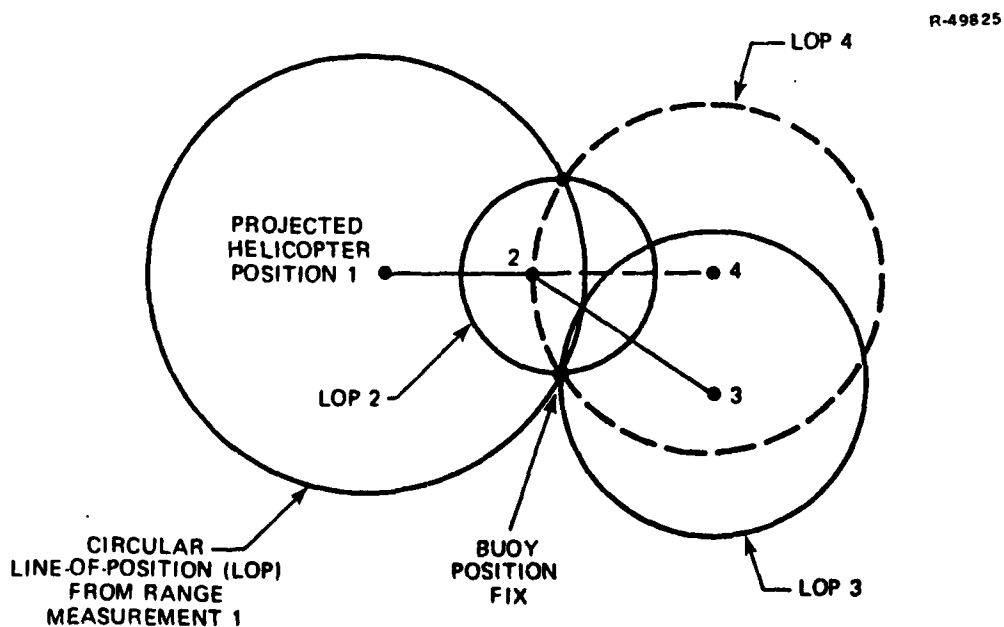
Figure C.1-1 Computation of Coarse Buoy Position Fix

measurement errors. The buoy position fix is the common in-
tersection of the circular LOPs associated with range measure-
ments at helicopter positions 1, 2, and 3. Note that an am-
biguity remains if measurements are made from the three co-
linear positions 1, 2, and 4.

In the case of measurement errors of the magnitude
expected in the Variable Geometry configuration, this method
of buoy position computation is suitable only for a "coarse"
indication of buoy position. The accuracy desired in the BPAS
application is obtained by processing redundant range, alti-
tude, and Loran-C data to reduce the impact of measurement
errors. The following advantages are afforded by processing
redundant information:

- Errors which are constant from measure-
  ment to measurement (bias errors) can be
  calibrated

- The impact of errors which are random
  from measurement to measurement (noise
  errors) can be reduced by averaging.

The method chosen to process redundant measurements in the
Variable Geometry configuration is a least-squares estimation
algorithm, which iteratively computes a correction to the
"coarse" estimate of buoy position. The algorithm relies on
linearized equations which apply only when the estimated buoy
position is near to the actual position. Several iterations
are typically required to achieve the desired "fine" estimate
of buoy position. The simulations employed in this study
evaluate the steady-state error resulting from multiple itera-
tions of the least-squares algorithm. Issues such as the
number of iterations required for convergence or the accuracy
of the initial coarse fix are not addressed in this study.

The least-squares algorithm provides an optimal estimate of buoy position in the presence of bias and noise errors, which comprise the error model for this study. A more detailed error model may include errors with dynamic properties intermediate between biases and noises and would be well-suited to a Kalman filter approach (Ref. 17).* A dynamic model is not required for this study, however, because no error sources with time constants comparable to the time interval of the audit are expected. Error sources in the Variable Geometry configuration either change very slowly during the audit (and are modeled as biases), or change fast enough to be independent from measurement to measurement (and are modeled as noises).

C.2   MECHANIZATION AND ERROR MODEL

At each measurement point on the helicopter trajectory (flight pattern), the following quantities are available:

T = measured round-trip travel time of the microwave signal

T_d = specified transponder timing delay (time between reception and transmission of pulse)

z_a = measured helicopter altitude

x_a, y_a = helicopter horizontal position coordinates (east, north) indicated by Loran-C

x_b, y_b = prior estimate of buoy position coordinates (provided by coarse fix or by output of previous iteration of least-squares algorithm).

---

*The least-squares algorithm is a special case of a Kalman filter (i.e., with no dynamics).

From these values, the microwave-indicated (r_M) and Loran-indicated (r_L) ranges to the buoy are computed as follows:

$$r_M = \tfrac{1}{2} c \, (T-T_d)$$
$$r_L = [(x_b-x_a)^2 + (y_b-y_a)^2 + z_a^2]^{\frac{1}{2}} \qquad \text{(C.2-1)}$$

where c is the microwave propagation velocity. The "observation" processed by the least-squares algorithm (Δr) is the difference between the microwave- and Loran-indicated ranges:

$$\Delta r = r_M - r_L \qquad \text{(C.2-2)}$$

The observation Δr can be written in terms of the errors in the microwave-indicated and Loran-indicated ranges, δr_M and δr_L, as follows:

$$\Delta r = (\text{true range} + \delta r_M) - (\text{true range} + \delta r_L)$$
$$= \delta r_M - \delta r_L \qquad \text{(C.2-3)}$$

The errors are expressed by the first ("linear") term of a Taylor Series expansion:

$$\delta r_M = \tfrac{1}{c} r_L \, \delta c + \tfrac{1}{2} c \, \delta T - \tfrac{1}{2} c \, \delta T_d$$

$$\delta r_L = \frac{1}{r_L} z_a \, \delta z_a + \frac{1}{r_L} (x_b-x_a) \, \delta x_b - \frac{1}{r_L} (x_b-x_a) \, \delta x_a$$

$$+ \frac{1}{r_L} (y_b-y_a) \, \delta y_b - \frac{1}{r_L} (y_b-y_a) \, \delta y_a \qquad \text{(C.2-4)}$$

where δ indicates the error in the associated quantity. Note that the Loran-C errors δx_a and δy_a are given by δE and δN, respectively, in Appendix A (Eq. A.4-9). By combining Eqs. C.2-3 and C.2-4 and expressing in state variable notation, the

k^{th} observation can be related to the error parameters by the equation:

$$\underline{\Delta r}_k = H_k \ \underline{\delta x} + \underline{\delta v}_k \qquad (C.2-5)$$

where

$\underline{\Delta r}_k$ = vector which includes observation k for each buoy

$\underline{\delta x}$ = state vector of bias errors (including north and east buoy position errors)

$\underline{\delta v}_k$ = vector of noise errors associated with observation k

H_k = matrix of coefficients which defines the geometry for observation k. Loran-C and microwave ranging contributions to H_k are from Eqs. A.4-9 and C.2-4, respectively.

The least-squares algorithm provides a recursive estimate of all bias errors, $\underline{\delta \hat{x}}_k$, (including buoy position error) based on the previous estimate, $\underline{\delta \hat{x}}_{k-1}$, given by the following computational procedure (Ref. 17). The "gain" matrix is first computed by:

$$K_k = P_{k-1} H_k{}^T \ [H_k P_{k-1} H_k{}^T + R_k]^{-1} \qquad (C.2-6)$$

where R_k is the noise error covariance matrix and P_{k-1} is the error covariance matrix for the bias estimate given by the previous step of the recursion algorithm. The initial covariance P_o is a diagonal matrix composed of the initial variances of the bias error sources, as specified in Section C.3. The bias error estimate is given by:

$$\underline{\delta \hat{x}}_k = \underline{\delta \hat{x}}_{k-1} + K_k \ [\underline{\Delta r}_k - H_k \ \underline{\delta \hat{x}}_{k-1}] \qquad (C.2-7)$$

The initial error estimate $\underline{\delta \hat{x}}_o$ is chosen to be zero. The error covariance matrix is updated by the equation:

$$P_k = [P_{k-1}^{-1} + H_k{}^T R_k^{-1} H_k]^{-1} \qquad (C.2-8)$$

The error estimate $\hat{\delta x}_k$ and its covariance matrix P_k include all bias error sources. The position error ellipse and rms error (defined in Section 3.2) for each buoy are computed from the appropriate 2 x 2 submatrix of P_k associated with the north and east buoy position errors.

C.3   NOMINAL PARAMETER VALUES

The structure and magnitudes of microwave ranging error parameters were deduced from discussions with manufacturers of microwave ranging systems and experience with similar systems. Table C.3-1 contains a summary of the nominal parameter values. Microwave propagation velocity error, δc, is assumed to be caused by variations in refractive index by the equation:

$$\delta c = -c \, \delta n \qquad (C.3-1)$$

where δn is refractive index error, with standard deviation 50 x 10^{-6} (see Appendix A, Section A.5.1). Microwave timing error is comprised of a component assumed to be random from measurement to measurement (measurement noise, δT), and a component with a constant magnitude over the interval of a buoy audit (bias, δT_d). A representative value for microwave measurement noise standard deviation is 0.01 µsec. The bias timing error is separated into two components:

- A common bias, which has the same value for measurements to all buoys and could arise from a helicopter receiver bias or a common temperature dependence of the signal delay in each transponder

C-6
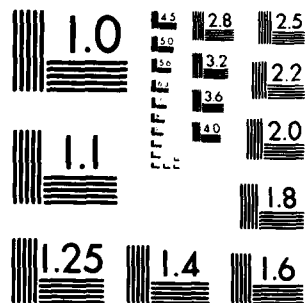
MICROCOPY RESOLUTION TEST CHART
NATIONAL BUREAU OF STANDARDS 1963 A

TABLE C.3-1

NOMINAL ERROR SOURCES FOR VARIABLE GEOMETRY CONFIGURATION

ERROR SOURCE	SYMBOL	TYPE	STANDARD DEVIATION
Microwave Propagation Velocity Error	δc	Bias	0.015 m/μsec
Microwave Measurement Noise	δT	Noise	0.01 μsec
Common Microwave Timing Error	δT_d	Bias	0.02 μsec
Independent Microwave Timing Error			0.02 μsec
Altitude Error	δz_a	Bias	10 m
Helicopter Loran-C Position Error	$\delta x_a, \delta y_a$	See Appendix A	
A Priori Buoy Position Error	$\delta x_b, \delta y_b$	Bias	Infinite

● A bias which is independent from buoy to buoy and could arise from a random difference in buoy signal delay caused by hardware variability.

The nominal standard deviation of each type of timing bias error is conservatively assumed to be 0.02 μsec in this study.

The helicopter is assumed to be equipped with a radar altimeter characterized by a bias error with a standard deviation of one percent of altitude. For the assumed altitude of 300 m, nominal altitude error (δz_a) standard deviation is conservatively chosen to be 10 m.

The errors δx_a and δy_a represent Loran-C position-fix errors for the helicopter. These errors are described by the east and north Loran-C position errors, δE and δN, respectively, in Appendix A (Eq. A.4-9).

The buoy position errors δx_b and δy_b are assumed to have an infinite a priori standard deviation. That is, the estimate of buoy position error from the least-squares algorithm is based only on Loran-C, microwave ranging, and altimeter measurements; the final estimate is not influenced by an initial estimate of buoy position. Note that δx_b and δy_b are modeled as biases, since it is assumed that the buoy does not move during the audit.

APPENDIX D
CORRESPONDENCE WITH MICROWAVE RANGING SYSTEM MANUFACTURERS

This appendix contains copies of correspondence be-
tween TASC and two manufacturers of microwave ranging systems,
Del Norte Technology, Inc. and Motorola.

TASC

THE ANALYTIC SCIENCES CORPORATION

28 August 1979

Mr. George Sickler
Del Norte Technology, Inc.
1100 Pamela Drive
Box 696
Euless, Texas   76039

Dear Mr. Sickler:

  Please find enclosed tentative requirements for the micro-
wave ranging system which we discussed during our July telephone
conversations. TASC is assisting the Transportation Systems Center
and U.S. Coast Guard in evaluating a positioning system which would
utilize the specified microwave ranging system in conjunction with
airborne Loran-C to audit the positions of U.S. Coast Guard navi-
gational buoys. The microwave ranging/airborne Loran-C system con-
figuration is being compared with an alternative configuration
consisting of a Loran-C receiver on each buoy from which time dif-
ference data are transmitted over a VHF telemetry link to a shore
station or helicopter. Therefore, to provide a meaningful compari-
son of the candidate systems, TASC needs an estimate of the per
unit production costs of buoy equipment and helicopter equipment
required for the microwave ranging system, and the cost of developing
equipment for experimental system verification.

  The microwave ranging system specifications may be modified
prior to hardware procurement if a decision is made by the U.S.
Coast Guard to pursue the concept. Your inputs to this evaluation
are greatly appreciated.

         Very truly yours,

         Leon M. DePalma

         Leon M. DePalma

LMD/p
Enclosures

cc: Mr. Joseph Wolfson (letter only)
  Transportation Systems Center
  U.S. Department of Transportation
  Kendall Square
  Cambridge, MA   02142

TASC

21 August 1979

TECHNOLOGY SCIENCES CORPORATION

Mr. William O'Donnell - T2020
Motorola - Government Electronics Division
7402 South Price Road
Tempe, Arizona 85282

Dear Mr. O'Donnell:

Please find enclosed tentative requirements for the microwave ranging system which we discussed during our telephone conversation of 1 August 1979. TASC is assisting the Transportation Systems Center and U.S. Coast Guard in evaluating a positioning system which would utilize the specified microwave ranging system in conjunction with airborne Loran-C to audit the positions of U.S. Coast Guard navigational buoys. The microwave ranging/airborne Loran-C system configuration is being compared with an alternative configuration consisting of a Loran-C receiver on each buoy from which time difference data are transmitted over a VHF telemetry link to a shore station or helicopter. Therefore, to provide a meaningful comparison of the candidate systems, TASC needs an estimate of the per unit production costs of buoy equipment and helicopter equipment required for the microwave ranging system, and the cost of developing equipment for experimental system verification.

The microwave ranging system specifications may be modified prior to hardware procurement if a decision is made by the U.S. Coast Guard to pursue the concept. Your inputs to this evaluation are greatly appreciated.

Very truly yours,

Leon M. De Palma

Leon M. DePalma

LMD/p
Enclosures

cc: Mr. Joseph Wolfson
    Transportation Systems Center
    U.S. Department of Transportation
    Kendall Square
    Cambridge, MA 02142

DESIGN REQUIREMENTS FOR A MICROWAVE RANGING SYSTEM
FOR BUOY POSITION AUDIT

1. INTRODUCTION

The role of the microwave ranging system in the Buoy
Position Audit System is illustrated in Fig. 1-1. The micro-
wave ranging system measures the ranges from a helicopter to a
number of code-identified buoys, at various points along a
helicopter track. The ranges are stored together with synchro-
nous Loran-C and altimeter measurements on magnetic tape for
post-mission processing. Data processing consists of (1) com-
puting helicopter position fixes via differential Loran-C by
utilizing helicopter and pattern monitor time difference meas-
urements, and (2) establishing buoy positions by combining
the helicopter position data with range and altitude data in
a least-squares algorithm. This document deals only with the
helicopter and buoy equipment required to obtain the range
measurements.

2. BUOY INTERROGATION SCENARIO

The control unit which schedules and commands buoy
range measurements is not considered part of the microwave
ranging system. However, a brief description of scheduling is
provided here to aid in the selection of a microwave ranging
system concept which is consistent with the requirements
listed in Section 3.
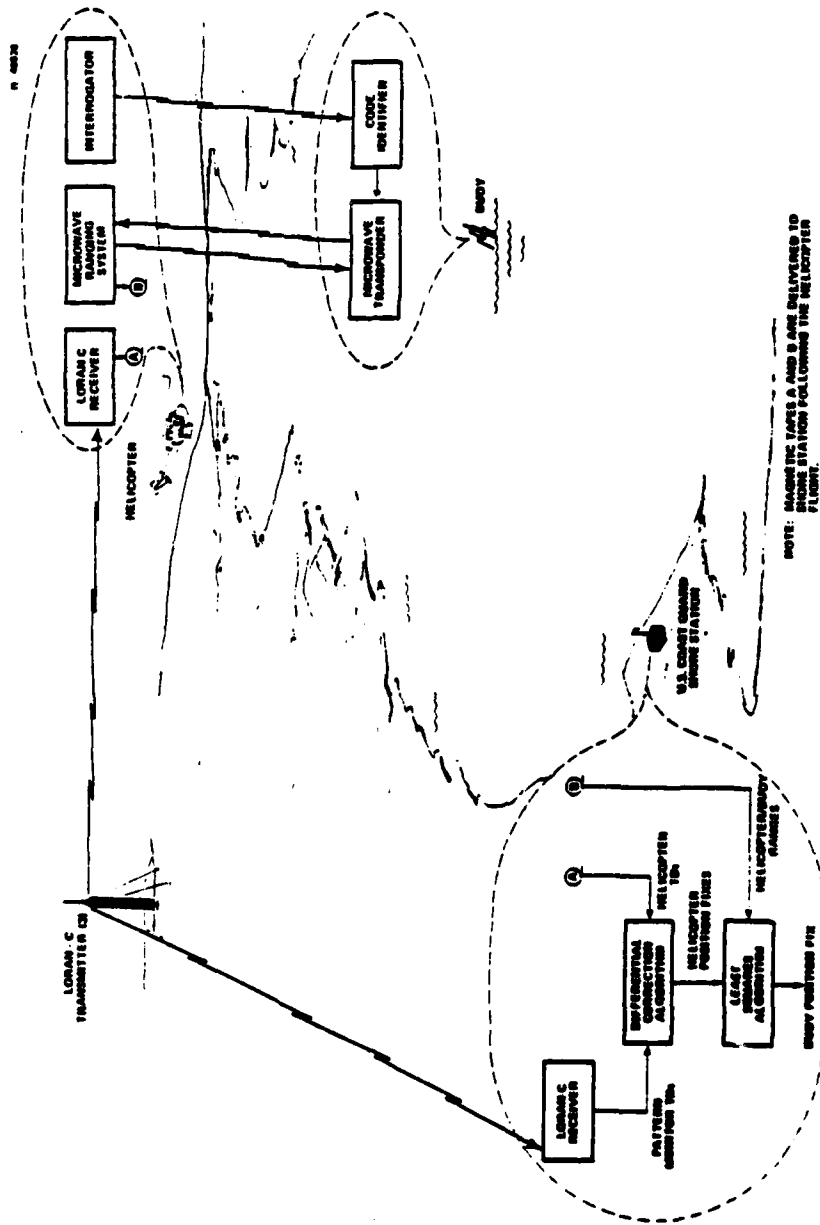
Figure 1-1   Candidate Buoy Position Audit System

Although the helicopter flight pattern is chosen to minimize the separation of the helicopter and buoys, the helicopter is not dedicated to the buoy position audit mission. Therefore, in order to collect sufficient data to guarantee acceptable geometry and to avoid the position-fix ambiguity associated with straight-line flight, ranges to all buoys must be measured at points scattered over the entire round-trip flight path. The recommended scenario is to interrogate all the buoys in sequence and to repeat the sequence at equally-spaced times during the helicopter flight. The following considerations are relevant to this scenario:

- If the buoy response is not obtained within a specified period of time, the buoy is assumed to be out of range of the interrogation signal

- To guarantee that buoy responses are of adequate signal strength (thus avoiding unnecessary buoy battery drain), the transmitters on the helicopter and buoys should be of equal power

- The system must not mistake passive reflections of the interrogation signals from the ocean surface or other buoys as active buoy responses.

Alternative scenarios may be considered in the context of the system requirements listed in Section 3.

3. REQUIREMENTS

The following requirements impact the microwave ranging system design:

- Maximum helicopter-to-buoy range of interest is 30 nm which may be reduced, if necessary, to meet specifications on buoy battery drain; reduction below 10 nm would severely constrain helicopter operations

- Buoy power source is a 12 volt, 1000-6000 amp-hr battery presently on all lighted buoys; battery drain of 7 amp-hr is available for each audit

- Audits are performed once per week on the average; buoy equipment should not require servicing more often than once per year

- Buoy equipment is housed in two cylindrical battery compartments, each measuring at least 22 in. inside diameter by 65 in. deep; one compartment is partially occupied by a 36 in. battery rack; the remainder of this compartment and the entire spare compartment are available for buoy audit equipment

- Battery compartments are vented to the atmosphere, thereby acquiring the temperature (within ±10°F) and humidity of the air above the ocean surface

- Weight of buoy equipment must not exceed 100 lb

- In any particular audit mission, fewer than 300 buoys would be interrogated; therefore, a nine-bit identification code is required

- Range measurement accuracy should be on the order of 10 ft rms at maximum range

- The separation of the buoy antenna and buoy electronics package could vary from 2 ft to 15 ft, depending on the location of the antenna on the buoy structure (see Fig. 3-1 for illustration of a typical buoy); the buoy antenna must have a hemispherical beam pattern

- Maximum helicopter velocity is 80-120 kt, depending on helicopter model; maximum round-trip helicopter flight time is 3 hrs

1962 TYPE STANDARD

Function. The 8X26 LBR buoy is designed and constructed for exposed or semiexposed locations. This buoy configuration is used with a 225-lb bell, wave-actuated sound signal. The basic buoy is the same as the 8X26 LR.

Physical Characteristics

Buoy weight	11,917 lb
Buoy draft (no mooring)	10 ft-3 in.
Focal height of light (no mooring)	15 ft-8 in.
Freeboard (no mooring)	3 ft-1 in.
Minimum freeboard	1 ft-3 in.
Pounds per inch of immersion	270

Related Equipment

Power units (maximum number and size)	2-830
Sound equipment	225-lb bell
Bridle size (chain diameter and length)	1½ in.X15 ft
Mooring chain size	1½ in.
Sinker size	8,500 lb

Operational Characteristics

Nominal visual range of daymark	3.2 nmi
Radar range	3.7 nmi

Operational Characteristics (cont'd)

Maximum current		4 kn
Visual range of light	(see Chapter 6)	
Minimum mooring depth		25 ft
Maximum mooring depth	(810)	220 ft
	(830)	190 ft

Figure 3-1   Characteristics of Typical Buoy (Model Number 8X26 LBR)
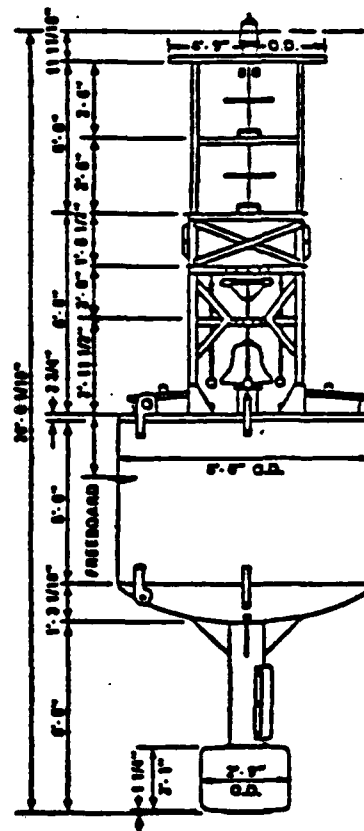
- The helicopter-borne unit must be capable of displaying the status of the range measurement process -- e.g., a warning could be displayed if no responses are received from a particular buoy; this would prompt the pilot to do a visual survey of the area in which the buoy is expected to be located

- The helicopter-borne unit must be equipped with standard RS-232C digital interfaces to accept interrogation scheduling data from the control unit and to output range data to a tape cassette recorder

- The helicopter-borne unit (excluding antenna) must be portable and capable of being hand-carried by one person; the antenna should be permanently mounted and have a hemispherical beam pattern.

4. COSTING CONSIDERATIONS

The following cost information is required to determine the economic feasibility of the microwave ranging/airborne Loran-C Buoy Position Audit System configuration:

- Production cost per buoy unit (including electronics, antenna, and calibration) for 1000 to 4000 units

- Production cost per helicopter unit (including electronics, display, antenna, and calibration) for fewer than 100 units

- Development and equipment costs for eight buoy units and one helicopter unit for experimental system verification.

A brief description of the recommended design should be provided together with a discussion of potential cost savings afforded by relaxing system specifications or by revising the recommended buoy interrogation scenario.

JACK McCARTHY ASSOCIATES, INC.
Box 436
Cohasset, MA 02025
(617) 383-0720

11-3-79

Leon DePalma
TASC
6 Jacobs Way
Reading, MA 01867

Dear Mr. DePalma:

In response to your inquiry, Motorola has asked me to pass
on to you the results of their review of the buoy audit app-
lication of the Mini-Ranger Positioning System.
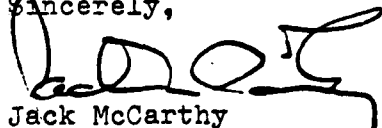
There seems to be little question that all technical/perform-
ance objectives can be met with modified Mini-Ranger designs.
Motorola is prepared to respond to equipment requirements of
this kind on a fixed price basis.

The Mini-Ranger management has reviewed rough cost project-
ions for a large quantity of Mini-Ranger reference stations,
customized to meet mission objectives as outlined by TASC.
They have concluded that a reference station for buoy use
would cost between $2500 and $3500 based on large quantities,
and on Motorola's estimated range of purchase specifications.
In other words, the current reference station design is cost-
reducible for the quantities and specifications anticipated,
but not to the point where there is any reasonable chance of
achieving a $2000/unit cost.

To determine whether a $2000/unit cost objective could be met,
it would be necessary to engage in an in-depth engineering
study on a wholly new design. If funding were to be available
for such a study, Motorola would be interested in conducting
it.

Thank you for your consideration. If we can be of further
help, please call on us at your convenience.

Sincerely,

Jack McCarthy

cc: Bill O'Donnell, Motorola
    Norm Iverson, Motorola

APPENDIX E
BUOY-TRACKING TECHNOLOGY

      In addition to their role as aids to navigation, buoys are applied extensively in hydrographic research. Technology for locating and tracking buoys has received particular attention in the area of ocean current mapping, because the buoys used for this purpose are in a free-drifting mode. Documented methods which have been employed or considered for locating and tracking buoys are summarized in Table E-1. The methods are categorized according to the type of buoy (free-drifting or moored) with which they are associated in the referenced literature. The systems listed in Table E-1 represent a wide range of methods, employing both passive techniques (radar, photography, visual) and active techniques (beacons, transponders, retransmission) and differing significantly in position accuracy, cost, coverage and flexibility.

TABLE E-1

METHODS FOR LOCATING AND TRACKING BUOYS

	METHOD	CHARACTERISTICS	REPORTED ACCURACY
FREE-DRIFTING BUOYS	Radio Direction Finding (Ref. 1)	Radio beacon on buoy, direction finder on search vehicle (primarily ships)	Homing mode
	Over-The-Horizon Radar (Ref. 2)	HF skywave transmission, transmitter on land, transponder on buoy, 1500-3500 km range	± 10 km
	Interrogation, Recording, and Location System (IRLS) (Ref. 3)	Ranging from NIMBUS Satellites	5-7 km
	EOLE Satellite (French System) (Ref. 3)	Ranging and doppler	1-2 km
	Striffler Buoy Tracking System (Ref. 4)	Hyperbolic system using transmitter on buoy and receivers at land stations, 500 km range	±2 km
	Sonar Ranging (Ref. 5)	SOFAR sound channel, range to shore stations measured, range at least 1500 km	±1 km
	NAVSAT Retransmission (Ref. 6)	NAVSAT signals received at buoy, retransmitted to land directly or via communications satellite	90 m, rms
	Consolan Retransmission (Ref. 1)	Retransmission of Consolan signals	5 m per km from station
	S-Band Radar (aerospace quality) (Ref. 7)	Line-of-sight, transmitter on land, transponder on buoy, 30 km range	<5 m
	Omega Position Location Equipment (Ref. 3)	Omega retransmission via communications satellite	2-4 km, rms
MOORED BUOYS	Side-Looking Airborne Radar (Ref. 8)	High quality commercial system not presently available	Accurate if buoy is detectable
	Aerial Photography (Ref. 8)	Requires good visibility, inaccurate greater than 1.6 km from shore	
	Visual Observations from Light Aircraft (Ref. 8)	Requires shore landmarks, accurate within 300 m of shore	Variable
	Beukers Laboratories LO-CATE® III System (Ref. 9)	Omega retransmission, differential mode	<500 m

E-2

APPENDIX F

EFFECT OF PULSE RETRANSMISSION ON
LORAN-C THIRD-CYCLE IDENTIFICATION

F.1   SIMULATION MODEL

The model utilized in the Pulse Retransmission simu-
lations is illustrated in Fig. F.1-1. The ideal Loran-C
current pulse assumed to be received at the buoy is described
by the equation

$$i(t) = A (t/\Delta)^2 e^{2 (1 - t/\Delta)} \sin(2\pi ft) \qquad (F.1-1)$$

where
A = peak envelope current = 1 unit

Δ = peak envelope time = 65 μsec

f = 0.1 cycle/μsec = 100 kHz

t = time (μsec) referenced to start of envelope

Effects of skywave interference, atmospheric noise, and non-
zero Envelope-to-Cycle Difference (ECD) are not included in
the simulations. The received pulse is passed through a band-
pass filter whose transfer function and frequency spectrum are
detailed in Appendix B. The bandpass filter parameters --
bandwidth and center frequency -- may vary slightly from buoy
to buoy as a result of manufacturing tolerances.

The filtered Loran-C pulse is then distorted by a
static (i.e., memoryless) nonlinearity, which is a simple
representation of the retransmission process -- including
modulation (at the buoy), telemetry, and demodulation (at the
shore station or helicopter). A more realistic representation

F-1
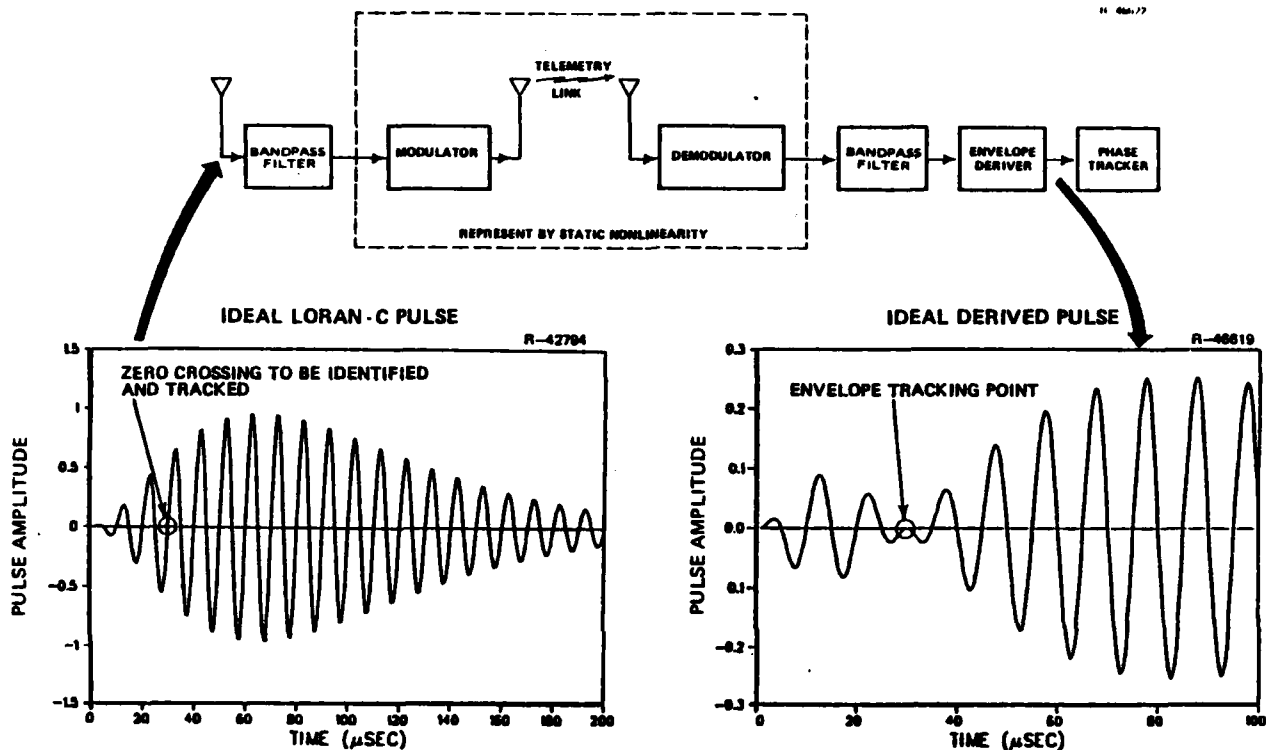
Figure F.1-1 Model Used in Loran-C Pulse
Retransmission Simulation

may be a nonlinear _dynamic_ system, structured to approximate
the modulation/demodulation process. The distorted pulse at
the output of the nonlinearity is passed through a second
bandpass filter, which would be part of the specialized
Loran-C receiver at the shore station or helicopter. Note
that the issue of filter parameter tolerances is not important
for this filter because a single Loran-C receiver processes
the retransmitted pulses from all buoys in a harbor.

The Loran-C receiver must be capable of identifying the third cycle of the 100 kHz carrier and of tracking the positive-going zero crossing associated with the third cycle (nominally, the 30 μsec point). A common technique for identifying the third cycle is to form a <u>derived pulse</u> by delaying the original pulse by a half cycle (5 μsec), scaling the delayed pulse by a gain (k) equal to 1.23466, and adding the scaled pulse to the original pulse (Ref. 20). If the ideal Loran-C pulse is processed by such a technique (termed "delay and add"), the <u>envelope</u> of the derived pulse equals zero at the 30 μsec point of the pulse, as shown in Fig. F.1-1. This envelope null is referred to as the <u>envelope tracking point</u>. The objective of the simulations herein is to determine the effect of the filters and nonlinearity on the envelope tracking point.

F.2 EFFECT OF BANDPASS FILTERS

The result of passing the ideal Loran-C pulse through a bandpass filter is to shift the envelope tracking point determined by the "delay and add" envelope deriver. The derived pulses for bandpass filters with bandwidths of 10 and 30 kHz, centered at 100 kHz, are illustrated in Fig. F.2-1 (compare with ideal derived pulse in Fig. 1.1-1). The envelope tracking point[*] is shifted to the right (>30 μsec) and the length of the shift increases with decreasing bandwidth. Although a bandpass filter causes large shifts in the envelope tracking point, the Loran-C receiver can be calibrated by adjusting the gain k used in the "delay and add" operation. Proper adjustment of k places the envelope tracking point at 30 μsec.

---

[*]Envelope tracking point is uniquely defined as the derived pulse zero crossing which is not associated with a carrier zero crossing.

R—46617

a) 10 kHz BANDWIDTH

R—46618
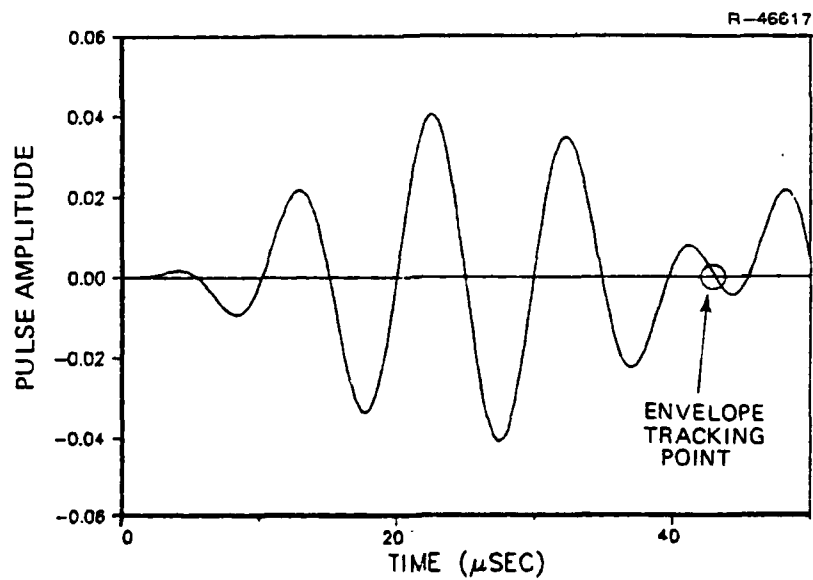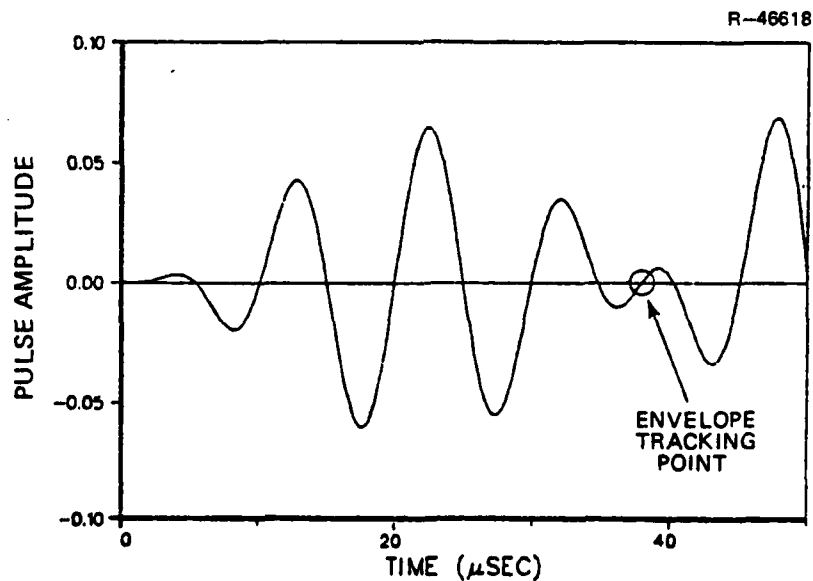
b) 30 kHz BANDWIDTH

Figure F.2-1   Derived Pulse for Single Bandpass Filter
(100 kHz Center Frequency)

However, the Loran-C receiver in the shore station or
helicopter in the Pulse Retransmission BPAS configuration must
function properly for all buoys in the harbor. Consequently,
k must be chosen to guarantee satisfactory envelope tracking
for the retransmitted Loran-C pulses from all buoys. It is
noted in Ref. 21 that manufacturing tolerances on the bandpass
filters utilized at the buoys must be small enough to permit
an acceptable harbor-wide calibration. To examine this issue
further, the envelope tracking point has been computed versus
filter bandwidth (Fig. F.2-2) and versus filter center fre-
quency (Fig. F.2-3). In these simulations, the bandpass fil-
ter in the Loran-C receiver is <u>fixed</u> with a bandwidth of 30
kHz and a center frequency of 100 kHz. Slopes of the curves
in Figs. F.2-2 and F.2-3 determine the sensitivity of the
envelope tracking point to deviations in bandwidth and center
frequency, respectively. For a nominal bandwidth of 30 kHz
and a nominal center frequency of 100 kHz, the sensitivities
are 0.2 μsec per kHz of bandwidth and 0.3 μsec per kHz of
center frequency. Since manufacturing tolerances less than
1.0 kHz are easily achievable, the envelope tracking point
will vary less than 0.3 μsec from buoy to buoy. If the aver-
age envelope tracking point is calibrated to a value of 30 μsec,
no third-cycle identification problems due to bandpass filter
variability are expected to be encountered.[*]

F.3   EFFECT OF NONLINEAR MODULATION/DEMODULATION

The effect of a nonlinear modulation/demodulation
process on the envelope tracking point is investigated using
the model depicted in Fig. F.1-1. Both bandpass filters are

---

[*]Third-cycle identification problems may occur if the cali-
brated envelope tracking point lies outside the 25 to 35
μsec time interval.

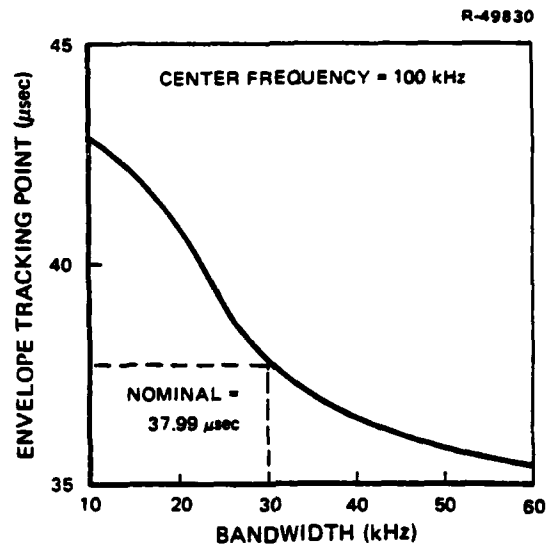Figure F.2-2   Envelope Tracking Point versus
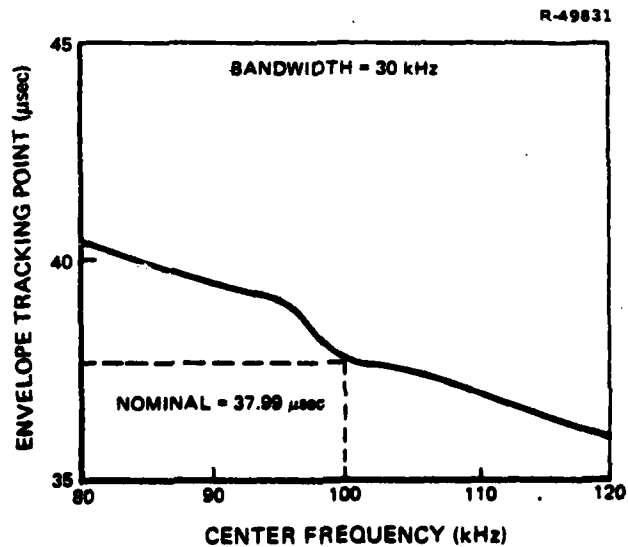   Bandpass Filter Bandwidth

Figure F.2-3   Envelope Tracking Point versus
                Bandpass Filter Center Frequency

assumed to have a 30 kHz bandwidth and 100 kHz center fre-
quency. Two classes of static nonlinearity are considered,
hard-limiting and "serpentine". The impact of a nonlinearity
on the envelope tracking point is an important issue due to
the large amplitude range expected between the weakest and the
strongest Loran-C pulses received at each buoy. It is shown
in Ref. 21 that the modulation/demodulation process must ex-
hibit a minimum dynamic operating range of 78 dB. If a 78 dB
dynamic range cannot be achieved due to cost or technical
constraints, the strongest pulses would be distorted by non-
linearities. Since the character of the distortion differs
for different pulse amplitudes, it may not be possible to
compensate for envelope tracking point differences introduced
by the distortion.

The hard-limiting nonlinearity is described by the
input-output characteristic shown in Fig. F.3-1. The satura-
tion level α determines the degree to which the leading edge
of the filtered Loran-C pulse (with peak value of unity) is
distorted by the nonlinearity. The output of the hard-limiting
nonlinearity is illustrated in Fig. F.3-2 for a saturation
level of 0.1. Although the leading edge of the pulse is ap-
parently distorted beyond recognition by the nonlinearity,
information regarding the pulse envelope is not lost. The
information is contained in the slopes of the carrier below
the saturation level. Indeed, passing the distorted pulse
through the second bandpass filter nearly replicates the pulse
which enters the nonlinearity. This somewhat surprising re-
sult can also be explained by the frequency spectrum of the
distorted pulse which is plotted in Fig. F.3-3. The shape of
the spectrum in the Loran-C band (90-110 kHz) is not signifi-
cantly different from the shape of the Loran-C spectrum.
Harmonics of 100 kHz are introduced by the nonlinearity but
are removed by the 30 kHz bandpass filter. The envelope
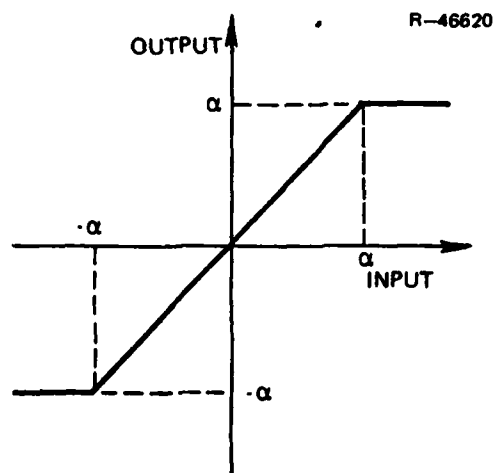
Figure F.3-1   Hard-Limiting Nonlinearity
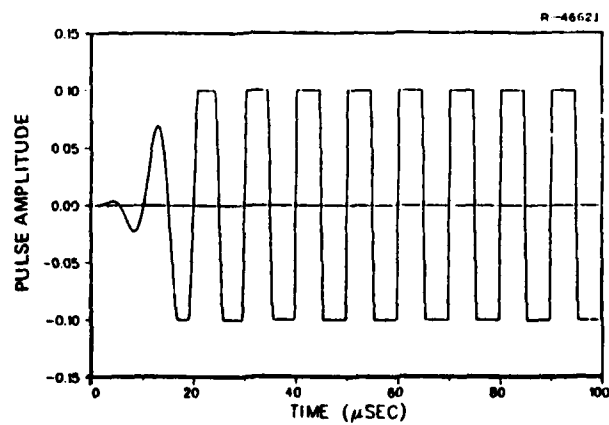
Figure F.3-2   Output of Hard-Limiting Nonlinearity
for $\alpha = 0.1$
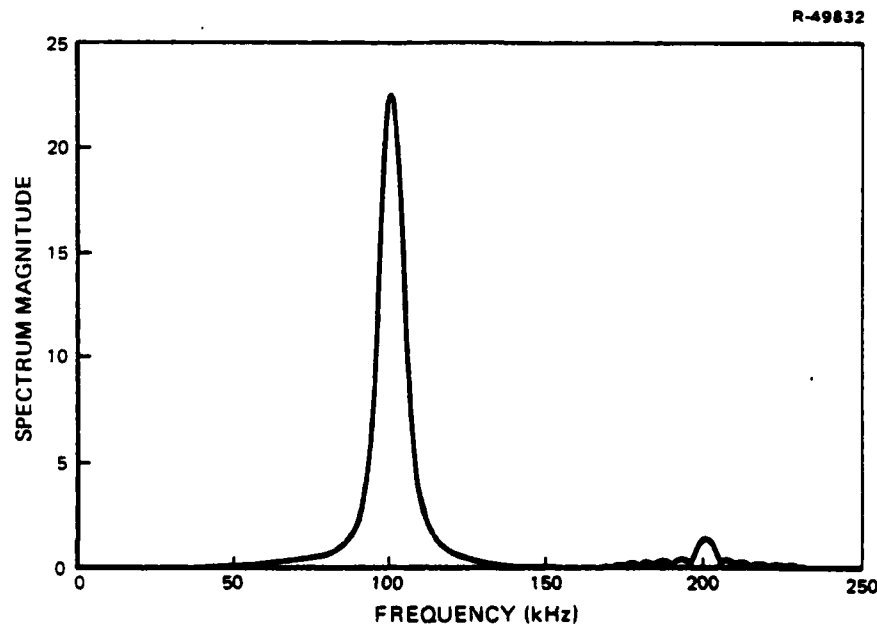
Figure F.3-3   Spectrum of Distorted Loran-C
                Pulse (α = 0.1)

tracking point is presented in Table F.3-1 for various values
of α.   Deviation from the nominal value of 37.99 μsec (for no
nonlinearity) is less than 0.1 μsec.   Therefore, a hard-limiting
nonlinearity has no detrimental effect on Loran-C third-cycle
identification.

     The serpentine nonlinearity has the smooth input-
output characteristic illustrated in Fig. F.3-4.   The devia-
tion from linearity is expressed by β sin(2πx), where β is the
maximum deviation and x is the input to the nonlinearity.
Pulse distortion depends on the parameter β and the peak ampli-
tude of the input pulse; e.g., maximum pulse distortion occurs
for large β and large peak amplitudes.   The output of the
serpentine nonlinearity is shown in Fig. F.3-5 for β equal to

TABLE F.3-1

ENVELOPE TRACKING POINT (μsec)
FOR HARD-LIMITING NONLINEARITY

SATURATION LEVEL, α	ENVELOPE TRACKING POINT (μsec)
0.1	37.96
0.2	37.93
0.3	37.90
0.4	37.97
0.5	37.91

R-46623
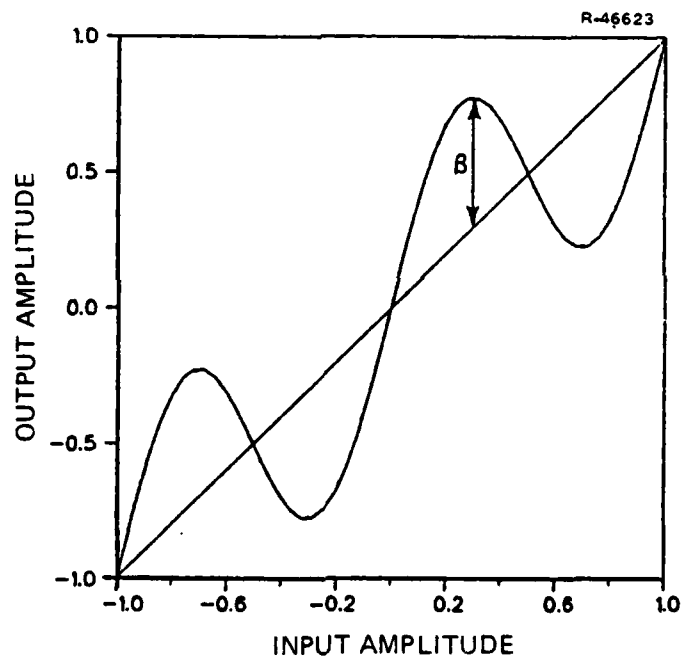
Figure F.3-4   Serpentine Nonlinearity

0.5 and a peak amplitude equal to 2.0. As in the case of the hard-limiting nonlinearity, significant distortion is introduced by the serpentine nonlinearity but is nearly eliminated by the bandpass filter. A range of envelope tracking points from 37.68 to 38.39 μsec (compared to 37.99 μsec for no nonlinearity) results for the values of β and pulse amplitude indicated in Table F.3-2 (for sine error characteristic).

F-10
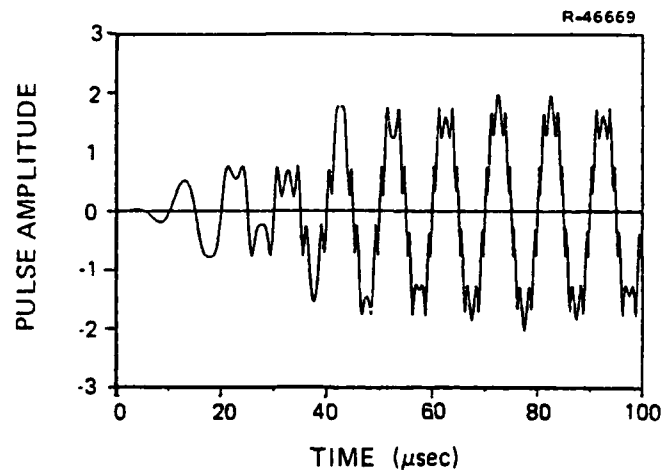
Figure F.3-5   Output of Serpentine Nonlinearity for
β=0.5 and a Peak Amplitude of 2.0

The hard-limiting and serpentine nonlinearities dis-
cussed above are both symmetric with respect to the origin --
i.e., f(-x) = -f(x) where f and x denote the nonlinear func-
tion and input current value, respectively. An asymmetric
nonlinearity was simulated by a serpentine nonlinearity with a
cosine rather than a sine characteristic. A somewhat greater
effect on the envelope tracking point is found, as shown in
the last column of Table F.3-2. However, the maximum deviation
from the nominal envelope tracking point is only 2.34 μsec,
still within the acceptable ±5 μsec limits.

TABLE F.3-2

ENVELOPE TRACKING POINT (μsec)
FOR SERPENTINE NONLINEARITY

PEAK PULSE AMPLITUDE	MAXIMUM DEVIATION FROM LINEARITY, β				
	0.01[*]	0.10[*]	0.20[*]	0.50[*]	0.50[†]
0.5	37.98	37.93	37.86	37.68	37.98
1.0	37.98	37.90	37.81	37.53	38.96
1.5	37.99	38.01	38.03	38.07	39.22
2.0	38.00	38.08	38.16	38.39	40.33

[*]Sine Error Characteristic

[†]Cosine Error Characteristic

APPENDIX G

COMMERCIAL EQUIPMENT DATA SHEETS

(1) COMMUNITRONICS LTD.
    Telemetry Systems
    Models MT-11 and MR-11

(2) COMMUNITRONICS LTD.
    VHF Telemetry Transmitter
    Model T-111

(3) COMMUNITRONICS LTD.
    FM VHF Receiver
    Model MR-18-FM

(4) INTERNAV
    Loran-C Navigation and Monitor Receiver
    Model LCM 404
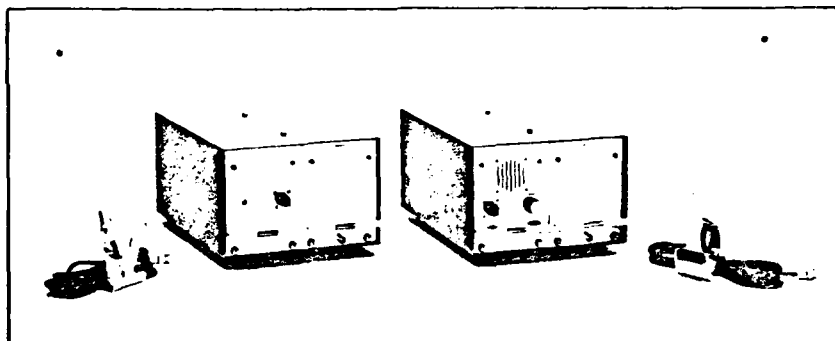
TELEMETRY SYSTEMS

Both the MT-11 and MR-11 were originally designed for systems manufactured by Communitronics. This telemetry capability fills the need of dedicated wide band communications packages for both remote and local transmissions. Typical applications for the telemetry systems have been in short haul digital transmission (2400 Baud) for hospital computer systems, remote meteorological data transmission and fire fighting links for pump control.

The modular housing of the units enables interfacing to both the transmitter and receiver in digital or analog formats. Specialized signal conditioning is available and is handled as a plug-in card in the system.

MODEL MT-11

The Model MT-11 Transmitter is a crystal controlled transmitter operating in the 400 to 500 MHz band. A unique modulator is utilized which provides the user with narrow band or wide band capability. The unit is all solid state and can withstand infinite VSWR.

Specifications of the MT-11 are listed below.

SPECIFICATIONS

Frequency Band	–	400 to 500 MHz (crystal selectable)
Accuracy	–	±.0005%
Power Output	–	100 mw – (2W, 7W, 15W optionally available)
Stability	–	±.001% (voltage and temperature)
Power	–	+12 volts at 100 ma (100 mw output)
Spurious	–	More than 60 db below carrier
Modulation Bandwidth	–	100 Hz to 5 KHz (standard)
Modulation Sensitivity	–	10 KHz/volt
Size	–	5 3/4" x 4" x 10"
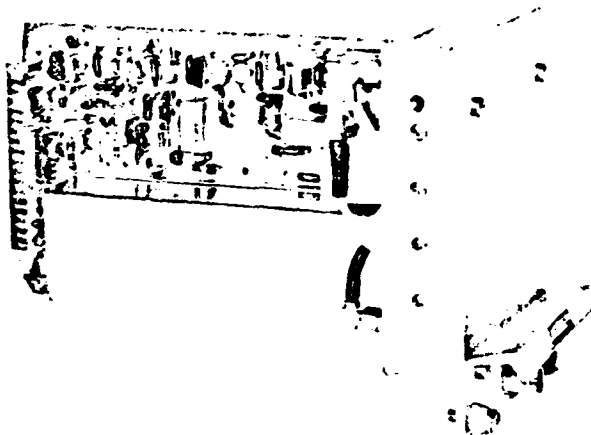
MODEL MR-11

The Model MR-11 Receiver is a crystal controlled dual conversion FM receiver. Utilizing an all solid state construction, the unit can be powered by 115 VAC power or +12 VDC. Since the construction of the MR-11 is modular, a change in the band pass filters allows the unit to process wide or narrow band information. The specifications of the MR-11 are listed below.

SPECIFICATIONS

Frequency Band	–	400 to 500 MHz
Accuracy	–	±.001%
Sensitivity (10 db Sinad)	–	Less than 1 uv
Noise Figure	–	3 db
Bandwidth (Post Detection)	–	10 KHz (standard)
Image Rejection	–	Greater than 60 db
Spurious Rejection	–	Greater than 60 db
Power Requirement	–	+12 VDC or 115 VAC
Size	–	5 3/4" x 4" x 10"

MODEL T111

VHF TELEMETRY TRANSMITTER

RF Output	.75 Watts nominal
Frequency Stability	.001%
Modulation Response	5 Hz - 30 kHz
Spurious & Harmonics	more than -50 dB
Efficiency	40%
Frequency Range	140-175 MHz - crystal select
Antenna Jack	BNC
Modulation Input Conn.	Feed-thru
D.C. Input	Feed-thru
Supply	12V D.C. nom.
Size	1.6" x 8" x 2"
Weight	1/2 pound (less batteries)
Temperature Range	-20°C to $+60^{\circ}$C
Output Z	50 Ohms nominal
Output Mismatch	Unit can withstand infinite VSWR any phase

PRELIMINARY DATA SHEET

MR-18 FM VHF Receiver

The Communitronics Ltd. MR-18 FM VHF Receiver offers the user a reliable, lo power FM receiver. A unique feature of the receiver is its wide demodulated bandwidth (30 kHz). The MR-18 FM's small size plus low power consumption makes it ideal for compact, battery powered use, such as sonobuoys, command receiver, homing devices and distress beacons. Custom tailoring at the factory allows for different bandwidths as well as channel selection for any frequency irom 30-300 MHz.

SPECIFICATIONS

Frequency	30-300 MHz
RF Bandwidth	200 kHz
Modulation Acceptance	FM
Sensitivity	½V for 20 dB quieting
Baseband Frequency Response	+3 dB 5 Hz to 30 kHz
Distortion	<1% @ 30 kHz peak deviation
Supply Voltage	12-15V D.C. (15 typical)
Temperature Range	$0^{o} - 50^{o}$ C.
RF Input Impedance	50 Ohms nominal
Size	2" x 4" x 1" height
Weight	5 oz.

MODEL LCM 404

Loran-C Navigation

And Monitor Receiver

PRODUCT DESCRIPTION

I. Features

- Low instrumental error (less than 40 nanoseconds)
- Low power consumption (15 watts in monitor mode)
- Two way communications
  a. Outputs TD's on command
  b. Outputs status information on command
  c. Reinitiates search on command
  d. Tracking cycle can be changed on command
- High resolution tracking loops
- Measures signal to noise ratio
- Blink indication
- Master independent
- Visual readout of TD's or SNR
- Local or remote control of receiver

II. General Description

The LCM 404 is designed to be a highly accurate Loran-C receiver for precision navigation or monitoring. It will operate as a standard navigation receiver and it contains a two way communication ability which will recognize a message sent to it from a polling unit and respond by sending back time differences and/or other data and execute certain other commands.

Control of the LCM 404 can be either LOCAL (front panel) or REMOTE. In either mode, the LCM 404 will transmit data in response to remote polling commands.

A. Local Mode - In this mode of operation, the LCM 404 is controlled from the front panel and can be used as a normal navigation receiver. The GRI, the secondaries in use, and the cycle sampling points are controlled from the front panel. Simultaneously, the unit can be remotely polled and will reply upon command with time differences and other Loran-C data.

GRI - Determined by Front Panel Switches

TD's displayed - Controlled by front panel switches S1 and S2.

Data to Remote Accessories - Controlled by switches S1 and S2.

Cycle Select Enable/Disable - Controlled by front panel

Up or Down Cycle Commands - From front panel

SNR - Can be displayed on front panel through use of front panel controls.

Communciations - Responds to external requests for time difference or status information.

B. Remote Mode - In this mode, certain receiver functions can be controlled remotely through the communications channel.

GRI - Determined by internal DIP switches (Front Panel GRI switches are ignored)

Secondaries Tracked - Determined by internal DIP switches.

TD's displayed - Selected by front panel switches S1 and S2.

Data to remote accessories - Selected by front panel switches S1 and S2.

Cycle Select Enable/Disable - Remotely controlled

UP of DOWN Cycle Commands - Remotely controlled.

SNR - Can be displayed on front panel using front panel switches

Communications - Same as Local Modes

Search Initiation - Remotely Controlled

Low Power Operation - When in the REMOTE mode
the LCM 404 front panel may be disconnected
completely thus conserving power usage.

III. Communications Function

The LCM 404 will recognize polling requests which
are sent to it and will respond with the requested time
difference or status information. Each unit is assigned
an ID number from 0 to 255 (set via the internal DIP
switches). The polling unit sends out a polling message
which contains the ID of the unit it wishes to respond,
the type of information requested, and, in the REMOTE
mode, whatever commands it wishes the receiver to execute.

If time differences are requested, the receiver res-
ponds with up to four TD's and an alert bit for each sig-
nal being tracked. If status information is requested,
the receiver sends back a status byte for each signal and
a measure of oscillator offset.

Details of the POLLING and REPLY messages are given
in Sections V and VI.

IV. Detailed Specifications

A. Absolute Accuracy

The error due to any of the following individual
range of signal conditions will be less than 25 nano-
seconds.

a. Absolute signal level 25 to 105 DB/luv/meter.

b. Differential signal levels 0 to 60 DB.

c. Differential ECD - plus or minus 4μ sec.

d. Signal-to-noise -10 DB atmospheric or greater.

e. Crossing rate interference S/CRI greater than
-20 DB.

f. CW interference S/CWI greater than -20 DB (when
notched.

G-8

B. Noise

   The standard deviation of the time differences will be less than 20 nanoseconds at a signal-to-atmospheric noise ratio of 0 DB.

C. Tracking

   Receiver will maintain track over the following range of signal conditions.

   a. Signal-to-noise greater than -23 DB atmospheric or better.

   b. CW interference S/CWI greater than -40 DB (when notched).

   c. Envelope to cycle difference plus or minus 4 μsec.

   d. Absolute signal level 10 to 114 DB/luv/meter.

D. Acquisition and Settling

   Receiver will acquire and settle to the correct cycle over the following range of signal conditions.

   a. Signal-to-noise greater than -15 DB atmospheric.

   b. CW interference S/CWI greater than -32 DB (when notched).

   c. Envelope to cycle difference plus or minus 3.5 μsec.

   d. Absolute signal level 25 to 105 DB/luv/meter.

E. Temperature Range - 0 to 55 degrees C.

F. Size - 5.7" high x 12.6" wide x 13.2" deep.

G. Weight - 20 lbs.

H. Resolution of tracking loop steps 10 nanoseconds.

I. Tracks Master and up to four secondaries.

J. Supply Voltage - 10 to 15 volts DC, 15 watts (with front panel display off).

K. TD Resolution - 1.0 nanosecond - transmitted data

0.1 microsecond - front panel readout

L. Data output device - USART INTEL 8251A.

M. Baud rate - 1200 asynchronous.

N. Four internal notch filters can be set by a technician. (Not operator tuneable.)

O. The LCM-404 is Master independent in that if Master Lost Signal is detected for a period of 100 GRI's, oscillator compensation is switched to the first secondary that was acquired. Thus time differences between secondaries remain valid.

P. Time differences output remotely are sampled simultaneously.

Q. The LCM 404 contains Modulator and Demodulator IC's for receiving or sending tones.

V. Format of Polling Message

Byte 1 - Receiver ID - 0 to 255 LSB first.

Byte 2 - First Digit - Type of reply requested.

Bit 0 = 1 - Send back TD's

Bit 1 = 1 - Send back Status Message

Bit 2 = 1 - Send back all 8's

Second Digit - Type of command - Binary encoded.

0 - Do nothing

1 - Up one cycle

2 - Down one cycle

3 - Drop signal

4 - Search for Signal

5 - Cycle Select Enable

6 - Cycle Select Disable

Byte 3 First Digit - Execute Command on Signal X.

    0 = Master

    1-8 = MSD of Signal TD

    9 = All

    Second Digit - Spare

VI.   Format of Reply Message

A.   TD Reply

    Byte 1 - Receiver ID 0 - 255 LSB first

    Byte 2 - TDA 1 nanosecond digit LSB first

           TDA 10 nanosecond digit

    Byte 3 - TDA 100 ns digit

           TDA 1 μsec digit

    Byte 4 - TDA 10 μsec digit

           TDA 100 μsec digit

    Byte 5 - TDA 1 MS digit

           TDA 10 MS digit

    Byte 6-9 TDB 1 nsec digit first

    Byte 10-13 TDC (if active)

    Byte 14-17 TDD (if active)

    Byte 18 - Signal Alert

      Bit 0 = 1 if M = $\overline{LS} \cdot \overline{BLK} \cdot STLD$

      Bit 1 = 1 if S1 = $\overline{LS} \cdot \overline{BLK} \cdot STLD$+Not Active

      Bit 2 = 1 if S2 = $\overline{LS} \cdot \overline{BLK} \cdot STLD$+Not Active

      Bit 3 = 1 if S3 = $\overline{LS} \cdot \overline{BLK} \cdot STLD$+Not Active

      Bit 4 = 1 if S4 = $\overline{LS} \cdot \overline{BLK} \cdot STLD$+Not Active

      Bit 5 = 1 if command executed

      Bit 6 = 1 if command rejected.

B. Status Reply

Byte 1 - Unit ID

Byte 2 - Master Status

   Bit 0 = 1 if $\overline{LS}$

   Bit 1 = 1 if $\overline{BLK}$

   Bit 2 = 1 if STLD

   Bit 3 = 1 if Cycle Select Enabled

   Bit 4 = 1 if tracking too high

   Bit 5 = 1 if tracking too low

   Bit 6 = 1 if Search

   Bit 7 = Spare

Byte 3 - S1 Status

Byte 4 - S2 Status

Byte 5 - S3 Status

Byte 6 - S4 Status

Byte 7 - Master SNR - SNR in db. LSD first. If
       first digit is 5 or greater the number is nega-
       tive. Subtract 5 and append minus sign. 08
       equals + 8db. 58 equals -8db. SNR is measured
       by determining the percent of time the noise
       amplitude exceeds signal amplitude. Thus it is
       most sensitive to atmospheric impulses and
       crossing rates. SNR tends to become insensi-
       tive to SNR's greater than +10db.

Byte 8 - S1 SNR   Byte 12-15 GRI (Oscillator Offset)
                        LSB first - LSD = 1 n sec.
Byte 9 - S2 SNR

Byte 10 - S3 SNR

Byte 11 - S4 SNR

VII. DIP Switches

DIP Switches are arranged on PC Card as shown:

```
 ┌──────────────────────────────────────────────┐
 │                                                │
 │  ┌──┐   ┌──┐   ┌──┐   ┌──┐      ┌──┐  |₁       │
 │  │5 │   │4 │   │3 │   │2 │      │1 │  |₂ ₃     │
 │  │  │   │  │   │  │   │  │      │  │  |₄ ₅     │
 │  └──┘   └──┘   └──┘   └──┘      └──┘  |₆ ₇ ₈   │
 │                                                │
 └──────────────────────────────────────────────┘
```
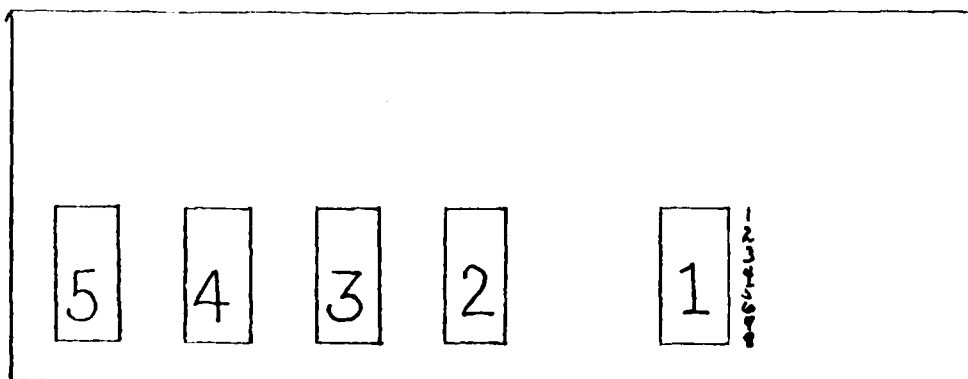
DIP Switch 1 -
  Positions 1-4 MSD of GRI (Binary Encoded)
    1 = 1 bit, 2 = 2 bit, 3 = 4 bit, 4 = 8 bit
    To get 9, set positions 1 and 4.
  Positions 5-8 2nd MSD of GRI
    5 = 1 bit, 6 = 2 bit, 7 = 4 bit, 8 = 8 bit
DIP Switch 2 -
  Positions 1-4 Third Digit of GRI
  Positions 5-8 These positions determine whether the
    receiver is in LOCAL or REMOTE mode. If no switch
    positions are set, receiver is in LOCAL mode. If

one or more positions are set receiver is in
REMOTE mode.

DIP Switch 3 -

Receiver ID Number - 0 to 255 binary encoded.

Position 1 = 1 bit

Position 8 = 128 bit

DIP Switch 4 -

Secondaries to acquire

Position 1 - Set if MSD of desired TD = 1

Position 2 - Set if MSD of desired TD = 2

.

.

.

Position 8 - Set if MSD of desired TD = 8

DIP Switch 5 -

Receiver Calibration Factor - Nanoseconds

Position 1 - If 0 Cal Factor Positive

If 1 Cal Factor Negative

Position 2-4 - Binary Encoded Value of
1st digit. Range is 0 to 7.

Position 5-8 - BCD Encoded Value of 2nd
digit. Range is 0 to 9.

APPENDIX H[*]

VARIABLE GEOMETRY PN RANGING SYSTEM

For this buoy position measuring system a two way pseudo-noise (PN) ranging signal is contemplated to be utilized. A duplex channel is required. One channel for the forward link (helicopter to buoy) and the other for the return link. To provide frequency isolation, a separation of at least 60 MHz between the channels is desirable. The experimental communication link may operate either microwave (L-Band) or UHF frequencies. The communication requirements are therefore computed for both frequency bands; at these frequencies free space propagation is valid. The free space attenuation between isotropic antenna is given by:

$$\alpha = 37 + 20 \log f + 20 \log d \tag{7}$$

where

α = free space attenuation in dB

f = frequency in MHz

d = distance in miles.

In Table 3 are given the availabile carrier-to-noise ratios at the assumed parameters with the baseline values of P_T = 1 watt and d = 25 N.M. where

P_T = transmitter power

d = distance to buoy

P_r = received signal power

*Appendix H was extracted from an internal memorandum. For reasons of expediency equations, tables, and figures were not renumbered.

TABLE 3.   L-BAND AND VHF POWER BUDGET CALCULATIONS

PARAMETER	AT L-BAND	AT UHF
f	1,500 MHz	450 MHz
d	25 N.M.	25 N.M.
P_T	+30 dBm	+30 dBm
T_o	290°K	290°K
T_e	1,000°K (30 dB)	1,000°K (30 dB)
k	-198.6 dBm	-198.6 dBm
kT_e	-168.6 dBm	-168.6 dBm
α	129.5 dB	119 dB
P_r	-99.5 dBm	-89 dBm
C/N_o dB-Hz	69.1 dB-Hz	79.6 dB-Hz

$$C/N_o = \frac{\text{carrier signal power}}{\text{noise spectral density}}$$

$$C/N_o = B_{RF}(SNR)_{RF}$$

$$B_{RF} = \text{RF Bandwidth}$$

$$F = \text{Noise Figure} = \frac{T_e}{T_o} + 1$$

T_o = reference noise temperature

T_t = equivalent system noise temperature

k = Boltzman constant (1.38×10^{-23} w/oK/Hz)

Note that the received signal power P_r is proportional to

$$P_r \; \alpha \; \frac{P_T}{d^2} \qquad (8)$$

so that P_r and hence C/N_o can be readily scaled as a function of P_T, and d.   Table 3 will be used as a baseline reference for estimating the communication requirements for the PN ranging system.

3.1 PN RANGING CODE REQUIREMENTS

An envelope correlating, delay-lock tracking loop is to be used in the PN ranging system. A diagramatic representation of the receiver structure is shown in Figure 2.[2] The PN code must satisfy several requirements.

    a) It must provide unambiguous range.

    b) It must satisfy the measurement accuracy requirements.

    c) It must provide a tolerable acquisition time.

Unambiguous Range: To provide unambiguous range the code length must be chosen so that

$$n\Delta \geq 12 \, d \text{ in usec.} \qquad (9)$$

H-3

FIGURE 2. ENVELOPE CORRELATING, DELAY LOCK LOOP (SCHEMATIC REPRESENTATION)
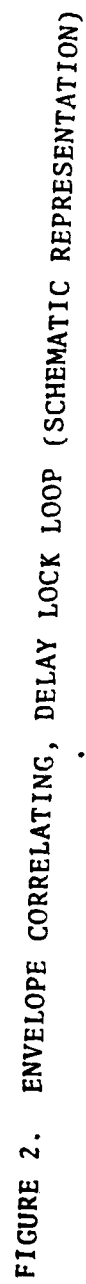
where

  d is the distance in N.M.

  Δ is the width of each code chip in usec.

  n is the number of chips in the ranging code

If the distance d = 25 N.M., then the code length must be
at least 300 usec. If we pick a code chip of Δ = 1 usec
and n = 512 chips, an unambiguous range will be provided to
approximately 42.6 N.M.

Tracking Accuracy: Another requirement is to adjust the
system parameters so as to achieve good tracking accuracies
with the envelope correlating, delay-lock loop (shown in
Figure 2). The jitter in the delay measurements is given
by:[3]

$$\frac{\sigma_t}{\Delta} = [\frac{B_L}{2C/N_0} (1 + \frac{2B_{1F}}{C/N_0})]^{1/2} \tag{10}$$

where

  σ_t = tracking rms error in feet

  Δ = chip duration in usec

  B_{1F} = receiver post correlation 1F bandwidth

  B_L = tracking loop bandwidth

Furthermore, if $C/N_0 \gg 2 B_{IF}$, the second term in the
above equation can be neglected. If we let B_{IF} = 10 KHz
(taking into account oscillator drifts), the value of $2 B_{IF}$
is 43 dB. From Table 3, it is seen that even at L-Band
and only with 0.1 watts of transmitted buoy power, the available

H-5

C/N_o ratio is 59 dB-Hz at 25 N.M. and 53 dB-Hz at 50 N.M.
Thus, for all practical purposes, the second term in
Equation 10 can be neglected. If we let:

$$B_{1F} = 10 \text{ KHz}$$

$$B_L = 20 \text{ cycles}$$

$$\Delta = 1 \text{ usec. } (\approx 1,000 \text{ ft})$$

$$C/N_o = 60 \text{ dB-Hz}$$

then

$$\sigma_t \approx 3.3 \text{ ft rms}$$

This of course does not include other systematic, geometric
and instrumentation errors. The point is that with this
postulated PN ranging code, the rms tracking delay jitter
can be reduced to a small value.

Spectral Requirements: The signal spectrum requirement is a
function of the code chip duration. Suppose that a clock x
code signal, suitable for range code tracking, is utilized.
The clock rate is usually two times the code bit rate. In
Figure 3 is shown the spectrum of clock x code signal. If
$\Delta = 1$ usec., as postulated, the first nulls occurs at 2 MHz.
If the clock x code signal biphase modulates an RF carrier,
a total RF signal bandwidth of 4 MHz is required for the
ranging code.

Acquisition Time: Before tracking can be initiated, the PN
ranging code must first be acquired. If the distance to the
buoy is known approximately, the search needs to be made only
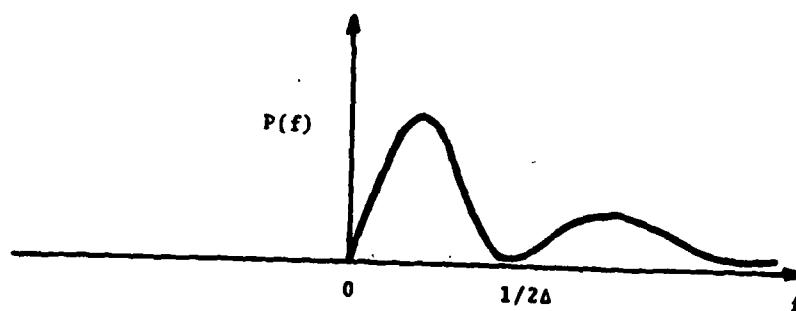over several code chips. Otherwise, the acquisition must be
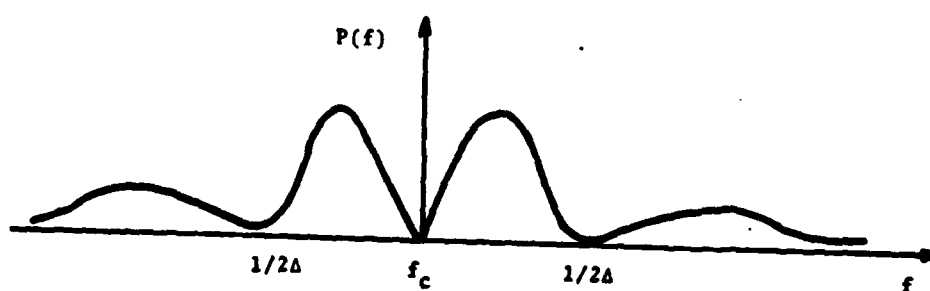
FIGURE 3a.   CLOCK X CODE SPECTRUM

FIGURE 3b.   SPECTRUM OF MODULATED CARRIER

H-7

carried out over the entire 512 chip interval. Suppose that code acquisition is accomplished by stepping the reference code in 1/2 bit intervals. For each step, the output is integrated over the entire code lenght of 512 usec. Since there are 1,024 such steps, the total acquisition time is at most 0.52 sec. and on the average about 0.26 sec. When the codes are fully correlated, the output clock x code x code = clock will be at maximum amplitude. The tracking loop may add another o.1 sec. to the total acquisition time. In Table 4 are listed the tentative parameters of the PN ranging code. In the next section, the communication requirements associated with the above specified ranging code are deter-mined.

TABLE 4.   RANGING CODE PARAMETERS

PN code length...................... = 512 µsec.

        n..................... = 512 (number of chips in
                                             the ranging code)

        Δ..................... =   1 µsec. (width of each
                                             chip)

Unambiguous range.................. = 42.6 N.M.

Correlator processing gain......... = 27 dB

Post-correlator IF Bandwidth, B_{IF}.. = 10 KHz

Tracking loop bandwidth B_L......... = 20 Hz

Tracking delay jitter rms, σ_t...... = less than 3.3 ft for
                                             $C/N_o > 60$ dB

Average estimated acquisition time. $\approx$ 0.36 sec.

3.2 COMMUNICATION REQUIREMENTS FOR PN RANGING

A two way ranging code will be transmitted by the helicopter to the buoy and retransmitted back to the helicopter for on-board processing. Assume that the ranging code is transmitted by bi-phase modulating the RF carrier. At the buoy, the signal is received, amplified to the desired power level and retransmitted back to the helicopter. The requirement for the forward link (helicopter to buoy) and the return link (buoy to helicopter) are now examined.

The Forward Link: In Table 3, it is shown that 1 watt of transmitted power will produce at a distance of 25 N.M. a C/N_0 of 79.6 dB-Hz at UHF and 69.1 dB-Hz at L-Band. Since the signal bandwidth is 4 MHz or 66 dB, the available RF signal to noise ratio at the receiver is 13.6 dB at UHF and 3.1 dB at L-band frequencies. If we assign a 20 watt transmitter to the helicopter, the available RF signal to noise ratio at the buoy receiver is:

$$(SNR)_{RF} \text{ at buoy } = \begin{cases} 26.6 \text{ dB at UHF} \\ \\ 16.1 \text{ dB at L-Band} \end{cases} \quad (11)$$
$$(d=25 \text{ N.M.})$$

The Return Link: Table 3 applies also to the buoy to helicopter link, but in addition, the buoy receiver also amplifies and retransmits its own receiver noise. However, if the transmitted helicopter power is much larger than the retransmitted buoy signal, the impact of the amplified buoy

noise will be small and for all practical purposes can be neglected. The amplified buoy signal will be in all probability band-pass limited. Since the $(SNR)_{RF}$ at the buoy receiver is larger than unity, there will be some enhancement in the output signal to noise ratio. If the input SNR to the band-pass limter were smaller than unity the output signal to noise ratio would be somewhat degraded. Here, we assume that a band-pass limiter will not degrade system performance. Our task now is to determine the (C/N_o) at the input to the helicopter reciever required for proper operation of the PN ranging system. The post correlation 1F signal to noise ratio $(SNR)_{IF}$, at the input to the envelope detectors preceeding the delay lock loop, is given approximately by:

$$(SNR)_{IF} \approx \frac{(SNR)_{RF} \; B_{RF}}{L \quad B_{IF}} \qquad (12)$$

where

$(SNR)_{RF}$ = SNR at the input to the envelope correlator

$(SNR)_{IF}$ = post correlation IF signal to noise ratio

$(B)_{RF}$ = 4 MHZ (RF bandwidth)

$(B)_{IF}$ = 10 KHz (post correlation IF bandwidth)

L = 3 dB (assumed decorrelation loss)

Suppose that we require that the $(SNR)_{IF}$ at the input to the delay lock loop be at least 10 dB and preferably 20 dB. Such signal to noise ratios should be adequate for proper operation of the tracking loop since they are above the threshold values of typical phase lock loops.

H-11

If we specify a $(SNR)_{IF}$ of 20 dB, the required (C/N_o), and RF signal to noise ratio at the input of the helicopter receiver is computed from Equation 14 to be as follows:

$$(C/N_o)_{helicopter} \approx (SNR)_{RF}B_{RF} = (SNR)_{IF}B_{IF}L = 63 \text{ dB-Hz}$$

(13)

$$\text{Helicopter } (SNR)_{RF} = -3 \text{ dB}$$

From Table 3 it is computed that such signal to noise ratios can be readily obtained even at L-Band with a transmitted buoy power of 6.1 dB below 1 watt (that is, with 0.246 watts) at a distance of 25 N.M. Thus, at L-Band, the return link communication parameters required for the PN ranging code are as follows:

Frequency = 1,500 MHz (L-Band)

P_B = 0.246 watts (transmitted buoy power)

RF Bandwidth = 4 MHz

Available C/N_o = 63 dB-Hz (at helicopter)

In Table 5 are summarized the forward and return communication link parameters required for the PN ranging system. To provide an additional fading signal margin, it would be desirable to utilize a 1 watt buoy transmitter. Note also from Table 3 that operation at UHF would result in an additional 10.5 dB signal margin.

TABLE 5. L-BAND COMMUNICATION PARAMETERS

Forward Link: (Helicopter to buoy)

P_H = 20 watts (Helicopter transmitted power

d = 25 N.M.

f = 1,500 MHz (assumed)

RF Bandwidth = 4 MHz

Modulation = PSK

data = PN ranging code with 512, 1 usec. code chips

Available $(SNR)_{RF}$ = 16.1 dB (at buoy receiver

Return Link: (Buoy to helicopter)

P_B = 0.246 watts (Buoy transmitted power)

f $\doteq$ 1,500 MHz

RF Bandwidth = same as above

Modulation = same as above

data = same as above

Available C/N_o = 63 dB-Hz

Available $(SNR)_{RF}$ = - 3 dB (at input to helicopter reciever)

Available $(SNR)_{IF}$ = 20 dB (at input to delay lock loop)

Command Link: Can utilize a data link or other means to "turn on" the buoy receiver/transmitter electronics.

REFERENCES

1. K. Bullington, "Radio Propagation at Frequencies Above 30 Megacycles" Proceedings of the I.R.E., October 1947.

2. J. J. Spilker, Jr. "Ditigal Communications Satellite", Prentice Hall, Inc., Englewood Cliffs, New Jersey, 1977 Chapter 18.

3. W. J. Gill, "A Comparison of Binary Delay-Lock Tracking Loop Implementation", IEEE Transactions on AES, July 1966.

APPENDIX I

DESIGN AND PERFORMANCE OF A TONE RANGING SYSTEM FOR BUOYAUDIT

Tone ranging is a range measurement technique which phase modulates an RF carrier with a set of sidetones or sine waves. The sidetones are generated from a master oscillator by digital division. The highest frequency tone is determined by the desired ranging precision; range is determined by measuring the phase shift between transmitted and received tones. The lower frequency tones are used for coarse range measurement, i.e., the phase shift of a lower frequency tone is used to resolve the number of whole wavelengths of phase shift which the higher frequency tone has incurred.

The specific technique described here is derived from an implementation originally proposed and analyzed by J.J. Stiffler (Ref. 36). It is basically a tone ranging system wherein a carrier is angle-modulated by a set of CW tones which are commensurate in frequency and coherent in phase. In his analysis Stiffler showed that under certain constraints, a tone frequency ratio of 2:1 would minimize the time required for signal acquisition. It also results in a particularly simple implementation scheme.

The signal generation process requires a signal countdown chain which divides in frequency by factors of two from the system oscillator to generate the ranging tones. The highest tone is called the clock; it determines the precision of the ranging system. The lowest frequency tone is chosen to have a half-wavelength longer than the minimum range required, thus eliminating range ambiguity problems. The set of tones is then combined in a majority-logic adder (equivalent to hard-limiting) thus providing a binary waveform to the modulator. In practise this same digital logic would drive the buoy clock.

RANGE TONE SELECTION AND IMPLEMENTATION

The block diagram of the chosen tone generator is shown in Figure 1. The highest frequency component has been chosen to be 100 khz; the lowest frequency component is 1.5625 khz. This component has a wavelength of 105.33 nautical

miles; there'ore the unambiguous one-way range is greater than 100 nautical miles, which is well beyond the helicopter line of sight. The combiner output is phase-modulated on the transmitted carrier which is assumed to be at an L-band frequency of approximately 1.6 ghz.
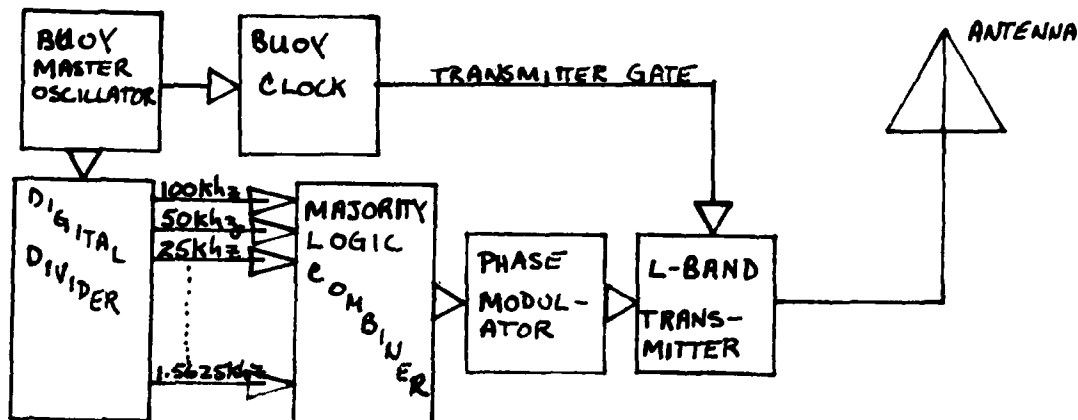
Figure 1. Buoy Ranging Signal Generator

The transmitter is gated on by the system clock, and transmits at a power level of approximately one watt for 10 seconds. The RF signal bandwidth is 200 khz.

SIGNAL RECEPTION AND PROCESSING

The RF signal from the buoy is received, demodulated and processed aboard the helicopter. The functions of reception and demodulation are performed by a relatively conventional phase-locked demodulator, whose block diagram is shown in Figure 2.
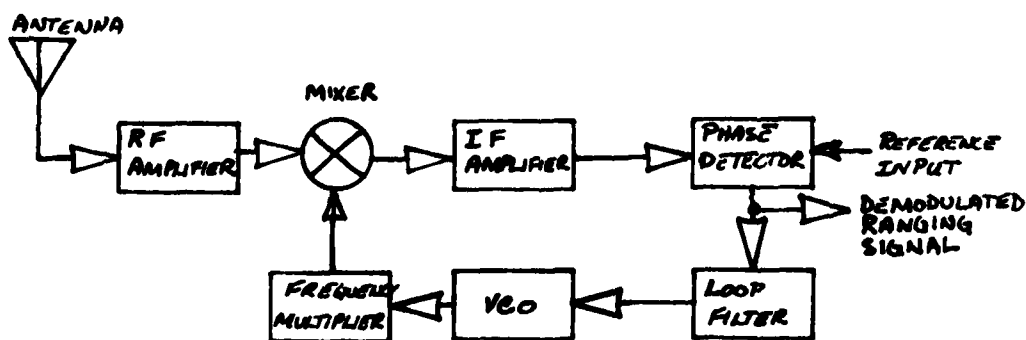
Figure 2. RF Demodulator

I-2

The phase-locked loop in Figure 2 locks to the carrier component of the received signal spectrum (Figure 3).
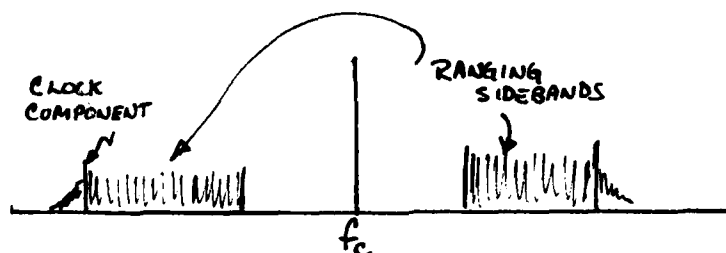

Figure 3. RF Signal Spectrum

The spectrum of the signal has very little energy in the region between the carrier and the lowest frequency tone (1.5625 khz). Consequently, the carrier-tracking loop can have a wide enough bandwidth to insure rapid lock-on, thus minimizing signal acquisition time.

The loop phase detector also functions as a linear phase demodulator. Consequently, the detector output signal contains the ranging signal, which goes from here to the ranging signal processor. The processor filters the noisy receiver output and generates a replica which is coherent in frequency and phase with the received ranging signal.

RANGING SYSTEM PERFORMANCE

The transmission frequency assumed here is about 1600 MHz. At this frequency, transmitter power level on the buoy need be no more than 1 watt. Assuming a range of 25 nautical miles from buoy to helicopter, the signal level received by the helicopter is calculated as follows:

Transmitter Power (1 watt)	+30dBm
Total Net Antenna Gain	0dB
Space Loss (free space)	-130.0dB
Signal Level at Helicopter	-100dBm
Noise Figure	+3dB
System Noise Power Density (assumes antenna temperature of 290°k)	-171dBm/Hz
Received Carrier / Noise Power Density (C/No)	+71dB-Hz

I-3

The ranging signal modulates the carrier at a modulation index of 1.2 radians. Then the power in the carrier component is reduced below total power by:

$$\cos^2 (1.2 \text{ radians}) = -8.82 \text{dB}$$

so that the net C/No in the carrier component is:

$$(C/No)_{carrier} = +71 - 8.8 = +62.2 \text{dB-Hz}$$

Similarly, the power in the ranging signal becomes:

$$(C/No)_{ranging} = +71 - 10 \log \sin^2(1.2) = +70.4 \text{dB-Hz}.$$

The RF demodulator must acquire the signal and demodulate. the ranging code in a small fraction of 10 seconds. This must be accomplished over a total frequency range of $\pm$ 2000 Hz, to allow for drift in the oscillator over one year plus doppler shift due to motion of the helicopter. Assume that the RF demodulator is a high-gain, second-order phase-locked loop; then the time to acquire an uncertain frequency is (Ref. 39):

$$T_{acq} \cong \frac{(\Delta\omega)^2}{2 \, \zeta \, \omega_n^3}$$

$\Delta\omega$ = radian frequency uncertainty
ζ = loop damping factor
ω_n = loop natural frequency

Then, if $\Delta\omega = 2\pi (4000)$; $\zeta = 0.5$ and The one-sided loop noise bandwidth is 500 hz :

$$T_{acq} = 0.63 \text{ seconds}.$$

The total signal-noise ratio in the demodulator is:

$$S/N = \left(C/N_o\right) \cdot 2B_L = 62.2 - 30 = +32.2 \, dB.$$

Therefore, the RF demodulator will have an S/N of +32.2dB and will acquire, track and demodulate the received signal in 0.63 seconds or less.

RANGING SIGNAL PROCESSOR - ACQUISITION AND PRECISION

The processor performs a sequential acquisition, first locking to the clock in a phase-locked loop, and then sequentially dividing its output by factors of two, comparing each output with the demodulated signal and making a binary (inphase-out of phase) decision. The decision time is (for each component), an integer multiple of the code length, which is essentially the period of the lowest-frequency code component (1/1562.5 or 0.64 milliseconds.) The clock loop bandwidth will be 20Hz, which will result in an acquisition time of approximately $3/20 = 150$ milliseconds.

Each of the other components will require 0.64 milliseconds; therefore, the total system acquisition time, for each buoy transmission, will be:

$$T = 0.63 + 0.15 + (6) \times 0.64 \times 10^{-3} = 0.784 \text{ sec.}$$

which leaves a little over 9 seconds for the actual range measurement.

The precision of the ranging measurement is determined by the clock phase jitter, which in turn is a function fo the clock loop S/N.

$$\sigma^2 = \frac{1}{2\, S/N} (\text{rad})^2 \,; \quad \begin{array}{l} \sigma^2 = \text{Variance of clock phase.} \\ S/N = \text{clock signal/noise ratio.} \end{array}$$

$$(\text{Ref. 39})$$

The clock signal noise ratio is:

$$S/N\Big)_{cL} = \left(C/N_0\right)_{ranging} \cdot 2\, B_{L,cL} \cdot \rho \,;$$

$B_{L,cL}$ = clock tracking loop noise bandwidth.

ρ = clock component power relative to total ranging power.

The value of ρ is derived in Ref. 36; for this design, it is -2dB. So

$$S/N\Big)_{cL} = +70.4 - 13 - 2 = +55.4 \text{ dB}$$

Since the clock wavelength is

$$\lambda_{CL} = \frac{c}{f_{CL}} \approx \frac{10^9}{10^5} = 10^4 \text{ feet.}$$

c = velocity of light ($\pm 10^9$ feet/sec)

f_{CL} = clock frequency (100khz)

the standard deviation of the ranging measurement becomes

$$\sigma_r = \frac{\lambda}{2\pi} \frac{c}{f_{cl}}$$

σ_r = ranging standard deviation (in feet rms)

$$\sigma_r = \frac{10^4}{2\pi} \sqrt{\frac{1}{2(S/N)_{cl}}} = \boxed{1.91 \text{ feet rms}}$$

The actual ranging error will be dominated by internal error sources such as timing errors and resolution in counters. A preliminary assessment gives an overall precision, for this system, of 12 feet.

REFERENCES

1. Walden, R.G., and Webb, D., "Methods of Locating and Tracking Buoys," Trans. Buoy Technology Symposium, (Washington, D.C.) March 1964, pp. 317-324.

2. Werner, C.D., "Buoy Tracking With Over-the-Horizon (OTH) Radar," Proc. AIAA Drift Buoy Symposium, (Hampton, Virginia) May 1974, pp. 18-33.

3. Cote, C., "The Development of the Satellite Location and Data Collection System Within the National Aeronautics and Space Administration," Proc. AIAA Drift Buoy Symposium, (Hampton, Virginia) May 1974, pp. 351-371.

4. Bumpus, D.F., "The Striffler 'Talking Drift Bottle,' a Free-Drifting Buoy-Location System," Proc. AIAA Drift Buoy Symposium, (Hampton, Virginia) May 1974, pp. 9-17.

5. Webb, D.C., "Measurement of Open Ocean Circulation Using Neutrally Buoyant Floats," Proc. AIAA Drift Buoy Symposium, (Hampton, Virginia) May 1974, pp. 47-55.

6. Turner, S., "The Navy Navigation Satellite System for Buoy Location," Proc. AIAA Drift Buoy Symposium, (Hampton, Virginia) May 1974, pp. 56-70.

7. Johnson, R.E., "A Near Shore Circulation Study of the Chesapeake Bay Entrance Using Radar Tracked Buoys," Proc. AIAA Drift Buoy Symposium, (Hampton, Virginia) May 1974, pp. 34-46.

8. Giovane, F., "A Study of Aerial Semi-Precise Survey Systems for Position Auditing of Coast Guard Aids to Navigation," U.S. Coast Guard Research and Development Center, Report No. CG-D-61-77, October 1977.

9. Lindeblad, J.R., "The Distress Alerting and Locating System (DALS); Summary of Development and Documentation," U.S. Coast Guard Research and Development Center, Report No. CG-D-29-77, April 1977.

10. Swanson, E.R., "Geometric Dilution of Precision," Navigation: Journal of the Institute of Navigation, Vol. 25, No. 4, Winter 1978-1979, pp. 425-429.

REFERENCES (Cont.)

11. DePalma, L.M., and Gupta, R.R., "Seasonal Sensitivity
     Analysis of St. Marys River Loran-C Time Difference
     Grid," The Analytic Sciences Corporation, Technical
     Information Memorandum TIM-1119-3, June 1978.

12. Bean, B.R., Horn, J.D., and Ozanich, A.M., Jr., Climatic
     Charts and Data of the Radio Refractive Index for the
     United States and the World, National Bureau of Standards
     Monograph 22, Washington, D.C., 1960.

13. Fine, H., "An Effective Ground Conductivity Map for
     Continental United States," Proc. IRE, Vol. 42,
     September 1954, pp. 1405-1408.

14. Johler, J.R., Keller, W.J., and Walters, L.C., "Phase
     of the Low Radio Frequency Groundwave," National Bureau
     of Standards Circular 573, June 1956.

15. Millington, G., "Ground Wave Propagation over an
     Inhomogeneous Smooth Earth," Proceedings of the
     Institute of Electrical Engineers, Vol. 96, Pt. III,
     January 1949.

16. Bean, B.R., and Thayer, G.D., "On Models of the
     Atmospheric Refractive Index," Proc. IRE, Vol. 47, May
     1959, pp. 740-755.

17. Gelb, A., (Editor), Applied Optimal Estimation, MIT
     Press, Cambridge, 1974.

18. "Model LCM 404 Loran-C Monitor Receiver," International
     Navigation Corp., Product Description, July 1979.

19. Culver, C., and Haroldsen, D., "The Use of Marine Loran
     Receivers for the Wide Area Coverage AVM Application,"
     Micrologic, Inc., Final Report to Gould, Inc., December
     1978.

20. Roland, W.F. (Editor),"Loran-C Receiving Sets: Functions,
     Characterization, and Specification," Wild Goose
     Association Radionavigation Journal, 1976.

21. Poppe, M.C. Jr., "Loran-C Retransmission Bandwidth Re-
     duction Study," Cambridge Engineering, Report No.
     CE-4010, April 1975.

REFERENCES (Cont.)

22.   Goddard, R.B., "Differential Loran-C Time Stability
       Study," U.S. Coast Guard, Report No. DOT-CG-31146-A,
       November 1973.

23.   Lincoln, W.B., and Rush, R.G., "The Dynamic Behavior of
       a Particular Chain Mooring Under Tidal Current
       Excitation," U.S. Coast Guard, unpublished report,
       March 1978.

24.   Campbell, L.W., Doherty, R.H., Johber, J.R.,"Loran-C
       System Dynamic Model-Temporal Propagation Variation Study",
       U.S. Dept. of Transportation, Report # DOT-CG-D57-79, July 1979.

25.   Beukers, J.M., "Applications of Loran-C Retransmission,"
       Presented at the Wild Goose Association Annual
       Convention, October 1973.

26.   Cassis, R.H. Jr., "A Loran-C Airborne Navigator,"
       Proc. Offshore Technology Conference, (Houston, Texas)
       May 1976, pp. 251-257.

27.   Cassis, R.H. Jr., "An Operational Test and Evaluation
       of an Airborne Loran-C Navigator System," Proc. Offshore
       Technology Conference, (Houston, Texas) May 1977, pp.
       69-76.

28.   Adams, R.J., and McKinley, J.B., "Airborne Evaluation
       of the Production AN/ARN-133 Loran-C Navigator," Systems
       Control, Inc. (Vt), Report No. CG-D-32-79, July 1979.

29.   Munson, R.C., "Positioning Systems," presented at
       International Congress of Surveyors, (Stockholm, Sweden)
       June 1977.

30.   Hart, E.D., and Downing, G.C., "Positioning Techniques
       and Equipment for U.S. Army Corps of Engineers Hydro-
       graphic Surveys," U.S. Army, Report No. H-77-10, May
       1977.

31.   Couchman, R.L., "An Overview of Alternative Techniques
       for Determining Positions at Sea, with Emphasis on
       Applicability of Potential Use for Positioning Buoys,"
       U.S. Coast Guard Research and Development Center,
       Report No. CG-D-20-78, March 1978.

32.   "Coast Guard Action Needed to Promote Safer Marine
       Transportation," Comptroller General of the United
       States, Report No. CED-79-37, May 1979.

REFERENCES (Cont.)

33. "Light List, Volume I, Atlantic Coast, St. Croix River, Maine to Little River, South Carolina," U.S. Coast Guard, CG-158, December 1978.

34. Nautical Chart of Boston Harbor, National Oceanic and Atmospheric Administration, National Ocean Survey, Chart Number 13270, 43rd Ed., March 1979.

35. Roland, W.F. (Editor), "Loran Chain Data," Wild Goose Association Radionavigation Journal, 1978.

36. J.J. Stiffler, Theory of Synchronous Communications, Chapter 6, Prentice Hall, 1971.

37. P.G. Mauro, Digital Tone Ranging Modem: Design and Implementation, Dept. of Transportation Report # FAA-RD-76-16, 1976.

38. E.J. Habib, G.C. Kronmiller, P.D. Engels and H.J. Franks, Development of a Range and Range Rate Spacecraft Tracking System, NASA Technical Note D-2093, June, 1964.

39. F.M. Gardner, Phase Lock Techniques.

copies 150

END

DATE
FILMED

9-80

DTIC